

Dissertation zur Erlangung des Doktorgrades  
der Fakultät für Chemie und Pharmazie  
der Ludwig-Maximilians-Universität München



**Different approaches to influence the  
ischemia/reperfusion injury of the liver**

Andreas Hartkorn  
aus  
Koblenz am Rhein

2008



# ERKLÄRUNG

Diese Dissertation wurde im Sinne von § 13 Abs. 3 bzw. 4 der Promotionsordnung vom 29. Januar 1998 von Frau Prof. Dr. Angelika M. Vollmar betreut.

# EHRENWÖRTLICHE VERSICHERUNG

Diese Dissertation wurde selbständig, ohne unerlaubte Hilfe erarbeitet.

München, am 24. Juli 2008

.....  
Andreas Hartkorn

Dissertation eingereicht am:	24. Juli 2008
1. Gutachter:	Frau Prof. Dr. Angelika M. Vollmar
2. Gutachter:	Herr PD Dr. Stefan Zahler
Mündliche Prüfung am:	23. September 2008



**MY BROTHER**



# CONTENTS

**ABBREVIATIONS** \_\_\_\_\_ **V****1. INTRODUCTION** \_\_\_\_\_ **1****1.1. Background and aim of project** \_\_\_\_\_ **2****1.2. Hepatic ischemia/reperfusion injury** \_\_\_\_\_ **4**

## 1.2.1. Background \_\_\_\_\_ 4

## 1.2.2. Model differentiations \_\_\_\_\_ 4

## 1.2.3. General mechanisms \_\_\_\_\_ 5

## 1.2.4. Role of ROS \_\_\_\_\_ 8

1.2.5. Role of NF- $\kappa$ B \_\_\_\_\_ 12

## 1.2.6. Interventions \_\_\_\_\_ 16

## 1.2.7. Approaches of this study \_\_\_\_\_ 17

**1.3. Ginkgo biloba extract – EGb 761** \_\_\_\_\_ **18**

## 1.3.1. General aspects \_\_\_\_\_ 18

## 1.3.2. Molecular activities \_\_\_\_\_ 19

## 1.3.3. Experimental outline \_\_\_\_\_ 21

**1.4. Xanthohumol and 3-Hydroxyxanthohumol** \_\_\_\_\_ **22**

## 1.4.1. General aspects \_\_\_\_\_ 22

## 1.4.2. Molecular activities \_\_\_\_\_ 23

## 1.4.3. Experimental outline \_\_\_\_\_ 25

**1.5. NF- $\kappa$ B decoy nanoparticles** \_\_\_\_\_ **26**

## 1.5.1. Background \_\_\_\_\_ 26

## 1.5.2. Targeting Kupffer cells \_\_\_\_\_ 26

## 1.5.3. Experimental outline \_\_\_\_\_ 28

**2. MATERIALS AND METHODS** \_\_\_\_\_ **29****2.1. Materials** \_\_\_\_\_ **30**

## 2.1.1. Ginkgo biloba extract – EGb 761 \_\_\_\_\_ 30

## 2.1.1.1. Solutions and reagents \_\_\_\_\_ 30

## 2.1.1.2. General aspects \_\_\_\_\_ 30

2.1.2.	Xanthohumol and 3-Hydroxyxanthohumol	30
2.1.2.1.	Solutions and reagents	30
2.1.2.2.	General aspects	31
2.1.3.	NF- $\kappa$ B decoy nanoparticles	31
2.1.3.1.	Solutions and reagents	31
2.1.3.2.	General aspects	32
<b>2.2.</b>	<b>Cell-free system</b>	<b>33</b>
2.2.1.	Solutions and reagents	33
2.2.2.	Xanthine/xanthine-oxidase assay	33
<b>2.3.</b>	<b>Cellular systems</b>	<b>34</b>
2.3.1.	Solutions and reagents	34
2.3.2.	Cell line and cultivation	35
2.3.3.	Dihydrofluorescein diacetate assay	36
2.3.4.	NF- $\kappa$ B reporter gene assay	37
2.3.4.1.	Plasmid preparation	37
2.3.4.2.	Transfection of cells	37
2.3.4.3.	Luciferase assay	38
<b>2.4.</b>	<b>Animal models</b>	<b>39</b>
2.4.1.	Solutions and reagents	39
2.4.2.	Animals	39
2.4.3.	Blood pressure measurement - <i>in vivo</i>	40
2.4.3.1.	Surgical procedure	40
2.4.3.2.	Treatment protocol – EGb 761	40
2.4.4.	Warm ischemia/warm reperfusion – <i>in vivo</i>	41
2.4.4.1.	Surgical procedure	41
2.4.4.2.	Treatment protocols	41
2.4.4.2.1.	Ginkgo biloba extract – EGb 761	41
2.4.4.2.2.	Xanthohumol	42
2.4.5.	Cold ischemia/warm reperfusion – <i>ex vivo</i>	43
2.4.5.1.	Surgical procedure	43
2.4.5.2.	Treatment protocols	43
2.4.5.2.1.	Xanthohumol and 3-Hydroxyxanthohumol	43
2.4.5.2.2.	NF- $\kappa$ B decoy nanoparticles	44

2.4.5.3. Biodistribution	45
<b>2.5. Immunohistochemistry</b>	<b>46</b>
2.5.1. Solutions and reagents	46
2.5.2. Staining of liver tissue	46
<b>2.6. Antioxidant parameters</b>	<b>47</b>
2.6.1. GSH	47
2.6.2. SOD	47
2.6.3. MDA	47
<b>2.7. Electrophoretic mobility shift assay – EMSA</b>	<b>48</b>
2.7.1. Solutions and reagents	48
2.7.2. Preparation of nuclear extracts	49
2.7.3. Radioactive labeling of consensus oligonucleotides	49
2.7.4. Binding reaction and electrophoretic separation	50
2.7.5. Detection and evaluation	50
<b>2.8. ELISA</b>	<b>50</b>
2.8.1. Preparation of samples	50
2.8.2. Reaction mixture	50
2.8.3. Detection and evaluation	50
<b>2.9. Western blot</b>	<b>51</b>
2.9.1. Solutions and reagents	51
2.9.2. Preparation of samples	53
2.9.3. Electrophoresis	53
2.9.4. Electroblotting	53
2.9.5. Protein detection	54
2.9.5.1. Specific protein determination	54
2.9.5.2. Total protein determination	54
<b>2.10. Caspase-3 like activity assay</b>	<b>55</b>
2.10.1. Solutions and reagents	55
2.10.2. Preparation of samples	55
2.10.3. Detection and evaluation	55

<b>2.11. Protein quantification</b>	<b>56</b>
2.11.1. Solutions and reagents	56
2.11.2. Pierce assay	56
2.11.3. Bradford assay	56
<b>2.12. Tissue injury parameters</b>	<b>57</b>
<b>2.13. Statistical analysis</b>	<b>57</b>
<b>3. RESULTS</b>	<b>58</b>
<b>3.1. Ginkgo biloba extract – EGb 761</b>	<b>59</b>
3.1.1. Impact on warm ischemia/warm reperfusion	59
3.1.1.1. Hepatic tissue damage	59
3.1.1.2. Apoptosis	59
3.1.1.3. Blood pressure development during IR	60
3.1.2. Investigation of arterial blood pressure drop	61
3.1.2.1. eNOS inhibition – <i>in vivo</i>	61
3.1.2.2. eNOS expression in isolated thoracic aorta	61
<b>3.2. Xanthohumol and 3-Hydroxyxanthohumol</b>	<b>63</b>
3.2.1. Impact on ROS levels in a cell-free system	63
3.2.2. Influences on the redox status in a cellular system	65
3.2.3. Influences on NF- $\kappa$ B activity in a reportergene assay	66
3.2.4. Impact on warm ischemia/warm reperfusion	67
3.2.4.1. NF- $\kappa$ B binding activity	67
3.2.4.2. Liver tissue injury	68
3.2.5. Impact on cold ischemia/warm reperfusion	69
3.2.5.1. Endogenous antioxidant system	69
3.2.5.2. Oxidative damage	70
3.2.5.3. NF- $\kappa$ B binding activity	70
3.2.5.4. Protein levels	71
3.2.5.5. Apoptosis	73
3.2.5.6. TNF- $\alpha$ levels	73
3.2.5.7. Liver tissue injury	74

<b>3.3. NF-<math>\kappa</math>B decoy nanoparticles</b>	<b>75</b>
3.3.1. Biodistribution	75
3.3.2. Impact on cold ischemia/warm reperfusion	75
3.3.2.1. NF- $\kappa$ B binding activity	75
3.3.2.2. Liver tissue injury	76
<b>4. DISCUSSION</b>	<b>77</b>
4.1. Ginkgo biloba extract – EGb 761	78
4.2. Xanthohumol and 3-Hydroxyxanthohumol	81
4.3. NF- $\kappa$ B decoy nanoparticles	86
<b>5. SUMMARY</b>	<b>89</b>
<b>REFERENCES</b>	<b>91</b>
<b>ALPHABETIC LIST OF COMPANIES</b>	<b>105</b>
<b>CURRICULUM VITAE</b>	<b>108</b>
<b>PUBLICATIONS</b>	<b>110</b>
<b>ACKNOWLEDGMENTS</b>	<b>113</b>

# **ABBREVIATIONS**

---

Ac-DEVD-AFC	N-acetyl-Asp-Glu-Val-Asp-AFC
AFC	7-amino-4-trifluoromethyl coumarin
Akt	proteinkinase B
ALT	alanine amino transferase
ANP	atrial natriuretic peptide
AP-1	activator protein 1
APS	ammonium persulfate
AST	aspartate amino transferase
ATP	adenosine triphosphate
AUC	area under the curve
BCA	bicinchoninic acid
BSA	bovine serum albumin
CAPE	caffeic acid phenethyl ester
CAT	catalase
CLSM	confocal laser scanning microscopy
CXC	$\alpha$ -chemokines
DMEM	Dulbecco's modified eagle medium
DNA	desoxyribonucleic acid
DTT	dithiothreitol
ECL	enhanced chemoluminescence
EDTA	ethylenediaminetetraacetic acid
EGb 761	Ginkgo biloba extract of Dr. W. Schwabe GmbH
EGTA	ethylene-glycol-bis(2-aminoethylether)tetraacetic acid
ELISA	enzyme linked immuno sorbent assay
EMSA	electrophoretic mobility shift assay
eNOS/iNOS	endothelial/inducible NO synthetase
ET-1	endothelin-1
FCS	fetal calf serum
GC	guanylate cyclase
GFP	green fluorescent protein
GP <sub>x</sub>	glutathione peroxidase
GSH	glutathione

---

GTE	green tea extract
HEK 293	human embryonic kidney cell line 293
Hepes	N-(2-hydroxyethyl)piperazine-N'-(2-ethanesulfonicacid)
H <sub>2</sub> FDA	dihydrofluorescein diacetate
HRP	horseradish peroxidase
HSP	heat shock protein
HO-1	heme oxygenase-1
ICAM	intercellular adhesion molecule
IFN	interferon
Ig	immune globulin
I $\kappa$ B	inhibitory protein $\kappa$ B
IKK	I $\kappa$ B kinase
IL	interleukin
i.p.	intraperitoneal
IPC	ischemic pre-conditioning
IR	ischemia/reperfusion
IRI	ischemia/reperfusion injury
i.v.	intravenous
JNK	jun N-terminal kinase
KC	Kupffer cell
KH	Krebs-Henseleit
LB	Lennox Broth
LDH	lactate dehydrogenase
LFA-1	lymphocyte function-associated antigen-1
L-NAME	nitro-L-arginine methyl ester
LPO	lipid peroxidation
LPS	lipopolysaccharide
MAC-1	$\beta_2$ integrin (CD18/CD11B)
MDA	malondialdehyde
MPO	myeloperoxidase
mRNA	messenger ribonucleic acid
NAC	N-acetylcysteine

---

NAD(P)H	nicotinamide adenine dinucleotide phosphate
NEMO	nuclear factor $\kappa$ B essential modulator
NF- $\kappa$ B	nuclear factor $\kappa$ B
NO	nitric oxide
NP	nanoparticles
NP-40	non-ident P 40
Nrf2	nuclear receptor factor 2
ODN	oligodeoxynucleotide
OH-XN	3-Hydroxyxanthohumol
PAA	polyacrylamide
PAF	platelet activating factor
PAGE	polyacrylamide gel electrophoresis
PBS	phosphate buffered saline
PDTC	pyrrolidinedithiocarbamate
PE	polyethylene
PI3K	phosphoinositide 3-kinase
PMSF	phenylmethylsulfonylfluoride
RIPC	remote IPC
RLU	relative light units
ROS	reactive oxygen species
RT	room temperature
SAR	structure activity relationship
SB	sample buffer
Scr. ODN	scrambled ODN
SDS	sodium dodecyl sulfate
SEC	sinusoidal endothelial cell
Ser	serin
SOD	superoxide dismutase
TBARS	thiobarbituric acid reactive substance
T/E	trypsin/EDTA
TEMED	tetramethylethylenediamine
Thr	threonin

---

TNF- $\alpha$	tumor necrosis factor- $\alpha$
UW	University of Wisconsin solution
WB	Western blot
XN	Xanthohumol
XO	xanthine-oxidase

# INTRODUCTION

## 1.1 BACKGROUND AND AIM OF PROJECT

The ischemia/reperfusion injury (IRI) of the liver is a crucial pathologic process encountered in several clinical situations such as hemorrhagic shock, liver resection and transplantation which can lead to a significant amount of liver dys-function, liver non-function or possible mortality.<sup>1</sup>

Despite several promising interventions both pharmacological and physical in nature, including antioxidant therapy, storage manipulation and pre-conditioning, there are no clearly established methods available to prevent hepatic IRI at present.<sup>2-5</sup> Only through a better understanding of the complex ischemia/reperfusion process one can find interesting targets to develop new strategies to combat this serious injury.

This study is aimed at using products of natural and synthetic origin to examine their molecular function and their impact on hepatic IRI.

The three approaches are as follows:

- a. EGb 761 (Dr. Willmar Schwabe Pharmaceuticals) is a standardized extract from the dried leaves of the Ginkgo biloba tree. Its different constituents drawn from the plant offer a wide range of approved medicinal applications.<sup>6</sup> Due to its diverse molecular activities affecting the redox system, microcirculation, mitochondrial function to name a few, EGb 761 might be an interesting candidate to be challenged in the multifunctional IRI process (see section 1.3).
- b. Dietary flavonoids have shown to have beneficial therapeutic effects, attributed mainly to their antioxidant capacity.<sup>7-9</sup> Xanthohumol, the prominent flavonoid of the hop plant, *Humulus lupulus L.*, and its metabolic derivative 3-Hydroxyxanthohumol, both possess promising antioxidant properties *in vitro*.<sup>10, 11</sup> The IRI of the liver is a complex injury process driven by oxidative stress, in which these compounds might be interesting (see section 1.4).
- c. Selective NF- $\kappa$ B inhibition in Kupffer cells using NF- $\kappa$ B decoy nanoparticles is an approach shown to be of great value in the model of warm IR by Dr. Florian Hoffmann in his recent Ph.D. thesis. The cold IR model used in this case was

assigned as Kupffer cells are vigorously activated and as it is solely influenced by hepatic factors. Therefore, it is an appropriate model to specify the role of selective NF- $\kappa$ B targeting in the liver in the best possible way (see section 1.5).

## 1.2 HEPATIC ISCHEMIA/REPERFUSION INJURY

### 1.2.1 Background

At present, the ischemia/reperfusion injury (IRI) is a critical process as it has been recognized as significant source of morbidity and mortality in different clinical and environmentally induced situations.<sup>12</sup>

In general, ischemia is caused by partial or absolute blockage of physiological blood flow through an organ, which results in relative deficiency of oxygen supply, leading to tissue injury. During subsequent reperfusion and blood flow restoration once the graft is reoxygenated is assumed to seriously aggravate ischemic injury.<sup>13, 14</sup> Diseases such as stroke, cardiac infarction and hemorrhagic shock as well as surgical interventions such as liver resections, coronary bypass surgeries and whole organ transplantations are the main processes in which IRI occurs.<sup>15</sup>

Moreover, the use of marginal grafts for transplantation, due to an insufficient supply of available organs for transplantation, renders them to be more susceptible to ischemia followed by reperfusion.<sup>1, 5</sup> Subsequently, that leads in a noteworthy amount to organ dys-function or even non-function of the grafts, thus aggravating organ shortage.

The liver belongs to the most frequently transplanted organs. In up to 10 % of early organ failure the IRI phenomenon is involved.<sup>5</sup> Hence, to achieve new insights in possible treatment strategies, a better understanding of the molecular pathophysiology is of great value.

### 1.2.2 Model differentiations

In general it has to be distinguished between two different clinical models of IRI.

During surgical liver interventions, when low blood flow stops or whole perfusion interruptions are unavoidable to prevent excessive bleeding (e.g. during liver resections), the warm ischemia/warm reperfusion (warm IR) event occurs. It is often referred to as the so-called Pringle's maneuver. Characteristically, the liver temperature is kept on the physiological body temperature during the whole process, i.e. 37 °C.

In contrast, in the cold ischemia/warm reperfusion (cold IR) model the temperature is reduced after harvesting the liver and kept at 4 °C during the transport of the organ to

the recipient. The ischemic storage period can last for up to several hours, while the graft is stored at 4 °C in different solution media (e.g. University of Wisconsin (UW), Euro-Collins, Ringer), which contain several ingredients to mimic physiological blood composition and exert beneficial activities on the injury outcome.<sup>3</sup>

The impact of model differences regarding the injury outcome and general cellular and molecular mechanisms are mentioned in detail in the next section.

### 1.2.3 General mechanisms

The exact molecular mechanisms that lead to hepatic IRI are complicated and the underlying biochemical pathways of this phenomenon remain unclear. So far, in literature two distinct injury pathways are discussed. First, the injury caused by the ischemic period, second, the damage induced by reperfusion of the liver graft (Figure 1).<sup>16</sup>

#### ISCHEMIA

The ischemic period due to tissue anoxia leads to disturbance of the mitochondrial respiration. Followed by the depletion of intracellular ATP and deterioration of energy dependent metabolic processes, which display the hallmark of ischemia.<sup>13</sup> Subsequently, anaerobic pathways are favored, which result in cellular acidosis and tissue damage.<sup>3, 16</sup> Moreover, the failure of active transmembrane transport of the mitochondria follows an imbalance of intracellular ion status, resulting in endothelial and Kupffer cell swelling followed by narrowing of the sinusoidal lumen.<sup>17, 18</sup> Low temperatures during cold ischemia have shown to attenuate ischemic tissue damage, as the metabolic rates are significantly reduced and important metabolic functions could be maintained for longer periods.<sup>3</sup> However, experimental evidence suggested that sinusoidal endothelial cells (SEC) are more susceptible when subjected to hypothermic ischemia.<sup>18, 19</sup> The release of several proteases cause SEC detachment from the underlying hepatocytes.<sup>3</sup> Thus, the UW solution, which is at present the preferred storage solution, is assumed to be effective in attenuating cold ischemic liver injury, due to its protease inhibitor content.<sup>3</sup> Despite, SEC suffer seriously from the hypothermic period and are more vulnerable following reperfusion.<sup>18</sup> In contrast, during the warm ischemic period, hepatocytes are discussed to be the preferential cell-type susceptible.<sup>19</sup>

The release of non-lysosomal proteases (e.g. calpains) might be the causative factor. Meanwhile, calpains demonstrated to be involved in both the warm and the cold ischemic period.<sup>20, 21</sup> Indeed, hepatocellular injury during the cold ischemic period is rather mild.<sup>22</sup>

## REPERFUSION

The second injury pathway manifests itself when the ischemic liver is reperfused. Paradoxically, restoring the blood supply is assumed to be the more prominent injury pathway of IR, which is characterized by an excessive inflammatory response. It is reported that this pathway consists of two phases, depending on the duration of reperfusion. The initial (acute phase) and the late phase (subacute phase).<sup>16, 23</sup> Indeed, both phases cannot be separated clearly as they merge seamlessly.

### INITIAL PHASE

Within the first 6 hours of reperfusion the resident liver macrophages, the Kupffer cells (KCs), are assumed to be mainly involved in the pathomechanism leading to an excessive inflammatory response.<sup>16, 24</sup>

The liver consists of several cell-types. Hepatocytes, also referred to as parenchymal cells, account for 65 % of all liver cells. Non-parenchymal cell-types are endothelial cells, hepatic stellate cells and Kupffer cells. Kupffer cells contribute to 15 % of the liver cells and represent the greatest amount of macrophages of any organ in the whole body. They reside in the hepatic sinusoids, the area of blood flow circulation, and constitute the first macrophage population of the body exposed to pathogens of gastrointestinal origin (bacteria, bacterial endotoxines and microbial debris). Therefore, they represent a main component of the innate immune system.<sup>24, 25</sup>

Their activation during the initial phase of IR causes the release of large amounts of reactive oxygen species (ROS; see section 1.2.4) and leads to the activation of the proinflammatory transcription factor NF- $\kappa$ B (see section 1.2.5), resulting in the excessive secretion of proinflammatory cytokines, in particular TNF- $\alpha$ , IL-1 and IFN- $\gamma$ .<sup>24, 25</sup> As described in the according sections, various pathways result in tissue injury following ROS release and NF- $\kappa$ B activation. Interestingly, cold ischemia implicates a

more dominant Kupffer cell activation following reperfusion compared to livers which underwent warm ischemia.<sup>15</sup>

Furthermore, the release of the platelet activating factor (PAF), which mainly derives from KCs, might play a crucial role already in the initial phase. It upregulates neutrophil recruitment, which is actually assumed to be the hallmark of the late phase of reperfusion.<sup>26</sup> However, their adherence to the activated Kupffer cells contributes to plugging of the sinusoidal vessels which results in microcirculatory failure.<sup>27</sup>

Moreover, CD4<sup>+</sup> T-lymphocytes are activated early after reperfusion resulting in the release of several acute phase proteins (e.g. IL-17, IFN- $\gamma$ ), which activate KCs and stimulate neutrophil recruitment as well.<sup>28</sup> Similar effects are proposed for the complement system, as inhibition of several complement factors (e.g. C1-INH, sCR1, C5aR) reversed these effects.<sup>29</sup>

#### LATE PHASE

The late phase starts approximately 6 hours postreperfusion and is characterized by the massive accumulation of neutrophils in the sinusoids.<sup>16</sup> Multiple processes are taking place, in which chemokines (e.g. CXC) are released by activated endothelial cells which induce the recruitment of neutrophils into the sinusoidal vessels. The expression of selectins (e.g. E-selectin) on the surface of endothelial cells enables interactions with their counterparts on neutrophils.<sup>27</sup> Moreover, intracellular adhesion molecules (e.g. ICAM-1) expressed on hepatocytes and on the endothelial cell-surface interact with integrins (e.g. Mac-1, LFA-1) on the surface of neutrophils, which leads to firm adhesion. Finally, adhered neutrophils transmigrate from the sinusoidal side into the hepatic parenchyma leading to hepatocyte degranulation and long-lasting oxidative stress, due to the release of proteases (e.g. elastase, cathepsin G) and ROS, respectively.<sup>30</sup> Beside its direct impact on hepatocellular injury, the adhesion and plugging of neutrophils and platelets within the sinusoidal vessels can obstruct the lumen, which leads to microcirculatory disturbances of the blood flow, aggravating parenchymal tissue injury even further.<sup>13</sup>

Moreover, several other factors shall accompany in neutrophil recruitment such as IL-17 release by CD4<sup>+</sup> T-lymphocytes and complement factors which function as chemoattractants and prime neutrophils for ROS formation.<sup>28, 29</sup>

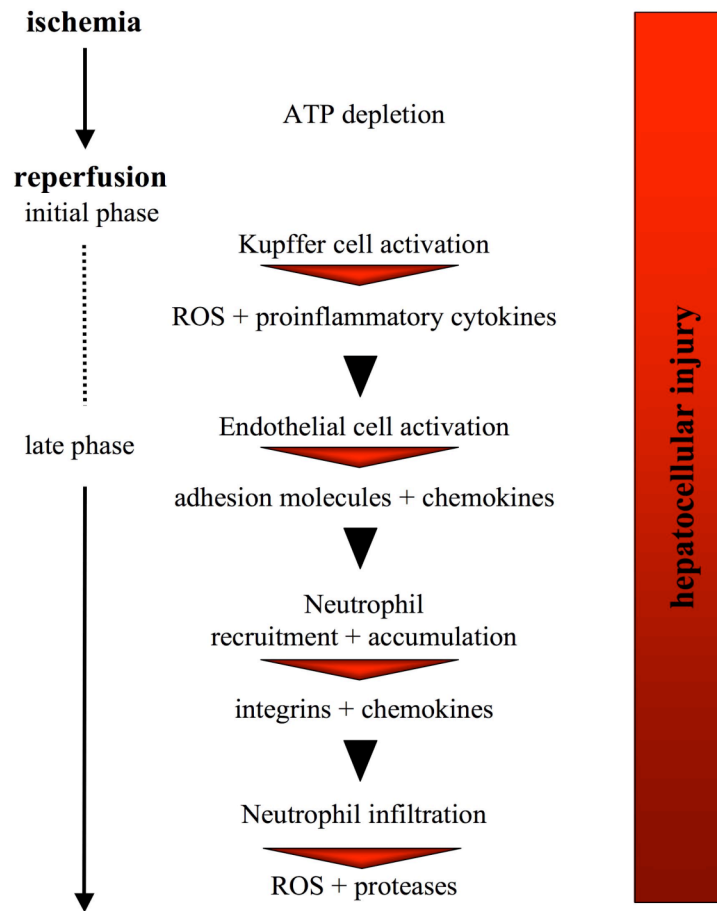


Figure 1 Putative mechanism of IRI in the liver.

### 1.2.4 Role of ROS

Reactive oxygen species (ROS) play a pivotal role in the hepatic IRI as they are released mainly during reintroduction of oxygen, thus early after reperfusion of the ischemic liver. Physiologically, ROS are either by-products generated of several processes (e.g. ATP generation, protein + lipid degradation) or second messengers controlling cell fates and inflammation.<sup>14</sup>

#### OXIDATIVE STRESS

A complex system of endogenous enzymatic (e.g. CAT, SOD, GPx) and non-enzymatic (e.g. GSH,  $\alpha$ -tocopherol, ascorbic acid) redox degrading antioxidants keep ROS on physiological harmless levels. During pathological situations such as IR, ROS levels exceed the endogenous capacities of removal, resulting in oxidative stress.<sup>2,31</sup>

ROS are generated in the liver during IR by different sources such as enzymes, organelles and specific cell-types, in particular phagocytes, which interdependently contribute to oxidative stress. The main intracellular sources are mitochondria, which predominantly generate ROS right after the onset of reperfusion within the respiratory chain. The xanthine-oxidase (XO), derived from conversion of xanthine-dehydrogenase during ischemia, is another intracellular source as well as activated NAD(P)H oxidases. Both enzymes generate ROS in several cell-types such as Kupffer cells, neutrophils, endothelial cells and hepatocytes. Eventually, the extracellular release of ROS by KCs is responsible for vascular oxidative stress in the sinusoid. Moreover, neutrophils contribute indirectly to oxidative stress after transmigration and adherence to the parenchyma. In conclusion, oxidative stress during IR evolves collectively from several pathways (Figure 2).<sup>14, 15, 32</sup>

However, it should be mentioned that superoxide anion radicals are also generated in low levels during the ischemic period in mitochondria within respiration, as total anoxia is unlikely, thus low molecular oxygen levels for radical formation still exist. Although its role in ischemia is not definitely clarified, beneficial effects for signaling pathways and cell adaptation are discussed.<sup>14</sup>

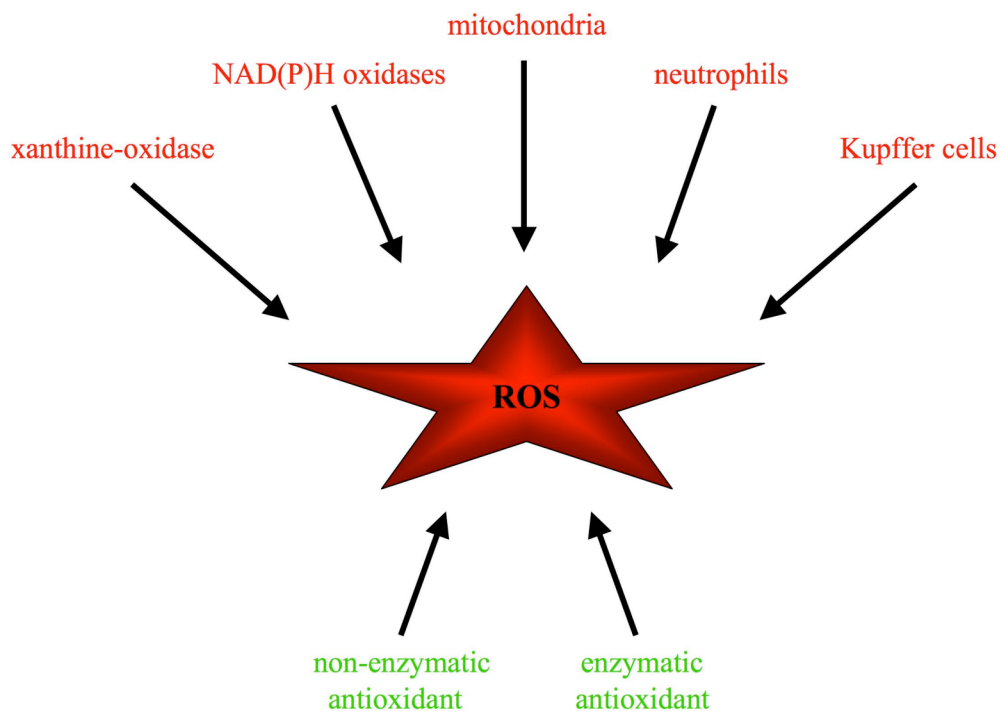


Figure 2 Sources of ROS generation (red) vs. endogenous antioxidants (green).

## DETRIMENTAL EFFECTS

Different pathways are leading to detrimental effects, as ROS affects the cellular system directly and indirectly (Figure 3). ROS react with important cellular components such as nucleic acids, polyunsaturated lipids and proteins. Membrane damage due to lipid peroxidation (LPO) is assumed to be a critical factor, as it is associated with loss of ion homeostasis followed by cell swelling. Moreover, mitochondria are particularly susceptible to oxidative damage, forming membrane permeability transition pores, which result in the breakdown of the membrane potential and in the release of substances such as cytochrome C, apoptosis-inducing factor and others. Subsequently the caspase cascade is activated which causes cell death. Furthermore, ROS are implicated in the activation of the platelet activating factor (PAF) and in the generation of proinflammatory cytokines, chemokines and adhesion molecules, primarily by activation of redox sensitive transcription factors, like NF- $\kappa$ B and AP-1.<sup>15, 33</sup> Ultimately, cellular damage and death of hepatocytes and endothelial cells are unescapable results.

However, postischemic ROS generation is also assumed to induce beneficial pathways such as upregulation of heme oxygenase-1 (HO-1) expression or indirect inhibition of ROS generating NAD(P)H oxidases.<sup>32</sup>

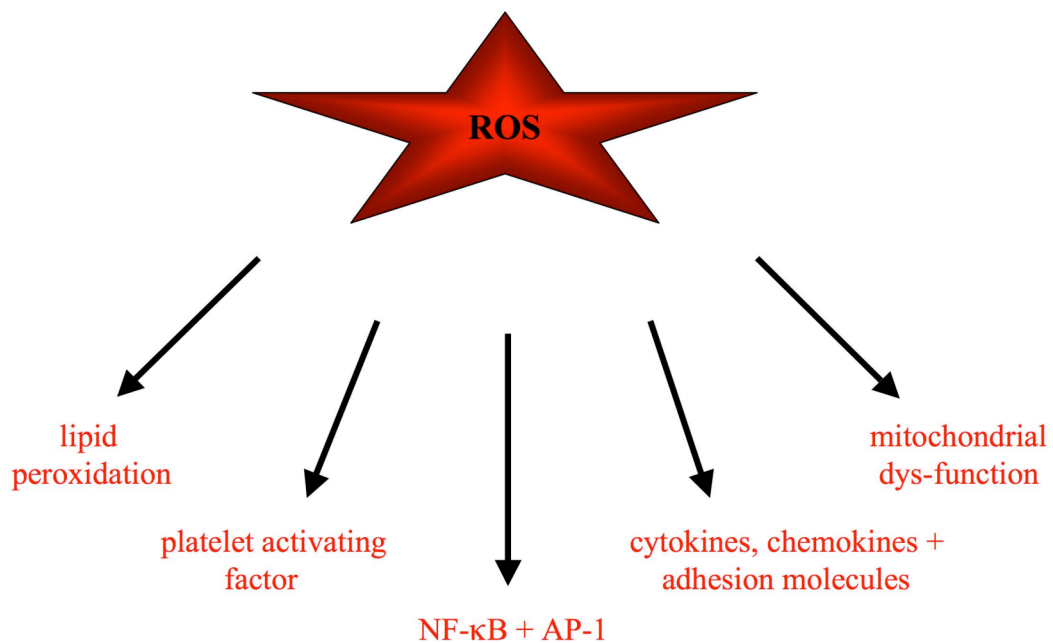


Figure 3 Reactive oxygen species (ROS) affect different pathways with detrimental outcome.

## NITRIC OXIDE

The major ROS, which are important in hepatic IRI include the superoxide radical ( $O_2^{\cdot-}$ ), hydroxyl radical (HO $\cdot$ ) and hydrogen peroxide ( $H_2O_2$ ). Additionally, some reactive nitrogen species (RNS) like nitric oxide (NO $\cdot$ ) and the strong oxidizing agent peroxynitrite ( $ONOO^-$ ) are crucial in the oxidative stress induced tissue injury.<sup>34</sup>

The enzyme family nitric oxide synthetases (NOS) generate NO by catalyzing the oxidation of L-arginine to L-citrulline (Figure 4). Its role for the aggravation of liver damage remains controversial, as low amounts of NO generated by the constitutively expressed isoform endothelial NOS (eNOS) have been assumed to be responsible for blood flow regulation, since it functions as potent vasodilator by activation of guanylate cyclase (GC).<sup>35</sup> In contrast, IR induces the generation of high NO amounts by the inducible NOS (iNOS), which react with superoxide anion ( $O_2^{\cdot-}$ ), followed by forming the high-potent reactive nitrogen species peroxynitrite. Hence, injury is primarily aggravated, by the predominance of the detrimental peroxynitrite and further on by general systemic effects due to high NO amounts leading to hypotension and shock.<sup>1</sup> Alternatively, Jaeschke et al. proposed that ROS contribute to microcirculatory failure, as the withdrawal of NO for peroxynitrite generation induced a shortage of vasodilators.<sup>32</sup> However, selective iNOS inhibition was reported several times to have beneficial effects in IRI.<sup>36-38</sup> In contrast, selective eNOS inhibition or eNOS gene knockout mice reduce microvascular perfusion, hence, worsening of tissue injury.<sup>39,40</sup>

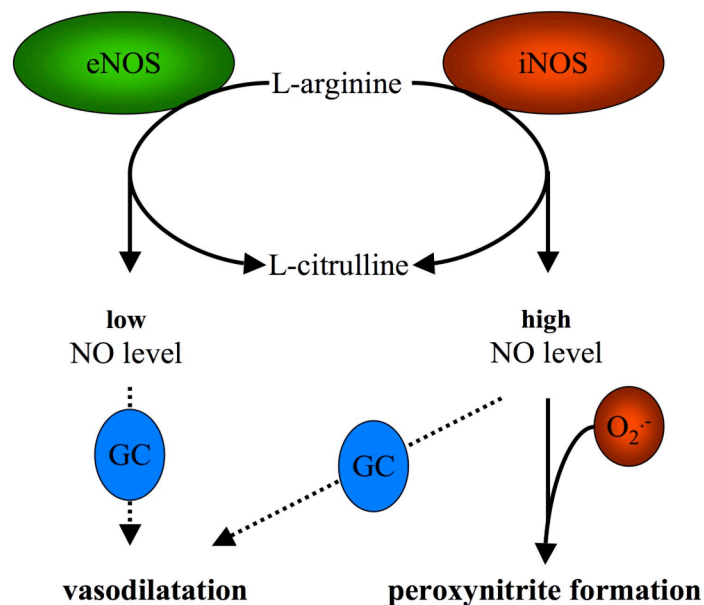


Figure 4 NO generation by eNOS and iNOS.

In that context endothelin-1 (ET-1), a potential vasoconstrictor released during the reperfusion period, also affects microcirculation of the liver tissue.<sup>17</sup> Interestingly, hepatic microcirculation has shown to correlate inversely with ET-1 levels, suggesting that microcirculatory failure is, at least in part, mediated by ET-1.<sup>41</sup> Moreover, an upregulation of the endothelin B receptor during reperfusion contributes to elevated sensitivity for endothelins, thus, receptor antagonists have shown to diminish IRI.<sup>1</sup>

#### ANTIOXIDANT THERAPY

The balance between detrimental and beneficial effects of ROS has to be kept in mind when oxidative stress driven diseases are treated therapeutically with antioxidants.

However, in the literature it has been shown by several studies that the treatment with antioxidants (e.g. NAC,  $\alpha$ -tocopherol, ascorbic acid, SOD, GSH) as well as graft storage in solutions containing potent antioxidants attenuate hepatic IRI, hence, increase graft survival (see section 1.2.6). Moreover, gene therapy using viral and non-viral vectors containing genes of endogenous antioxidants are currently under intensive research and offer a promising tool, as conventional delivery of endogenous enzymes are disadvantageous due to short half-lives and bad cellular uptake.<sup>2, 42</sup> However, the pro-oxidant activities of antioxidants under certain conditions should be taken into account as well, when their huge protective potential is emphasized.<sup>43</sup>

#### 1.2.5 Role of NF- $\kappa$ B

The nuclear factor  $\kappa$ -B (NF- $\kappa$ B) is a redox-sensitive transcription factor, which plays a crucial role in hepatic IRI. Beside others, the release of ROS during reperfusion in huge amounts activates NF- $\kappa$ B. Hence, antioxidant and radical scavenging approaches like administration of the well-known antioxidant NAC<sup>44</sup>, green tea extract<sup>45</sup> or the delivery of antioxidant enzyme genes (SOD, CAT) by nanoparticles<sup>42</sup> inhibited NF- $\kappa$ B activation and improved injury outcome markedly.

Physiologically, NF- $\kappa$ B dependent genes play a central role in the regulation of the innate and adaptive immune response, lymphocyte function and cell survival. Studies indicate that NF- $\kappa$ B transcribed proteins are involved in T-cell proliferation and B-cell generation and proliferation.<sup>46</sup> Moreover, the involvement of NF- $\kappa$ B in several

pathological conditions, like atherosclerosis<sup>47</sup>, asthma<sup>48</sup>, tumorigenesis<sup>49</sup>, heart diseases<sup>50</sup> and others could be demonstrated.

#### NF- $\kappa$ B ACTIVATION PATHWAY

Intriguingly, several signal transduction pathways of different inducing mechanisms do converge in the single transcription factor NF- $\kappa$ B. Hence, NF- $\kappa$ B displays pleiotropic effects during inflammation, immune response, cell survival and proliferation.<sup>51</sup> Five different members can form a variety of homo- or heterodimers. p50, p52, p65/RelA, p68/RelB and p75/c-Rel are described to that point, whereas the p50/p65 heterodimer is the predominant form mediating NF- $\kappa$ B signaling. Usually NF- $\kappa$ B is non-covalently bound to its inhibitory proteins I $\kappa$ Bs and retained in an inactive form in the cytoplasm, therefore preventing the translocation to the nucleus followed by gene transcription (Figure 5).

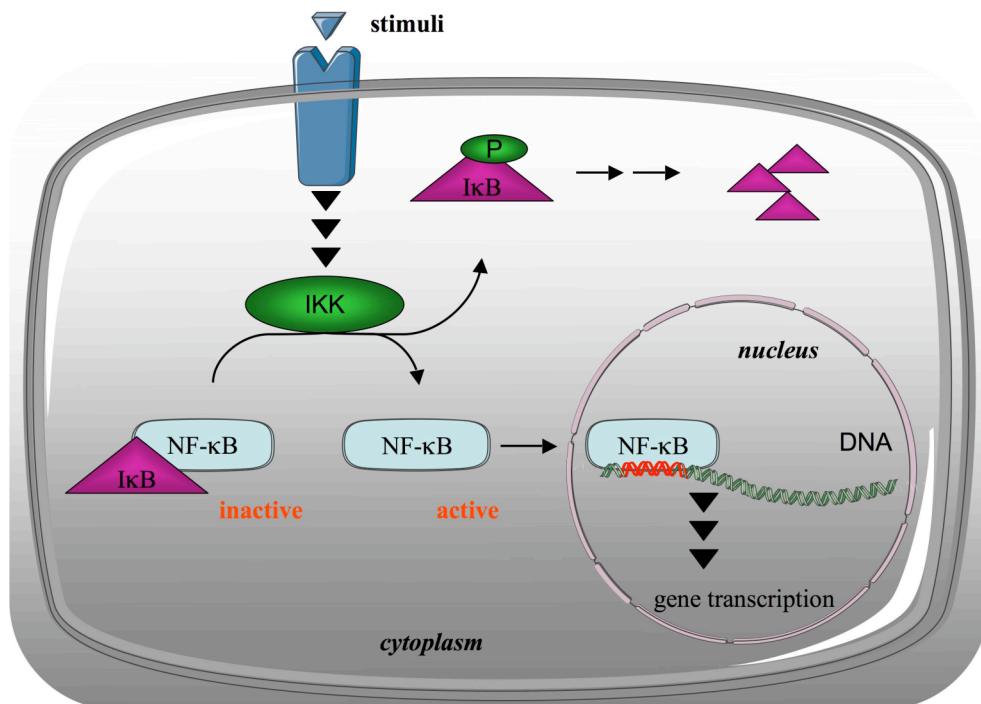


Figure 5 NF- $\kappa$ B activation pathway.

Certain stimuli, such as cytokines, viral and bacterial pathogens, and stress-inducing agents, stimulate phosphorylation of I $\kappa$ B via the I $\kappa$ B kinase (IKK). IKK is a kinase-complex containing three tightly associated IKK polypeptides: Two catalytic subunits

(IKK $\alpha$  and IKK $\beta$ ) and one regulatory subunit, the NF- $\kappa$ B essential modulator (NEMO), also referred to as IKK $\gamma$ . Additionally, an alternative way of NF- $\kappa$ B activation is proposed which does not require IKK mediated phosphorylation. Indeed, both mechanisms result in I $\kappa$ B phosphorylation and lead to the ubiquitination and degradation of I $\kappa$ B by the 26S-proteasome.

Subsequently, NF- $\kappa$ B translocates to the nucleus where it binds to its cognate DNA-binding site (5'-GGGZXXYYCC-3'; Z is purine, Y is pyrimidine, and X is any base) within the promoter region of specific genes, where it exerts its transcriptional activity. The targets for transcriptional activation of NF- $\kappa$ B include the genes of cytokines, chemokines, adhesion molecules, stress response, growth factors and antiapoptotic regulators.<sup>22, 52, 53</sup>

#### ESSENTIAL ROLE OF NF- $\kappa$ B

Several studies attempted to inhibit NF- $\kappa$ B activation systematically and observed its indispensable function. Mice lacking p50, p52 or c-Rel show defective immune functions, thus confirming its essential function in the immune system.<sup>46</sup> Moreover, p65 knockout mice are not viable due to strong hepatocyte apoptosis.<sup>54</sup> The treatment of mice with an adenoviral vector overexpressing a mutated form of I $\kappa$ B $\alpha$  (Ad5I $\kappa$ B), which is almost exclusively expressed in the liver, increased the susceptibility to inflammation *in vivo* and resulted in massive apoptosis of hepatocytes.<sup>55, 56</sup> Transgenic mice containing a genetically modified, degradation-resistant I $\kappa$ B $\alpha$  transgene confirmed these results.<sup>57</sup> Moreover, several approaches targeting subunits of the I $\kappa$ B kinase (IKK) complex by generation of constitutive knockout animals emphasized its essential role.<sup>58</sup> Eventually, it seems to be inadvisable to inhibit NF- $\kappa$ B in general.

#### DUAL ROLE OF NF- $\kappa$ B IN THE LIVER

The liver has a unique regenerative ability thanks to certain stimuli like inflammation, IRI, or liver resection. For example after partial hepatectomy of up to 70 %, hepatocytes proliferate and regenerate till the original liver mass is restored.

NF- $\kappa$ B activation shows to be essential for hepatocyte proliferation as it induces antiapoptotic and proliferative protein expression.<sup>59</sup> Recently, it was reported that the level of NF- $\kappa$ B activation in hepatocytes of IR treated livers showed a positive

correlation with protection.<sup>60</sup> Whereas, NF- $\kappa$ B activation in Kupffer cells initially induces the excessive release of proinflammatory cytokines, which is assumed to account predominately for tissue injury.<sup>24</sup> Moreover, NF- $\kappa$ B in endothelial cells is responsible for upregulation of adhesion molecules and chemokines, contributing to neutrophil accumulation and adherence.<sup>22</sup> Therefore it is apparent that NF- $\kappa$ B has a dual role in the liver depending on the cell-type addressed (Figure 6).

Generally, KC depletion is assumed to be the easiest method to inhibit NF- $\kappa$ B selectively in KCs. It has been shown that depletion with gadolinium chloride attenuated warm IRI.<sup>61</sup> However, as mentioned above, KCs are indispensable for immune function, and they are necessary regulators for liver regeneration. For example, after liver resection KCs release the NF- $\kappa$ B driven cytokines TNF- $\alpha$  and IL-6, which stimulate hepatocyte regeneration and induce restoration of organ mass.<sup>62</sup> Abshagen et al. recently demonstrated that regeneration after partial hepatectomy is strongly diminished when KCs were depleted,<sup>63</sup> and these results were confirmed by others as well.<sup>64, 65</sup>

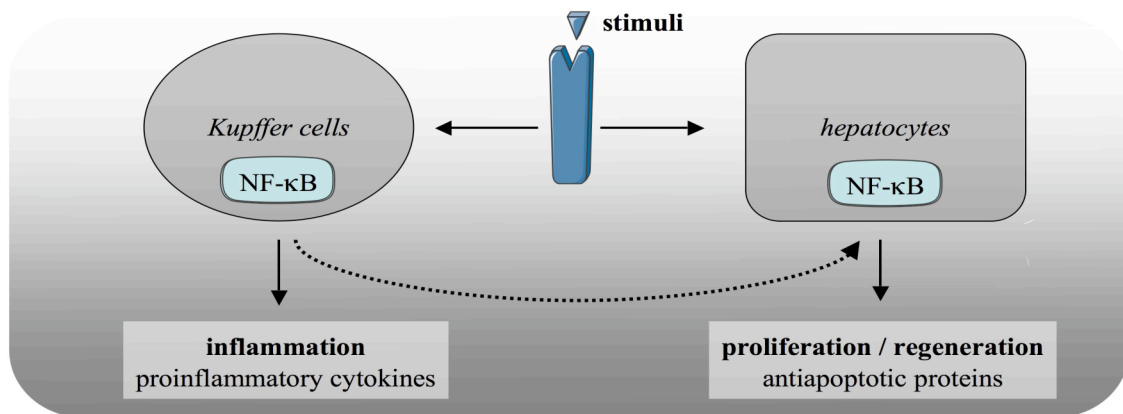


Figure 6 Dual role of NF- $\kappa$ B activation depending on the cell-type addressed.

In conclusion, the cell-type specific role of NF- $\kappa$ B and its essential function for liver regeneration have to be kept in mind when the NF- $\kappa$ B pathway is chosen to be influenced for therapeutic purposes.

For more detailed information the reader is kindly referred to the Ph.D. thesis of Dr. Florian Hoffmann, as it would exceed the main interest of this thesis.

### 1.2.6 Interventions

To counteract the burden and to reduce the adverse effects of hepatic IR, various strategies aimed at the different pathophysiological processes of IRI have been considered. These include both pharmacological approaches and physical interventions.

#### PHARMACOLOGICAL APPROACHES

Several antioxidants (e.g. NAC, GSH,  $\alpha$ -tocopherol) and direct radical scavengers (e.g. SOD, CAT), as already mentioned above, demonstrate huge potential in different models of hepatic IRI. High dosages of allopurinol demonstrated to have antioxidant potential in hepatic IR, as it inhibits the enzyme xanthine-oxidase which participates in ROS generation.<sup>2</sup>  $\alpha$ -Lipoic acid, a well described antioxidant, has shown to regulate several signal-transduction pathways resulting in tissue protection. Selective iNOS inhibitors have proved tissue protection during hepatic IR,<sup>36, 38</sup> as iNOS upregulation goes along with excessive NO production, which is linked to the formation of peroxynitrite and to its systematic impact on vasodilatation (see section 1.2.4). The pretreatment of livers suffering warm or cold ischemia followed by reperfusion, with the hormone atrial natriuretic peptide (ANP) reduced tissue damage and increased liver function, due to direct impact on several mediators of IR (NF- $\kappa$ B, AP-1, ROS, TNF- $\alpha$  and HSP 70).<sup>66, 67</sup>

However, none of the above mentioned pharmacological approaches have yet found access to clinical usage, apart from organ storage solutions. These display a mixture of several constituents, which provoke in combination beneficial effects. First developed in the late 1980s and now the most commonly used in clinical practice, is the University of Wisconsin (UW) solution. The protease inhibitor lactobionate and the endogenous antioxidant glutathione were identified to have a main impact. Lactobionate has shown to reduce hypothermic cell swelling during the cold ischemic period, and strong antioxidant capacity has been demonstrated for glutathione.<sup>3</sup>

#### PHYSICAL INTERVENTIONS

The term ischemic pre-conditioning (IPC) describes the process when organs are exposed to repetitive brief intervals of vascular occlusion prior to sustained IR. Murry and coworkers described this process first for the myocardium and characterized it as an

adaption of the myocardium to ischemic stress.<sup>68</sup> Meanwhile, this strategy was successfully applied to several organs and is used clinically as it reduces tissue injury and prolongs graft survival after IRI effectively. The underlying mechanism is very complex and not yet fully elucidated. Many factors seem to be implicated like adenosine, nitric oxide, oxidative stress, protein kinase C, mitogen-activated protein kinases, heat shock proteins and NF- $\kappa$ B activation.<sup>4</sup> Interestingly, NF- $\kappa$ B activation was associated with upregulated levels of cyclin D1, a crucial regulator of cell cycle progression, which is assumed to account specifically for hepatic recovery.<sup>22</sup> All these factors are assumed to participate in the strengthening of the liver graft resistance due to IPC.

In that context, remote ischemic pre-conditioning (RIPC) is another strategy, which is currently under intensive research. Brief intervals of IR to an other organ distant to the organ which undergoes sustained IR, results in increased tolerance and tissue protection.<sup>12</sup>

Heat pre-conditioning is a process in which the transplanted organ or the whole body is exposed to hyperthermia for a short interval before sustained IR, which results in increased graft survival.<sup>69</sup> Heat shock proteins (HSPs) are assumed to be mainly involved, in particular HSP 70, which is closely related to stress-tolerance.

Despite several promising interventions, there is no appropriate tool available to prevent hepatic IRI at present.

### **1.2.7 Approaches of this study**

Following substances have been investigated in IRI and are discussed as listed below:

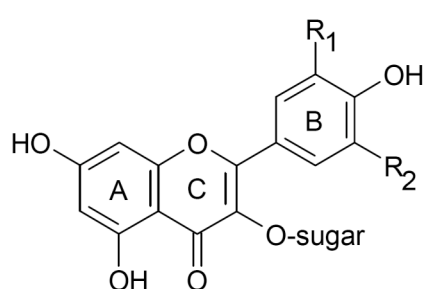
- a. EGb 761, kindly provided by Dr. W. Schwabe Pharmaceuticals (section 1.3).
- b. Xanthohumol and 3-Hydroxyxanthohumol, synthesized by Susanne Vogel of the University of Regensburg (section 1.4).
- c. NF- $\kappa$ B decoy nanoparticles, provided by Sebastian Fuchs of the Department of Technology (section 1.5).

## 1.3 GINKGO BILOBA EXTRACT – EGB 761

### 1.3.1 General aspects

Extracts from the dried leaves of the Ginkgo biloba trees are being used for decades in traditional Chinese medicine. EGb 761 is a standardized extract of the Ginkgo biloba leaves (Maidenhair tree) kindly provided by Dr. Willmar Schwabe Pharmaceuticals and commercially available under the trade name Tebonin® in different pharmaceutical intake-forms. It has been used effectively in the treatment of several pathological disorders related to oxidative stress. The German Kommission E has approved its usage for symptomatic treatment of cerebral disorders/dementia, peripheral arterial insufficiency, vertigo and tinnitus (Bundesanzeiger Nr. 133, 19.7.1994).

EGb 761 is extracted with a mixture of water/acetone giving a final ratio of 35-67:1 (plant : extract). Its essential compounds are 24 % flavonoids (Figure 7), which are nearly exclusively flavonol-O-glycosides, 7 % proanthocyanidins and 6 % terpene trilactones, which are divided in different subgroups.<sup>6</sup> First, the diterpenoid ginkgolides (3.2 %; Figure 8) and second the sesquiterpenoid bilobalides (2.9 %; Figure 9). Ginkgolic acids are downgraded to less than 5 ppm, since they are responsible for undesirable allergic effects.<sup>70</sup>



flavonoid structure	R <sub>1</sub>	R <sub>2</sub>
Kaempherol	H	H
Quercetin	OH	H
Myricetin	OH	OH
Isorhamnetin	OCH <sub>3</sub>	H

Figure 7

Chemical structure of flavonoid glykosides (24 %) in EGb 761.

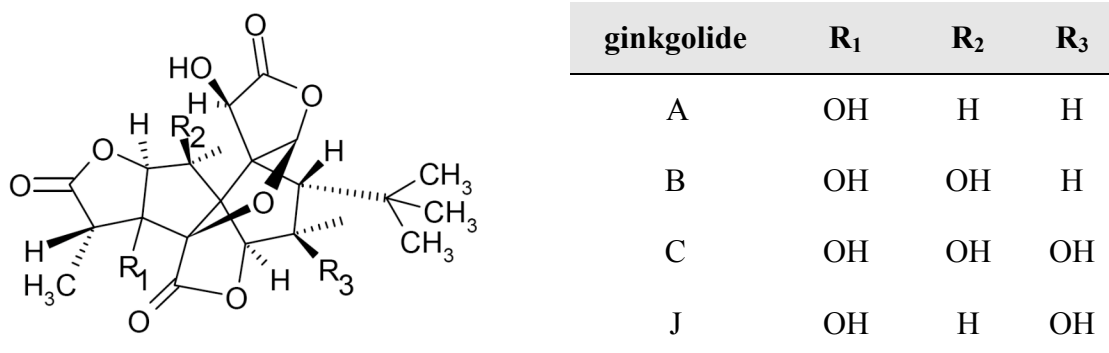


Figure 8 Chemical structure of ginkgolides A, B, C and J (approx. 3.2 %) in EGb 761.

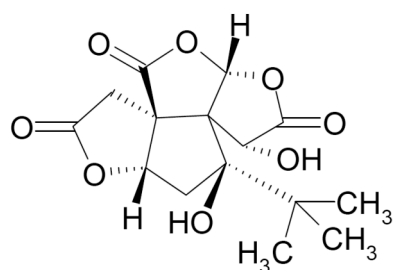


Figure 9 Chemical structure of bilobalides (2.9 %) in EGb 761.

### 1.3.2 Molecular activities

The molecular mechanism and therapeutic benefit of the complex Ginkgo biloba extract, EGb 761, is versatile, since its effects can evolve from additive, synergistic as well as antagonistic properties of the different constituents. In consideration of the complex injury pathway of hepatic IR, EGb 761 has several promising properties, which could be of great value for the IR injury process.

#### REDOX SYSTEM

EGb 761 is a polyvalent agent capable of scavenging free radicals like superoxide radical, hydrogen peroxide, hydroxyl radical and nitric oxide. Their antioxidant activities are mainly referred to its high flavonoid glycoside content.<sup>71</sup> Structure activity relationship (SAR) studies of flavonoids (Figure 7) have shown that the catechol group in the B-ring, the 2, 3-double bond conjugated with the 4-oxo function and the 3- (and

5-) hydroxyl group enable them to chelate metal ions and to scavenge directly ROS.<sup>6, 72, 73</sup> Contrary perspectives are given for the proanthocyanidines. On the one hand, they account for the antioxidant activities as direct radical scavengers, on the other hand, they are assumed to bind and inactivate antioxidant enzymes such as catalase and glutathione peroxidase.<sup>74, 75</sup> Several studies demonstrate reduced lipid peroxidation after subjection to IR when treated with EGb 761 before.<sup>76</sup> Interestingly, the activities of the endogenous enzymatic (SOD, GPx) and non-enzymatic (GSH) antioxidants were shown to be upregulated by EGb 761 treatment in different models. Additionally, the induction of mitochondrial SOD expression and heme oxygenase-1 (HO-1), as seen in microarray analysis, further supports this relationship.<sup>6, 76, 77</sup>

#### MICROCIRCULATION

The ginkgolides (A, B and C) have shown to inhibit platelet activation and aggregation, as they are potential PAF-receptor antagonists,<sup>6, 78</sup> thus influencing blood rheological properties and circulation positively. Interestingly, on oxidative stress induced aggregation ginkgolides had no impact, although the whole extract (EGb 761) inhibited platelet aggregation. That confirms that ginkgolides exert their activities without major impact on oxidative stress.<sup>79, 80</sup> Recently, Zhang et al. show that EGb 761 treatment in chronic liver injury improves hepatic microcirculatory and prevents sinusoidal endothelial cell damage.<sup>41</sup> Interestingly, the amount of ET-1, a potent vasoconstrictor, was significantly reduced, suggesting that ET-1 inhibition via EGb 761 is, at least in part, responsible for the improvement of microcirculation. Myeloperoxidase (MPO), an indicator of neutrophil accumulation, was reduced after EGb 761 treatment in different IR models. Moreover, sinusoidal microcirculation was significantly improved by EGb 761 pre-treatment prior to hepatic warm IR, which goes along with reduced leukocyte adherence in postsinusoidal venules.<sup>81</sup>

#### MITOCHONDRIAL FUNCTION

It is well-known that impairment of mitochondrial function occurs mainly during the ischemic period and results in ATP depletion (see section 1.2.3). Moreover, mitochondria are very susceptible to radicals, hence, the potential of EGb 761 to scavenge radicals protects the mitochondria indirectly.

Bilobalides are considered to be crucial for neuroprotection and have shown to be responsible for the reduction of cerebral damage after ischemia, as they improve cerebral energy metabolism by stabilizing mitochondria. Interestingly, increasing evidence emerges, that EGb 761 and in particular the bilobalides exert protective effects on the mitochondrial respiratory chain. Janssens and colleagues revealed that the respiratory chain activity is kept on high levels during ischemia when treated with bilobalides, thus preserving the ATP pool and limiting tissue damage induced by ischemia.<sup>82, 83</sup>

#### NF- $\kappa$ B SIGNALING

As mentioned above, the transcription factor NF- $\kappa$ B is crucial in hepatic IR. Since NF- $\kappa$ B is redox regulated, it was proposed that its inhibition in myocardial IR with EGb 761 is mainly due to ROS reduction.<sup>84</sup> Moreover, the inhibition of iNOS activation by EGb 761, as seen in different inflammatory models (LPS; LPS/IFN- $\gamma$ ) and in myocardial IR, respectively, was linked to the blockage of NF- $\kappa$ B activation.<sup>85-87</sup> In addition, attenuated TNF- $\alpha$  levels after Ginkgo biloba extract treatment confirm the impact on NF- $\kappa$ B, as this cytokine is NF- $\kappa$ B regulated.<sup>86</sup>

### 1.3.3 Experimental outline

This project aimed to elucidate the impact of the Ginkgo biloba extract, EGb 761, on the complex hepatic IR model. Therefore, following aspects were mainly considered:

- Effect on hepatic tissue injury.
- Impact on acute arterial blood pressure.
- Evaluation of eNOS expression *in vivo*.

## 1.4 XANTHOHUMOL AND 3-HYDROXYXANTHOHUMOL

### 1.4.1 General aspects

The principal prenylated flavonoid of the hop plant, *Humulus lupulus L.*, is Xanthohumol (XN), which constitutes approximately 82-89 % of the total amount of prenylated flavonoids of different hop varieties.<sup>88</sup> Xanthohumol (Figure 10) is characterized by an open C-ring flavonoid structure, a so-called chalcone. Chalcones are one of six major subgroups of flavonoids that are found in most higher plants. In plants, flavonoids are bio-synthesized through the phenylpropanoid pathway leading after the first committed step to chalcones.<sup>89</sup>

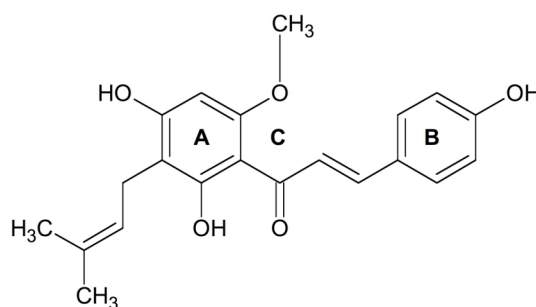


Figure 10 Chemical structure of Xanthohumol (XN).

Hop preparations are well-known in medicine for treatment of sleeping disorders as tranquilizer or for the activation of gastric function as bitter stomachic.<sup>90</sup> The German Commission E approved hops for the treatment of mood disturbances, such as restlessness and anxiety as well as sleep disturbances (Bundesanzeiger Nr. 50, 13.3.1990). In recent years, hop has attracted considerable interest since its constituent Xanthohumol was identified as broad-spectrum anti-cancer and chemopreventive compound.<sup>91</sup>

Beer is one of the most commonly consumed alcoholic beverages, and hop is added for bitterness and the typical flavor. Hence, beer is the primary dietary source of XN. Nevertheless, the concentration of XN in beer is very low (approx. 0.1 mg/l) due to thermal conversion to isoxanthohumol during the brewing process.<sup>92</sup> Moreover, orally administration revealed that XN is not detectable in plasma,<sup>93</sup> thus its impact as nutrient

constituent might be restricted due to its poor bioavailability and its low nutritional content.

Metabolic studies on human liver microsomes and feeding experiments have recently shown that Xanthohumol is subjected to strong biotransformation,<sup>11, 94, 95</sup> which leads, among others, to 3-Hydroxyxanthohumol (OH-XN; Figure 11). OH-XN emerges from B-ring oxidation of XN giving a hydroxyl substituent in ortho position, which is a so-called ortho-diphenoxyl functionality.

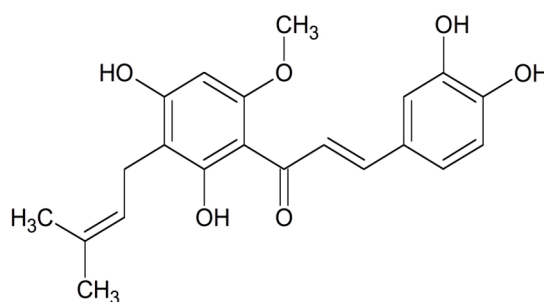


Figure 11 Chemical structure of 3-Hydroxyxanthohumol (OH-XN)

#### 1.4.2 Molecular activities

In recent years, the flavonoids Xanthohumol and 3-Hydroxyxanthohumol have shown promising properties primarily in *in vitro* experiments, which could be of interest for complex injury processes such as the hepatic IRI.

#### ANTIOXIDANT PROPERTIES

In general, it was assumed that the typical structure of flavonoids accounts for their antioxidant activities as they are able to scavenge ROS directly or to chelate metal ions, hence, preventing ROS formation as well (see section 1.3.2 Redox system).<sup>8, 96</sup> Beside, there is recent evidence that polyphenolics exert an indirect antioxidant effect as they induce endogenous antioxidant enzymes (e.g. SOD, CAT, GPx).<sup>97, 98</sup> Paradoxically, since antioxidants exert pro-oxidant activities in certain conditions, the indirect antioxidant effects of polyphenolics might be due to these contrary properties.<sup>97</sup>



polyphenolic flavonoid with strong antioxidant potential,<sup>114</sup> which has shown to inhibit NF- $\kappa$ B activation in a model of cold IR subjected to IPC.<sup>115, 116</sup>

Recently, different cancer cell models demonstrate that NF- $\kappa$ B activation was inhibited by XN.<sup>117, 118</sup> Interestingly, Albini et al. revealed that NF- $\kappa$ B inhibition was associated with markedly decreased I $\kappa$ B $\alpha$  phosphorylation and repressed Akt protein levels, which is an important upstream activator of the NF- $\kappa$ B pathway.<sup>88</sup>

These results raise the question if XN and OH-XN exert beneficial effects on oxidative stress driven diseases as they act simply as antioxidants or possibly through interaction with the NF- $\kappa$ B signal transduction pathway.

#### **1.4.3 Experimental outline**

This study elucidated the impact of the dietary flavonoid XN and its metabolic derivative OH-XN on a complex oxidative stress driven model, the hepatic IRI. For this purpose key-aspects were investigated as follows:

- Antioxidant potential *in vitro* and in the liver challenged to IR.
- Influence on NF- $\kappa$ B activation in a reportergene assay and in hepatic IR.
- Impact on pro- and antiapoptotic parameters.
- Consequence on hepatic tissue injury.

## 1.5 NF- $\kappa$ B DECOY NANOPARTICLES

### 1.5.1 Background

Interestingly, NF- $\kappa$ B in the liver has been assumed to have an ambiguous role depending on the cell-type addressed (see section 1.2.5). NF- $\kappa$ B activation in hepatocytes is reported to be essential for hepatocyte regeneration and proliferation i.e. cellular protection, since several antiapoptotic proteins like Bcl-2 and Bcl-xl are upregulated.<sup>119, 120</sup> In contrast, the activation of Kupffer cells during IR causes an increase in the expression of proinflammatory cytokines leading to inflammation and liver failure.<sup>3, 24</sup> However, the role of NF- $\kappa$ B in Kupffer cells is more complicated as they also trigger the regeneration of hepatocytes indirectly due to the release of TNF- $\alpha$  and IL-6.<sup>62</sup> Therefore, selective and transient NF- $\kappa$ B inhibition in Kupffer cells is a more promising approach than persistent NF- $\kappa$ B inhibition.<sup>60, 120</sup> That is confirmed by several studies, as unspecific NF- $\kappa$ B inhibition in the liver and general depletion of the Kupffer cells, respectively, affects negatively hepatocyte regeneration and proliferation following hepatic IR and impairs the physiological functions of Kupffer cells.<sup>54-56, 63-65</sup>

### 1.5.2 Targeting Kupffer cells

The challenge is to find an appropriate carrier, which enables exclusive transport to the liver resident macrophages, the Kupffer cells.

Liposomes were used as a promising approach as different substances can be encapsulated or bound to their surface and are taken up by Kupffer cells,<sup>121, 122</sup> but they are highly unselective as they tend to fuse with several cell-types.<sup>123</sup> Moreover, other carriers have shown insufficient selectivity as they are transported to endothelial cells as well or as they also result in a high inflammatory response, e.g. when adenoviral gene transfer is used.<sup>124-126</sup>

Dr. Florian Hoffmann described in his recent Ph.D. thesis for the first time a Kupffer cell specific carrier based on gelatin NP, which enables exclusive delivery of NF- $\kappa$ B decoy oligodeoxynucleotides to KCs without affecting NF- $\kappa$ B in hepatocytes or other cell-types, NF- $\kappa$ B decoy-NP.

NF- $\kappa$ B decoy-NP consist of positively charged gelatin NP, which interact ionically with negatively charged double-stranded oligonucleotides (ODN), encoding for the consensus sequence of the NF- $\kappa$ B promoter region (Figure 12).

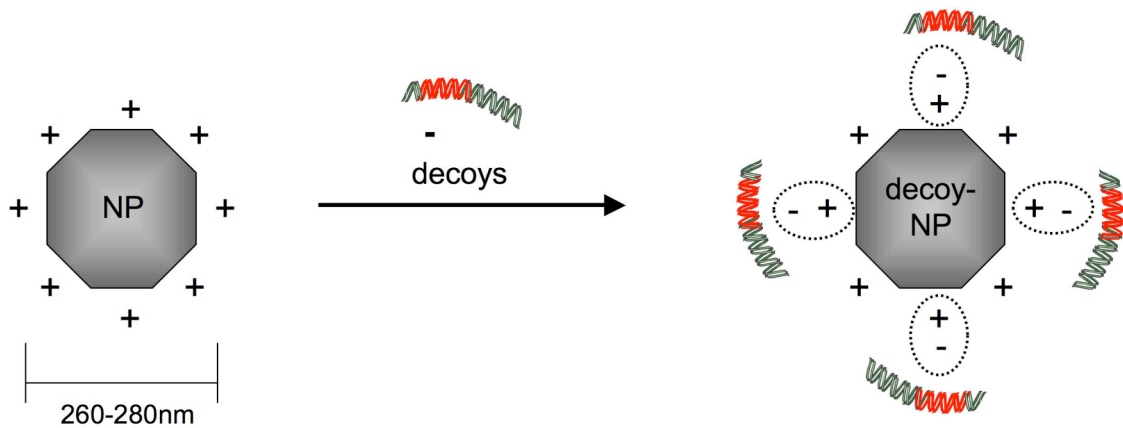


Figure 12 Ionic interactions between negatively charged decoys and positively charged NP results in decoy-NP.

Hence, the transcription factor NF- $\kappa$ B is selectively bound by NF- $\kappa$ B ODNs, which prevents binding to genomic DNA and impedes gene transcription (Figure 13). Gelatin NP are a selective carrier to deliver ODNs sufficiently to Kupffer cells when administered *in vivo* direct in the portal vein, as shown previously in Dr. Hoffmann's Ph.D. thesis. The specific size of gelatin NP (260-280 nm) and their stable, unflexible structure, hinders the penetration of the endothelial window (approx. 175 nm). Hence, the endothelial cell cover cannot be crossed. Moreover, the solid nanoparticles require a phagocytotic absorption, which prefers uptake by macrophages, thus, avoiding interaction with hepatocytes. Furthermore, gelatin is a biodegradable material, which limits the excessive inflammatory response as seen for adenoviral vectors and liposomes.<sup>126, 127</sup>

For more detailed information of gelatin nanoparticles, oligonucleotides and KC targeting the reader is kindly referred to the Ph.D. thesis of Dr. Florian Hoffmann and of Dr. Jan Zilies, as it would exceed the main interest of this thesis.

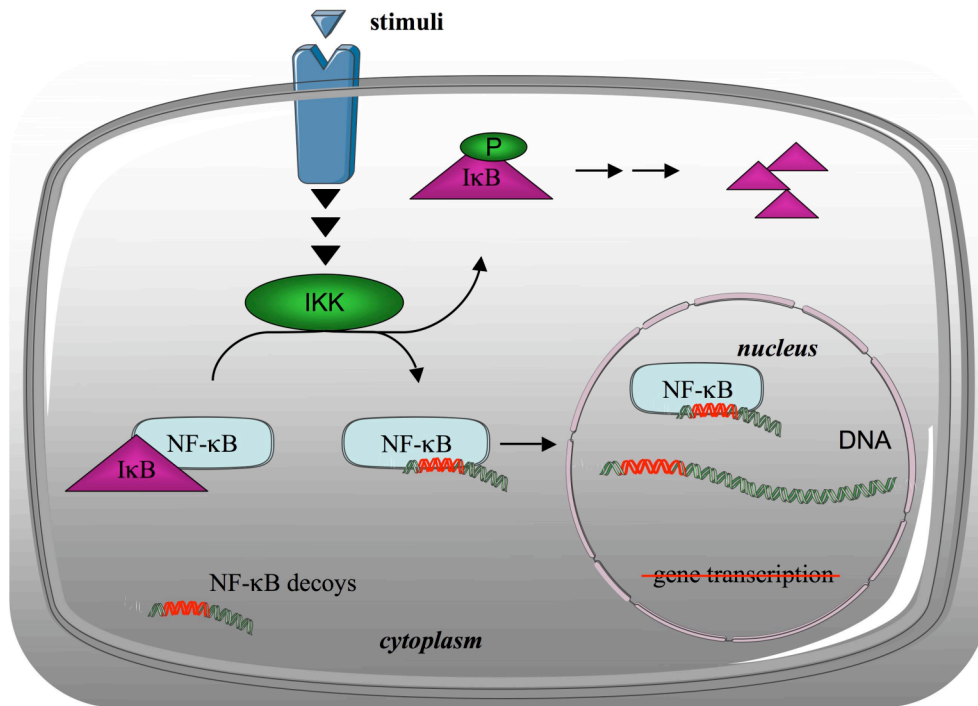


Figure 13 NF-κB oligonucleotide decoys interact with NF-κB avoiding gene transcription.

### 1.5.3 Experimental outline

The aim of this project was to specify the role of NF-κB in Kupffer cells. For this purpose, NF-κB decoy-NP were applied in the *ex vivo* model of hepatic cold IR. In order to clarify this intention, different aspects were considered as follows:

- Verification of exclusive delivery to Kupffer cells *ex vivo*.
- Impact on NF-κB activation induced by cold IR.
- Role of Kupffer cell derived NF-κB on the hepatic injury.

# **MATERIALS AND METHODS**

## 2.1 MATERIALS

### 2.1.1 Ginkgo biloba extract – EGb 761

#### 2.1.1.1 SOLUTIONS AND REAGENTS

Table 1 Phosphate buffered saline.

Phosphate buffered saline (PBS; pH 7.4)	
NaCl	123.2 mM
KH <sub>2</sub> PO <sub>4</sub>	3.16 mM
Na <sub>2</sub> HPO <sub>4</sub>	10.4 mM
H <sub>2</sub> O	

#### 2.1.1.2 GENERAL ASPECTS

EGb 761 is a well-defined, standardized preparation of the dried Ginkgo biloba leaves and was kindly provided by Dr. Willmar Schwabe Pharmaceuticals. The composition, therapeutic uses and molecular functions are described in section 1.3. The chemical structures of the main constituents of EGb 761 are displayed in the same section. For experiments, EGb 761 was freshly dissolved in PBS in different concentrations varying from 0.05 to 5 mg/ml extract.

### 2.1.2 Xanthohumol and 3-Hydroxyxanthohumol

#### 2.1.2.1 SOLUTIONS AND REAGENTS

Table 2 Solvents used for Xanthohumol or 3-Hydroxyxanthohumol.

Solvent for cell-free or cellular experiments		Solvent for rat liver experiments	
Ethanol (96 %)	50%	Propylenglycol	4 %
PBS		Tween 80	0.8 %
10 mM stock-solutions were dissolved with PBS or DMEM medium		PBS	

### 2.1.2.2 GENERAL ASPECTS

Both compounds were kindly provided by Prof. Dr. Jörg Heilmann of the University of Regensburg. Detailed synthesis description and identity approval was published recently by Vogel et al.<sup>128</sup> For experiments both substances were dissolved in their respective solvent (Table 2). The chemical structures and detailed information are given in section 1.4.

### 2.1.3 NF- $\kappa$ B decoy nanoparticles

#### 2.1.3.1 SOLUTIONS AND REAGENTS

Table 3 Reagents used for NF- $\kappa$ B decoy nanoparticles preparation.

Product	Company
Gelatin type A	Sigma-Aldrich
NF- $\kappa$ B decoy oligonucleotides (5'- AGT TGA GGG GAC TTT CCC AGG C -3', 5'- GCC TGG GAA AGT CCC CTC AAC T -3')	Biomers.net
Scrambled decoy oligonucleotides (5'- CCT TGT ACC ATT GTT AGC C -3', 5'- GGC TAA CAA TGG TAC AAG G -3')	Biomers.net
Alexa Fluor® 488 end-labeled decoy oligonucleotides	Biomers.net

Table 4 Solutions used for NF- $\kappa$ B decoy nanoparticles preparation.

KH solution (pH 7.4, 37 °C)		Rehydration at 20 nM/ml NF- $\kappa$ B decoy ODN	
NaCl	126 mM	Tween 80 (10 %)	34 $\mu$ l
KCl	4.7 mM	Sucrose	486.8 $\mu$ l
KH <sub>2</sub> PO <sub>4</sub>	1.2 mM	H <sub>2</sub> O	679.2 $\mu$ l
MgCl <sub>2</sub> x 6H <sub>2</sub> O	0.6 mM	1.2 ml was dissolved freshly before	
NaHCO <sub>3</sub>	24 mM	perfusion in 120 ml of KH solution	
CaCl <sub>2</sub> x 2H <sub>2</sub> O	1.25 mM		
Pyruvat-Na	126 mM		
Glucose	5.5 mM		
H <sub>2</sub> O			
saturated with			
95 % O <sub>2</sub> and 5 % CO <sub>2</sub>			

### 2.1.3.2 GENERAL ASPECTS

Preparation and loading of nanoparticles was kindly performed by Sebastian Fuchs (Pharmaceutical Technology, Department of Pharmacy, University of Munich). Dr. Florian Hoffmann (Pharmaceutical Biology, Department of Pharmacy, University of Munich) has previously given a detailed description in his Ph.D. thesis (2007).

In brief, aqueous nanoparticles dispersion containing surface modified gelatin NP was incubated with an oligonucleotide (ODN) solution containing the sequence for NF- $\kappa$ B decoy ODN or scrambled decoy ODN, which resulted in 10 % drug loading. For biodistribution analysis, nanoparticles were loaded with Alexa Fluor® 488 5'-end-labeled NF- $\kappa$ B decoy oligonucleotides.

For experiments, the freeze-dried gelatin nanoparticles were isoosmotic rehydrated, leading to a final volume of around 1.2 ml containing 20 nmol/ml NF- $\kappa$ B decoy ODN, which were dissolved 1:100 in KH (Krebs-Henseleit) buffer for animal studies.

## 2.2 CELL-FREE SYSTEM

### 2.2.1 Solutions and reagents

Table 5 Solutions and reagents used for cell-free experiments.

Product	Company
Xanthine	Sigma Aldrich
Luminol	Sigma Aldrich
Xanthine-oxidase	Sigma Aldrich

Xanthine-solution		Luminol-solution		Xanthine-oxidase 0.5 U/l	
Xanthine	1 mM	Luminol	1 mM	Xanthine-oxidase	35 U/l 50 $\mu$ l
PBS		PBS		PBS	3450 $\mu$ l

### 2.2.2 Xanthine/xanthine-oxidase assay

The chemiluminescence mixture was prepared immediately before analysis by mixing 230  $\mu$ l of 1 mM xanthine and 30  $\mu$ l of sample. To start the reaction, 20  $\mu$ l of 1 mM luminol and 20  $\mu$ l of 0.5 U/ml xanthine-oxidase were added to the mixture, which contained solvent (control), XN (40  $\mu$ M), or OH-XN (40  $\mu$ M), respectively. Chemiluminescence was measured for 100 seconds at 37 °C using an Orion II microplate luminometer (Berthold detection systems). The results were expressed as relative light units (RLU) or as area under the curve (AUC).

## 2.3 CELLULAR SYSTEM

### 2.3.1 Solutions and reagents

Table 6 Solutions and reagents used for cellular experiments.

Product	Company
Phenol-red free DMEM	PAA Laboratories
Culture flasks, plates and dishes	TPP
Fetal calf serum (FCS)	Biochrom KG
Glutamine	Merck
Dihydrofluorescein diacetate (H <sub>2</sub> FDA)	Invitrogen
TNF- $\alpha$	Calbiochem
PDTC	Sigma Aldrich

HEK 293 growth medium		HEK 293 freezing medium	
FCS	10 %	FCS	3 %
Glutamin	1 %	Glutamin	1 %
DMEM phenol-red free		DMEM phenol-red free	

PBS Ca <sup>2+</sup> /Mg <sup>2+</sup> solution (pH 7.4)		Trypsin/EDTA (T/E)	
NaCl	137 mM	Trypsin	0.05 %
KH <sub>2</sub> PO <sub>4</sub>	1.47 mM	EDTA	0.20 %
KCl	2.68 mM	PBS	
Na <sub>2</sub> HPO <sub>4</sub>	8.10 mM		
MgCl <sub>2</sub>	0.25 mM	Collagen G	
CaCl <sub>2</sub>	0.50 mM	Collagen G	0.001 %
H <sub>2</sub> O		PBS	

Plasmides	Company
pNF- $\kappa$ B-Luc, pFC-Mekk	Stratagene
pEGFP	Clontech
p $\beta$ -Gal	Promega

Lennox Broth (LB) Media (pH 7.2)		Lennox Broth (LB) Agar	
LB Base	2 %	LB Agar	3.2 %
H <sub>2</sub> O		H <sub>2</sub> O	

### 2.3.2 Cell line and cultivation

For experiments, cells of the human embryonic kidney cell line 293 (HEK 293; DSMZ-German collection of microorganisms and cell cultures, ACC 305) were cultured in a humidified atmosphere at 37 °C and 5 % CO<sub>2</sub> in an incubator (Heraeus). Contamination of mycoplasma was routinely tested with the PCR detection kit VenorGeM (Minerva Biolabs).

HEK 293 cells were grown in phenol-red free DMEM supplemented with 10 % FCS and 2 mM glutamine in 75 cm<sup>2</sup> tissue culture flasks or seeded in plates or dishes for experiments. Therefore, culture flasks, plates or dishes were coated with collagen G for 20 min at 37 °C before seeding. When reaching ~85-90 % confluency, cells were splitted 1:4. Hence, cells were washed twice with PBS and subsequently detached by incubation with T/E for 2 min. Then, cells were gradually detached and centrifuged in PBS at 1,000 rpm for 5 min at room temperature and the pellet was resuspended in HEK 293 growth medium.

### 2.3.3 Dihydrofluorescein diacetate assay

Cells were seeded in 24-well plates and when reaching ~85-90 % confluency, treated for two hours with XN and OH-XN (40  $\mu\text{M}$ ), respectively. After 90 minutes, the cells were loaded additionally with 20  $\mu\text{M}$  H<sub>2</sub>FDA by incubation for 30 min at 37 °C in the dark. Dihydrofluorescein, a ROS-sensitive fluorescence dye, is formed after penetrating the cell membrane and ester group cleavage. Eventually, cells were washed with PBS Ca<sup>2+</sup>/Mg<sup>2+</sup> and stimulated with 1 mM H<sub>2</sub>O<sub>2</sub> for 30 minutes (Figure 14).

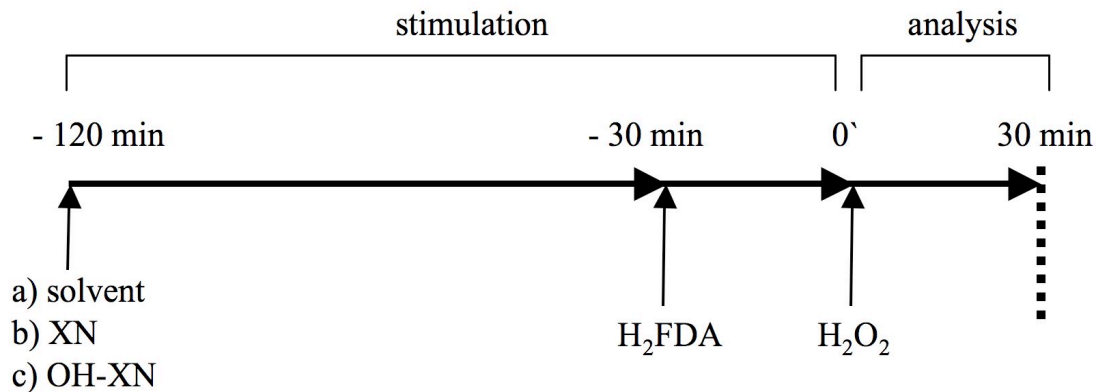


Figure 14 Time course of HEK 293 cell stimulation for the dihydrofluorescein diacetate assay.

Fluorescence was measured with a SpectraFluor Plus microplate reader (Tecan) using an excitation and emission wavelength of 485 nm and 535 nm, respectively.

### 2.3.4 NF- $\kappa$ B reportergene assay

#### 2.3.4.1 PLASMID PREPARATION

The plasmid preparation was kindly performed by Andrea Rothmeier (Pharmaceutical Biology, Department of Pharmacy, University of Munich).

In brief, 100  $\mu$ l of competent DH5 $\alpha$  bacteria were incubated for 20 minutes with 1-100 ng plasmid DNA on ice. Then the bacteria were heat-shocked for 90 seconds at 42  $^{\circ}$ C and afterwards kept on ice. 200  $\mu$ l LB-media were added and the bacteria were incubated at 37  $^{\circ}$ C for 30 minutes in a water bath. After incubation, up to 200  $\mu$ l of the bacteria suspension were plated on selective (ampicillin 100  $\mu$ g/ml or kanamycin 50  $\mu$ g/ml) LB-agar and incubated over night at 37  $^{\circ}$ C.

Single colonies of transformed DH5 $\alpha$  were picked and each colony incubated in 3 ml selective LB-media (37  $^{\circ}$ C) for 18 h at 150 rpm (Thermoshaker, Gerhardt). Subsequently, the cultured bacteria were centrifuged at 13,000 x g at 4  $^{\circ}$ C for 2 minutes and the mini preparation of plasmids was performed with a Plasmid MiniPrep-Kit (Qiagen) according to the manufacture's description. Plasmids were cut with appropriate restriction enzymes and then identified by size with agarose gel electrophoresis after ethidium bromide staining.

Following successful mini preparation, 3 ml of the transformed bacteria were pre-cultivated for 8 h at 37  $^{\circ}$ C and subsequently incubated in 100 ml selective LB-media overnight at 37  $^{\circ}$ C and 150 rpm (Thermoshaker, Gerhardt). After centrifugation at 6,000 x g for 15 minutes at 4  $^{\circ}$ C, the isolation was carried out with EndoFree<sup>®</sup> Plasmid Maxi-Kit (Qiagen) according to the manufacture's protocol.

#### 2.3.4.2 TRANSFECTION OF CELLS

HEK 293 cells were seeded at a concentration of 4 x 10<sup>6</sup> cells/100-mm dish. The next day, cells were transiently co-transfected with 2.8  $\mu$ g of a plasmid containing 5.7-kB of the human NF- $\kappa$ B promoter driving a firefly luciferase gene (pNF- $\kappa$ B-Luc) and 45  $\mu$ g of a  $\beta$ -galactosidase plasmid (p $\beta$ -Gal, 6.82-kB). Transfection was performed using the Ca<sup>2+</sup>-phosphate method for 6 hours, which is described in detail previously by Dr. Hans-Peter Keiss in his Ph.D. thesis (Pharmaceutical Biology, Department of

Pharmacy, University of Munich). For visual transfection efficiency, green fluorescent protein (GFP) was expressed using pEGFP transfected cells.

#### 2.3.4.3 LUCIFERASE ASSAY

Co-transfected cells were seeded in 24-well plates at a concentration of  $1 \times 10^5$  cells/well and grown for an additional 16 hours. Then cells were pre-incubated for 2 hours with different concentrations of XN and OH-XN (5, 10, 20, 40 and 60  $\mu\text{M}$ ), respectively, and subsequently stimulated with 1 ng/ml TNF- $\alpha$  for 6 hours (Figure 15). Cells preincubated with 50  $\mu\text{M}$  pyrrolidine dithiocarbamate (PDTC) served as positive control.

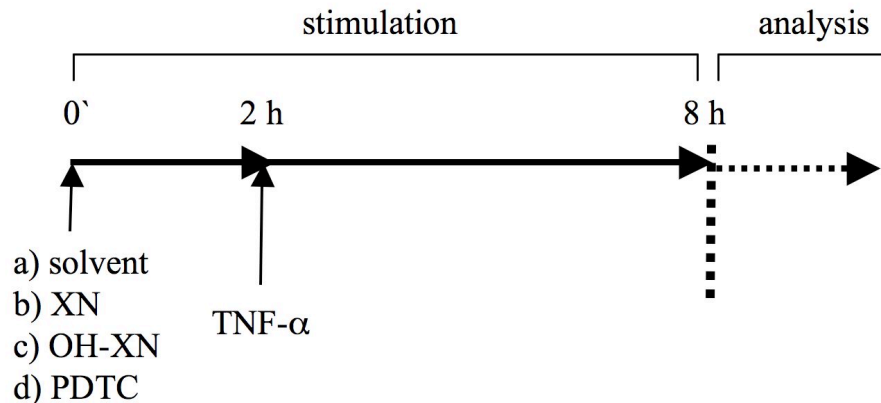


Figure 15 Stimulation of HEK 293 cells for the NF- $\kappa$ B reporter gene assay.

Finally, cells were washed with PBS, lysed and the NF- $\kappa$ B activity was measured with a commercial luciferase assay kit (Luciferase assay system, Promega) according to the manufacturer's instructions using a luminometer (AutoLumatPlus, Berthold Technologies) and normalized with  $\beta$ -galactosidase activities to correct for transfection efficiency. Relative luciferase activity is expressed as the normalized luciferase activity in percentage of solvent treated cells (control group).

Cells co-transfected with pFC-Mekk, pNF- $\kappa$ B-Luc and p $\beta$ -Gal served as negative control. Cells were transfected with pNF- $\kappa$ B-Luc or p $\beta$ -Gal alone, to eliminate interactions between different plasmids.

## 2.4 ANIMAL MODELS

### 2.4.1 Solutions and reagents

Table 7 Solutions and reagents used for animal experiments.

Product	Company
Chow	Ssniff
L-NAME	Cayman Chemical
Fentanyl	Janssen-Cilag
Midazolam	Ratiopharm
Isofluran	Abbott
Carbogen	Air Liquide
Formalin 10 %	Appli Chem
PE catheters	Portex
Heparin	Braun Melsungen AG
NORM-JECT® syringe	Henke Sass Wolf

### 2.4.2 Animals

6 week old male Sprague-Dawley rats, weighing 200-250 g, were purchased from Charles River Laboratories and housed in a climatized room with a 12 hours light-dark cycle. The animals had free access to chow and tap water up to the time of experiments. All animals received human care in compliance with the „Principles of Laboratory Animal Care“. The study was registered with the local animal welfare committee. Animals were anesthetized by i.p. injection of 0.005 mg/kg Fentanyl and 2.0 mg/kg Midazolam. For further maintainance of anesthesia, 1.5 % Isofluran was continuously conducted using a vaporizer with Carbogen (5 % CO<sub>2</sub> / 95 % O<sub>2</sub>) as a carrier gas.

### 2.4.3 Blood pressure measurement - *in vivo*

#### 2.4.3.1 SURGICAL PROCEDURE

Blood pressure was continuously monitored with a blood-pressure gauge after cannulation of the carotid artery with a 16 gauge-PE catheter.

#### 2.4.3.2 TREATMENT PROTOCOL – EGB 761

The first group received the respective solvent 30 minutes before an i.v. injection of EGb 761 (20 mg/kg), whereas the second group received an i.v. injection of L-NAME (16 mg/kg), a selective eNOS inhibitor, 30 minutes prior to the EGb 761 application (Figure 16). Blood pressure was monitored for 30 minutes right after EGb 761 administration.

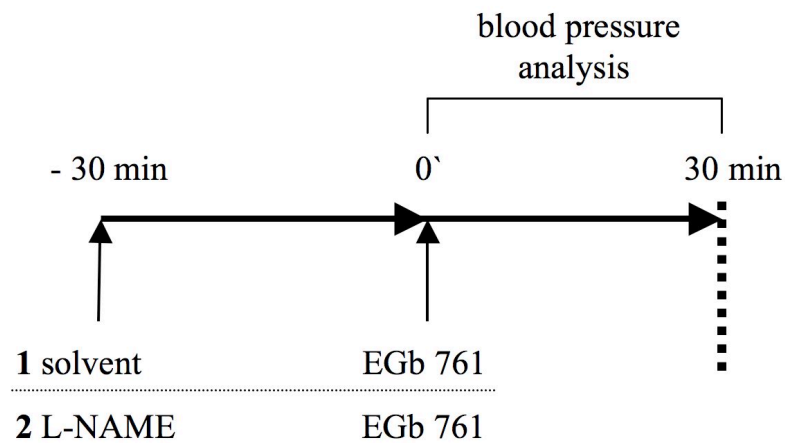


Figure 16 Treatment of rats with L-NAME (16 mg/kg) or solvent, respectively, 30 minutes prior to EGb 761 (20 mg/kg) administration. Continuously thereafter, blood pressure was monitored for 30 minutes.

## 2.4.4 Warm ischemia/warm reperfusion – *in vivo*

### 2.4.4.1 SURGICAL PROCEDURE

The abdomen was opened by midline-laparotomy and the portal triad was prepared. Throughout the experiment the body temperature was maintained between 36.0 °C and 37.0 °C with a warming lamp and blood pressure was detected as described before to supervise anesthesia.

The arterial and portal blood flow to the left lateral and median lobe of the liver was interrupted by applying an atraumatic clip, resulting in 70 % liver ischemia. After ischemia, the blood supply was restored by removal of the clip and the reperfusion period was initiated.

Blood samples were collected into heparinized tubes at the end of the reperfusion period and subsequently animals were sacrificed by bleeding. The organ was rinsed free from blood by perfusing the liver with PBS through the portal vein via a peristaltic pump (DigiStaltic from Watson-Marlow GmbH) at a flow of 55 ml/min for 2 minutes. The median lobe was excised and the remaining lobes were perfused with formalin 3 % in PBS for protein fixation.

All tissues were cut in 3 mm cubes, immediately snap frozen in liquid nitrogen and kept at -80 °C until further examination. After centrifugation of blood samples at 5000 U/min for 8 minutes, the plasma was stored in aliquots at -80 °C.

### 2.4.4.2 TREATMENT PROTOCOLS

#### 2.4.4.2.1 GINKGO BILOBA EXTRACT – EGB 761

Rats were exposed to 90 minutes of warm ischemia followed by 3 hours of reperfusion. Different concentrations of EGb 761 (0.2-20 mg/kg) or solvent, respectively, were applied intravenously via the jugular vein with a NORM-JECT® syringe 15 minutes before the onset of the ischemic period (preischemic). Untreated animals served as controls (Figure 17).

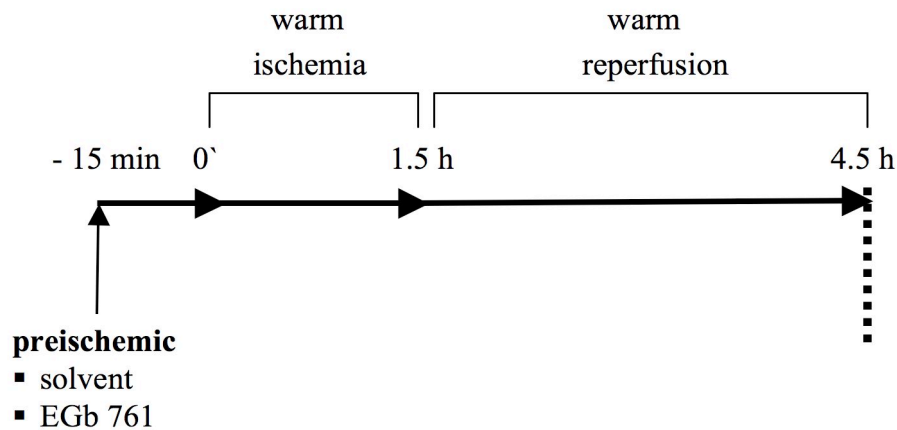


Figure 17 Treatment of rats with EGb 761 or solvent, respectively, prior to warm ischemia/warm reperfusion (1.5 h / 3 h).

#### 2.4.4.2.2 XANTHOTHUMOL

Xanthohumol (8 mg/kg) was dissolved in the respective dissolution medium and administered continuously with a NORM-JECT<sup>®</sup> syringe over 5 minutes via the leg vein preischemic, 15 minutes before the onset of warm ischemia (1 hour), and postischemic prior to the reperfusion period of 2 or 6 hours, respectively (Figure 18). Pre- and postischemic solvent administration served as control.

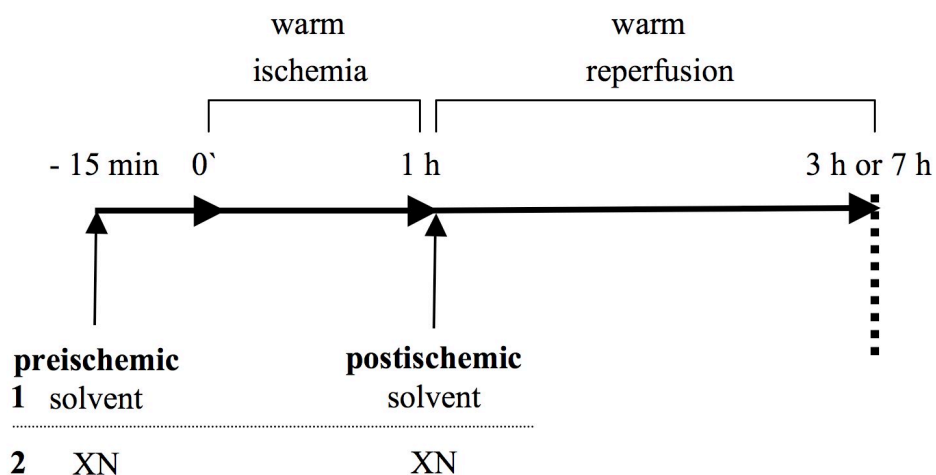


Figure 18 Pre- and postischemic treatment each with 8 mg/kg Xanthohumol or solvent, respectively, in the cold IR model with either 2 hours or with 6 hours of reperfusion.

### 2.4.5 Cold ischemia/warm reperfusion – *ex vivo*

#### 2.4.5.1 SURGICAL PROCEDURE

After opening the abdomen by a midline-laparotomy, the bile duct, portal vein, and suprahepatic inferior vena cava were cannulated with PE-catheters. The liver was drained and rinsed free from blood *in situ* with hemoglobin-free and albumin-free, bicarbonate-buffered Krebs-Henseleit (KH) solution (pH 7.4, 37 °C) saturated with 95 % O<sub>2</sub> and 5 % CO<sub>2</sub>. Additionally, the hepatic artery, the infrahepatic inferior vena cava, and the right kidney vein were ligated. The perfusion medium was pumped constantly through the liver with a peristaltic pump (Digi-Staltic from Masterflex) in a non-recirculating fashion (30 ml/min).

After 30 minutes of perfusion, livers were flushed with 100 ml ice-cold (4 °C) PBS solution, initiating the cold ischemic period. Then the perfusion was stopped and organs were preserved at 4 °C for 6 hours. Following the period of ischemia, livers were reperfused with KH buffer (pH 7.4, 37 °C) saturated with 95 % O<sub>2</sub> and 5 % CO<sub>2</sub> for 150 minutes at a flow rate of 3.0-3.5 ml x min<sup>-1</sup> x g liver in a non-recirculating fashion for 2.5 hours.

Perfusate samples were collected and kept at -80 °C for further transaminases and lactate dehydrogenase measurement. Moreover, bile production was determined throughout the reperfusion period and portal pressure rates were monitored on a hydrostatic column. Liver tissue samples were obtained at the end of reperfusion period and were either fixed in phosphate-buffered formalin for paraffin embedding or snap-frozen in liquid nitrogen until analysis.

#### 2.4.5.2 TREATMENT PROTOCOLS

##### 2.4.5.2.1 XANTHOHUMOL AND 3-HYDROXYXANTHOTHUMOL

2.26 mM of XN (16 mg/kg) and OH-XN (16.76 mg/kg), respectively, were dissolved in the respective dissolution medium and filled in NORM-JECT<sup>®</sup> syringes. The chilled solutions (4 °C) were injected into the portal vein after liver preparation right before the ischemic period (preischemic) and remained in the liver during ischemia. After 6 hours of cold ischemia, livers were reperfused with KH buffer for 2.5 hours. Injection of the solution medium served as control (Figure 19).

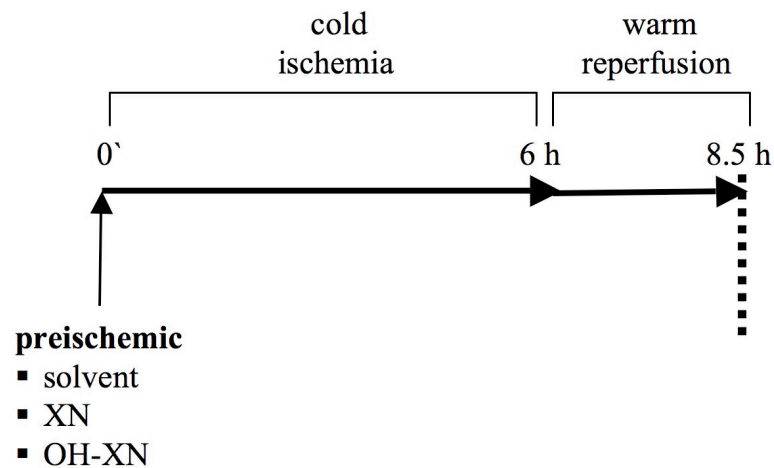


Figure 19 Treatment with 2.26 mM of Xanthohumol and 3-Hydroxyxanthohumol or solvent, respectively, prior to cold ischemia (6 hours) followed by 2.5 hours of warm reperfusion.

#### 2.4.5.2.2 NF- $\kappa$ B DECOY NANOPARTICLES

Subsequently after liver preparation, 120 ml of the KH solution containing 1.2 ml (20 nM) NF- $\kappa$ B decoy-NP or scrambled decoy-NP was perfused continuously (3 ml/min) through the liver graft before initiating the ischemic period. Ischemia was kept for 6 hours (Figure 20) and subsequently reperused for 2.5 hours with KH solution.

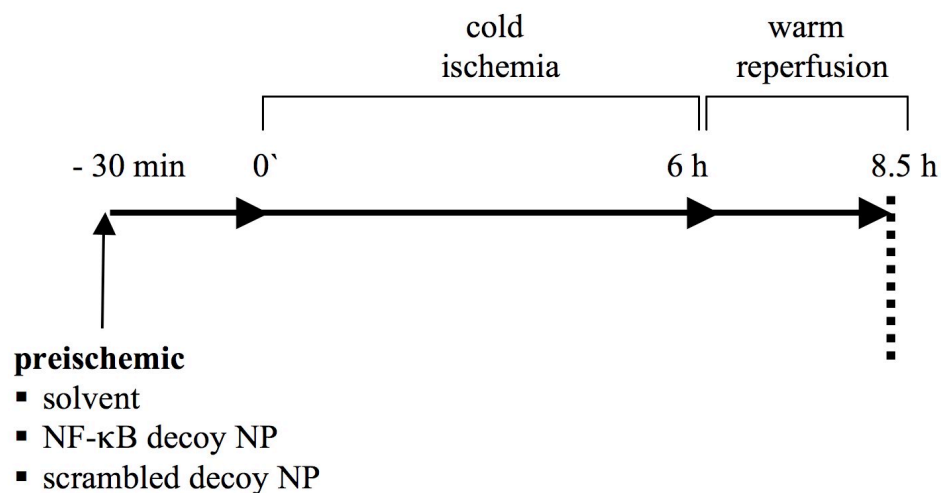


Figure 20 Treatment with NF- $\kappa$ B decoy-NP (20 nM), scrambled decoy-NP (20 nM) or solvent, respectively, prior to cold ischemia (6 h) followed by warm reperfusion (2.5 h).

### 2.4.5.3 BIODISTRIBUTION

It has been shown previously by Dr. Florian Hoffmann (Pharmaceutical Biology, Department of Pharmacy, University of Munich) in his Ph.D. thesis that nanoparticles are mainly absorbed by Kupffer cells after injection *in vivo*. To proof the suitability of nanoparticle exposure in the *ex vivo* model of ischemia/reperfusion, 120 ml KH solution containing 20 nmol of Alexa Fluor® 488 labeled oligonucleotides loaded onto nanoparticles was perfused continuously (3 ml/min) in a non-recirculating fashion through the liver graft (Figure 21).

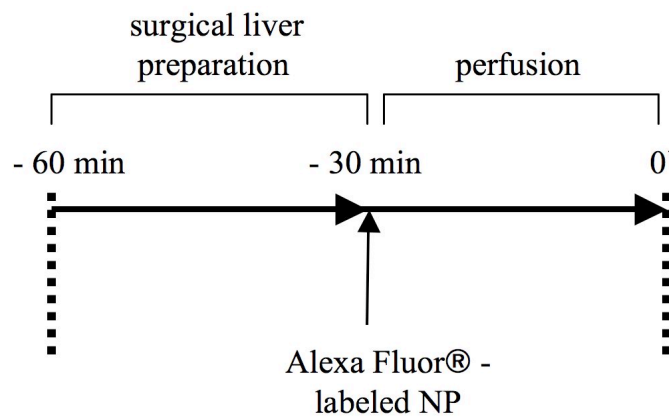


Figure 21 Liver perfusion with NP loaded with Alexa Fluor® 488 labeled oligonucleotides.

Subsequently, livers were harvested right after flushing with ice cold PBS and liver slices were analysed by confocal laser scanning microscopy after paraffin embedding (see section 2.5).

## 2.5 IMMUNOHISTOCHEMISTRY

### 2.5.1 Solutions and reagents

Table 8 Products used for immunohistochemistry.

Product	Company
Hoechst 33342	Invitrogen
Coverplate™	Thermo Shandon
PermaFluor® Mounting Medium	Beckman Coulter

Table 9 Primary and secondary antibody.

Antibody	Dilution	Company
CD 163 (MCA342R) mouse anti-rat IgG	1:100 in 0.2 % saline buffered BSA	AbD Serotec
Alexa Fluor® 633 goat anti-mouse IgG	1:400 in 0.2 % saline buffered BSA	Invitrogen

### 2.5.2 Staining of liver tissue

The formalin-fixed, paraffin embedded liver sample was cut into 8 µm thick slices and deparaffinized in xylene following rehydration through a declining ethanol-series. The staining procedure was carried out using Coverplate™ disposable immunostaining chambers.

For staining of Kupffer cells, sections were first incubated with a mouse anti-rat monoclonal CD 163-antibody overnight at 4 °C. After repeated washing with PBS, the secondary antibody Alexa® 633 goat anti-mouse was applied for 45 minutes. Subsequently, nuclei were stained with Hoechst 33342 for further 5 minutes. All sections were mounted with PermaFluor® Mounting Medium and analyzed by confocal laser scanning microscopy (LSM 510 Meta CLSM from Zeiss).

## 2.6 ANTIOXIDANT PARAMETERS

The GSH and SOD level determination was kindly performed by Dr. Hussam Ajamieh of the Klinikum Großhadern (University of Munich).

### 2.6.1 GSH

Glutathione (GSH) levels were measured using the colorimetric microplate assay from Oxford Biomedical Research. Briefly, the total GSH content of the liver tissue homogenate is determined after reduction of DTNB (5,5'-dithiobis(2-nitrobenzoic acid)), causing a colored ion which absorbs light at 405 nm. This color increase is proportional to the total GSH concentration. The results were expressed as percentage of untreated controls. Protein content was determined using the Bradford method (see section 2.11.3).

### 2.6.2 SOD

Superoxide dismutase (SOD) activity was analyzed using the pyrogallol method described by Marklund et al.<sup>129</sup> Briefly, 100 µl of the liver tissue homogenate was mixed with 2.8 ml of Tris-HCl (50 mM) and 50 µl of EDTA (1 mM) at pH 8.2. After pre-incubation for 5 min at 25 °C, the reaction was initiated by the addition of 50 µl pyrogallol solution with a final concentration of 0.124 mM. The change of absorbance at 420 nm measured after 10 seconds and 1 minute was calculated. The amount of enzyme, which inhibits the autoxidation rate of pyrogallol by 50 % is defined as one unit. The results were expressed as percentage of untreated controls. Protein content was determined using the Bradford method as described in section 2.11.3.

### 2.6.3 MDA

Malondialdehyde (MDA) concentration of liver homogenates was measured using the TBARS assay kit from Cayman Chemical. Briefly, MDA, the product of lipid peroxidation, reacts with thiobarbituric acid under acidic conditions at 95 °C to form a pink colored complex with an absorbance at 532 nm. The results were expressed as percentage of untreated controls. Protein content was determined using the Bradford method as described in section 2.11.3.

## 2.7 ELECTROPHORETIC MOBILITY SHIFT ASSAY – EMSA

### 2.7.1 Solutions and reagents

Table 10 Solutions and reagents used for EMSA.

Product	Company
consensus binding sequence for NF- $\kappa$ B (5'-AGT TGA GGG GAC TTT CCC AGG C-3')	Promega
[ $\gamma$ 32P]-ATP 3000 Ci/mmol	Amersham
T4 polynucleotide kinase	USB
Nuc Trap probe purification columns	Stratagene

Buffer A		Buffer B		Binding buffer	
Hepes (pH 7.9)	10 mM	Hepes (pH 7.9)	20 mM	Glycerol	20 %
KCl	10 mM	NaCl	400 mM	MgCl <sub>2</sub>	5 mM
EDTA	0.1 mM	EDTA	1 mM	EDTA	2.5 mM
EGTA	0.1 mM	EGTA	0.5 mM	NaCl	250 mM
H <sub>2</sub> O		Glycerol	25 %	Tris-HCl	50 mM
add freshly before use:		add freshly before use:		H <sub>2</sub> O	
DTT	1 mM	DTT	1 mM		
PMSF	0.5 mM	PMSF	1 mM		

STE buffer (pH 7.5)		Loading buffer		Reaction buffer	
Tris	10 mM	Tris-HCl	250 mM	Binding buffer	90 %
NaCl	100 mM	Bromphenolblue	0.2 %	Loading buffer	10 %
EDTA	1 mM	Glycerol	40 %	DTT	2.6 mM
H <sub>2</sub> O		H <sub>2</sub> O		H <sub>2</sub> O	

TBE 10 x		Polyacrylamide (PAA) gel		Reaction mix	
Tris	890 mM	TBE 10x	5.3 %	30 µg of nuclear	x µl
Boric acid	890 mM	PAA solution 30%	15.8 %	protein	
EDTA	20 mM	Glycerol	2.6 %	add after unfreezing:	
H <sub>2</sub> O		TEMED	0.05 %	poly(dIdC)	2 µl
Dilutions		APS	0.08 %	Reaction buffer	3 µl
were prepared with		H <sub>2</sub> O		H <sub>2</sub> O	ad 15 µl
purified water.					

### 2.7.2 Preparation of nuclear extracts

The electrophoretic mobility shift assay (EMSA) was performed as described previously.<sup>130</sup> Tissue samples were homogenized 1:10 with lysis Buffer A in a Potter S homogenizer from B. Braun Biotech. After centrifugation (1,000 rpm, 10 minutes, 4 °C) and incubation (4 °C for 10 minutes) in freshly added Buffer A, containing 6 % of Nonidet P-40 10 %, samples were centrifuged (14,000 rpm, 1 minute, 4 °C). The remaining pellet was suspended in Buffer B, followed by incubation (4 °C for 30 minutes) under continuous shaking. After centrifugation (14,000 rpm, 10 minutes, 4 °C) supernatants were frozen at -80 °C. The protein concentration was determined by the method of Bradford as described in section 2.11.3.

### 2.7.3 Radioactive labeling of consensus oligonucleotides

The consensus binding sequence for NF-κB was 5'end-labeled with [ $\gamma^{32}\text{P}$ ]-ATP by incubation for 10 minutes at 37 °C using T4 polynucleotide kinase. The reaction was terminated by addition of 0.5 M EDTA solution and radioactive labeled DNA was separated from unlabeled DNA by using Nuc Trap probe purification columns. Radioactive oligonucleotides were eluted from the column with 70 µl of STE buffer and frozen at -20 °C until used for EMSA.

### **2.7.4 Binding reaction and electrophoretic separation**

The freshly prepared reaction mix, containing 30 µg of nuclear protein, was incubated for 10 minutes at room temperature. Subsequently, the binding reaction was started by adding 1 µl of the radioactive labeled NF-κB oligonucleotide. Following incubation (30 minutes, RT), the protein-oligonucleotide complexes were separated by gel electrophoresis (Mini-Protean 3 form BioRad) with 0.25 x TBE buffer at 100 V for 60 minutes using non-denaturing polyacrylamide gels.

### **2.7.5 Detection and evaluation**

Gels were exposed to Cyclone Storage Phosphor Screens (Canberra-Packard) for 24 hours, followed by analysis with a phosphor imager station (Cyclone Storage Phosphor System from Canberra-Packard).

## **2.8 ELISA**

### **2.8.1 Preparation of samples**

Rat TNF-α UltraSensitive ELISA Kit was obtained from BioSource. Determination of serum TNF-α levels was performed according to the manufacturer's manual. Briefly, after centrifugation of heparinized blood samples for 8 minutes at 5,000 rpm, the supernatant was separated and stored at -80 °C until further analysis.

### **2.8.2 Reaction mixture**

Then 50 µl incubation buffer and 50 µl biotin conjugate were added to each 50 µl serum sample. Following a waiting period for 2 hours and several washing steps, the samples were incubated with 100 µl streptavidin coupled horse radish peroxidase (HRP) for 30 minutes. After further washing steps, 100 µl of stabilized chromogen was added to each well. Finally, the reaction was terminated by adding 100 µl of stop solution.

### **2.8.3 Detection and evaluation**

The absorbance was measured at 450 nm using the SUNRISE Absorbance Reader from TECAN. Color development was proportional to the amount of rat TNF-α in the blood.

## 2.9 WESTERN BLOT

### 2.9.1 Solutions and reagents

Table 11 Solutions and reagents used during Western blot.

Lysis buffer		Sample buffer (SB) 5x		Stacking gel	
NaCl	150 mM	Tris-HCl	312 mM	Rotiphorese®	17 %
Tris-HCl	50 mM	(pH 6.8)		Gel 30	
NP-40	1.00 %	Glycerol	50 %	Tris (pH 6.8)	125 mM
Desoxy- cholicacid	0.25 %	SDS	5 %	SDS	0.1 %
SDS	0.10 %	DTT	2 %	TEMED	0.2 %
H <sub>2</sub> O		Pyronin Y	0.125 %	APS	0.1 %
add before use:		(5 %)			
Complete®	4 mM	H <sub>2</sub> O			
PMSF	1 mM	Sample buffer (SB) 1x		Seperation gel 12.5 %	
Na <sub>3</sub> VO <sub>4</sub>	1 mM	SB (5x)	20 %	Rotiphorese®	40 %
NaF	1 mM	H <sub>2</sub> O		Gel 30	
				Tris (pH 8.8)	375 mM
				SDS	0.1 %
				TEMED	0.1 %
				APS	0.05 %
Electrophoresis buffer		Tank buffer 5x		Tank buffer 1x	
Tris	4.9 mM	Tris	125 mM	Tank buffer 5x	20 %
Glycine	38 mM	Glycine	200 mM	Methanol	20 %
SDS	0.1 %	H <sub>2</sub> O		H <sub>2</sub> O	
H <sub>2</sub> O					

TBS + T (pH 8.0)		Blotto 5 %		BSA 5 %	
Tris	24.6 mM	Blotto	5 %	BSA	5 %
NaCl	188 mM	TBS + T		TBS + T	
Tween 20	0.1 %				
H <sub>2</sub> O					

ECL solution A		ECL solution B	
Luminol	25 mM	H <sub>2</sub> O <sub>2</sub>	0.006 %
p-Coumaric acid	0.396 mM	Tris (pH 8.5)	100 mM
Tris (pH 8.5)	100 mM	H <sub>2</sub> O	
H <sub>2</sub> O			

Coomassie staining solution		Coomassie destaining solution		Ponceau solution	
Coomassie blue G	0.3 %	Acetic acid	10 %	Ponceau S	0.1 %
Acetic acid	10 %	Ethanol (96 %)	33 %	Acetic acid	5 %
Ethanol (96 %)	45 %	H <sub>2</sub> O		H <sub>2</sub> O	
H <sub>2</sub> O					

Table 12 Primary antibodies used for specific protein detection.

Antigen	Isotype	Dilution	Company
Actin	mouse monoclonal	1:1000; Blotto 1 %	Chemicon
Akt	rabbit polyclonal	1:1000; BSA 5 %	Cell Signaling
Phos.-Akt <sup>Ser 473</sup>	rabbit polyclonal	1:1000; BSA 5 %	Cell Signaling
Phos.-Akt <sup>Thr 308</sup>	rabbit monoclonal	1:1000; BSA 5 %	Cell Signaling
Bcl-xl	rabbit polyclonal	1:1000; BSA 5 %	Santa Cruz
JNK	rabbit polyclonal	1:1000; BSA 5 %	Cell Signaling
Phos.-JNK <sup>Thr183/Thr185</sup>	rabbit polyclonal	1:1000; BSA 5 %	Cell Signaling

Table 13 Secondary antibodies.

Antibody	Dilution	Company
Goat anti-mouse IgG1 : HRP	1:1000 in Blotto 1 %	Biozol
Goat anti-rabbit : HRP	1:1000 in Blotto 1 %	Dianova

### 2.9.2 Preparation of samples

Liver tissue (20-60 mg) was homogenized (Potter S, B. Braun Biotech) in 200-600  $\mu$ l lysis buffer. Following centrifugation (14,000 rpm, 4 °C, 10 minutes), an aliquot of sample was used for protein quantification by use of the Pierce assay as described in section 2.11.2.

The remaining supernatant was diluted 5:1 with 5 x sample buffer and probes were boiled at 95 °C for 5 minutes for protein denaturation. Samples were kept at -20 °C until Western blot analysis.

### 2.9.3 Electrophoresis

Equal amounts of protein were ensured by adding 1 x sample buffer to the respective probes and were separated according to their molecular weight by SDS-PAGE (Mini PROTSEAN 3, Biorad Laboratories). Proteins have been stacked at 100 V for 21 minutes and were separated at 200 V for 40 minutes.

### 2.9.4 Electroblotting

For wet transfer, the sandwich assembly was placed in the Mini Trans-Blot Cell buffer tank from Bio-Rad at 100 V for 1.5 hours. Transfer sandwich was assembled in a box containing tank buffer (1x) starting with a wetted pad. Subsequently, a soaked blotting paper, the gel followed by the nitrocellulose membrane, a second blotting paper and a wetted pad was added. The nitrocellulose membrane (Hybond<sup>TM</sup>-ECL<sup>TM</sup>, Amersham Biosciences) was previously activated by soaking in tank buffer (1x) for at least 30 min and the sandwich was assembled with the membrane facing the anode.

## 2.9.5 Protein detection

### 2.9.5.1 SPECIFIC PROTEIN DETERMINATION

To block unspecific protein binding sites, the membranes were either incubated with Blotto 5 % or BSA 5 % for 2 hours at room temperature. Immunological detection of proteins were identified by incubating the membrane with the respective primary antibody (4 °C, over night), followed by incubation with a HRP-conjugated secondary antibody (2 h, RT). After each antibody incubation step, the membrane was washed 4 times with PBS containing 0.1 % Tween 20 for 5 minutes. All incubation steps were performed under gentle shaking.

The reactive bands were visualized employing a chemiluminescent reaction by incubation the membrane (1 minute) with a 1:1 mixture of ECL solution A and B, containing luminol. The enzyme horseradish peroxidase (HRP), which is coupled to the secondary antibodies, catalyzes the oxidation of luminol in the presence of H<sub>2</sub>O<sub>2</sub>. Luminescence was detected by exposure of the membrane to an X-ray film (Super RX, Fuji) and subsequently developed with a Curix 60 Developing system (Agfa-Gevaert AG).

β-Actin was used as loading control (Millipore). Moreover, the molecular weight of proteins was determined by comparison with the prestained protein ladder (PageRuler™, Fermentas).

### 2.9.5.2 TOTAL PROTEIN DETERMINATION

Equal protein loading and blotting efficiency was ensured by staining gels as well as membranes with Coomassie (20 minutes, RT) or Ponceau (5 minutes, RT) staining solution, respectively, since all proteins were stained. Gels were extensively washed with Coomassie destaining solution for 30 minutes and subsequently with purified H<sub>2</sub>O until proteins appeared as blue bands. Moreover, membranes were washed in purified water until the background disappeared.

## 2.10 CASPASE-3 LIKE ACTIVITY ASSAY

### 2.10.1 Solutions and reagents

Table 14 Solutions and reagents used for caspase-3 like activity assay.

Lysis buffer (pH 7.5)		Substrate buffer	
Hepes (pH 7.5)	25 mM	Hepes (pH 7.5)	50 mM
MgCl <sub>2</sub>	5 mM	Sucrose	1 %
EDTA	1 mM	Chaps	0.1 %
		add before use:	
		DTT	10 mM
		Ac-DEVD-AFC	50 μM

### 2.10.2 Preparation of samples

Liver tissue was homogenized (Potter S, B. Braun Biotech) 1:10 with lysis buffer. Following centrifugation (14,000 rpm, 10 minutes, 4 °C), samples were used for protein quantification by Bradford assay as described in section 2.11.3. The remaining supernatants were stored at -80 °C until measurement. For analysis, extracts were incubated with the substrate buffer (1:10) containing Ac-DEVD-AFC.

### 2.10.3 Detection and evaluation

The generation of AFC was determined kinetically by fluorescence measurement (excitation: 385 nm; emission: 505 nm) using the SpectraFluor Plus microplate reader (Tecan). Samples containing lysis buffer were used as blank. Control experiments confirmed that the activity was linear with time and with protein concentration under the conditions described above.

## 2.11 PROTEIN QUANTIFICATION

### 2.11.1 Solutions and reagents

Table 15 Solutions and reagents used for protein quantification.

Product	Company
BCA Assay reagents	Interdim
Coomassie Brilliant Blue	BioRad

### 2.11.2 Pierce assay

Pierce Assay was performed as described by Smith et al.<sup>131</sup> Samples were incubated 1:20 with BCA Assay reagents for 30 min at 37 °C. Absorbance was measured photometrically with a Tecan Sunrise Absorbance reader (TECAN) at 550 nm. Protein standards were obtained by diluting a stock solution of Bovine Serum Albumin (BSA, 2 mg/ml). Linear regression was used to determine the actual protein concentration of each sample.

### 2.11.3 Bradford assay

Bradford Assay was performed as described by Bradford et al.<sup>132</sup> Samples were incubated 1:20 with a dilution of Coomassie Brilliant Blue (1:5 in water) for 5 min. Absorbance was measured photometrically with a Tecan Sunrise Absorbance reader (TECAN) at 592 nm. Protein standards were obtained by diluting a stock solution of Bovine Serum Albumin (BSA, 2 mg/ml). Linear regression was used to determine the actual protein concentration of each sample.

## **2.12 TISSUE INJURY PARAMETERS**

Activities of serum aminotransferases (alanine transferase (ALT) and aspartate transferase (AST)) as well as lactate dehydrogenase (LDH) of the collected perfusates or heparinized serum were determined as established markers of hepatic tissue damage. The data were kindly provided by Babett Rannefeld from the Institute for Clinical Chemistry of Klinikum Großhadern, (University of Munich, Germany) using a serum multiple analyzer (Olympus AU 2700, Olympus) at 37 °C.

## **2.13 STATISTICAL ANALYSIS**

Number of experiments is indicated in the respective figure legend. Data are expressed as mean  $\pm$  SEM. Statistical analysis was performed using the GraphPad Prism 3.03 software (GraphPad software Inc, San Diego, USA). Significance (\*, #) has always been calculated at the 95 % confidence interval between indicated groups, using an unpaired t-test.

# RESULTS

### 3.1 GINKGO BILOBA EXTRACT – EGB 761

#### 3.1.1 Impact on warm ischemia/warm reperfusion

##### 3.1.1.1 HEPATIC TISSUE DAMAGE

The impact of Ginkgo biloba extract (EGb 761) was elucidated in the *in vivo* model of 90 minutes warm ischemia followed by 3 hours of warm reperfusion by measuring the liver enzymes (AST + ALT), a parameter for hepatic tissue damage. Therefore, blood samples were collected at the end of reperfusion period. Pretreatment of rats with EGb 761, in concentrations varying from 0.2 mg/kg to 20 mg/kg was not protective (Figure 22). Instead, 2 mg/kg EGb 761 even significantly increased the liver enzymes. High toxic potential was observed when the concentration reached 20 mg/kg.

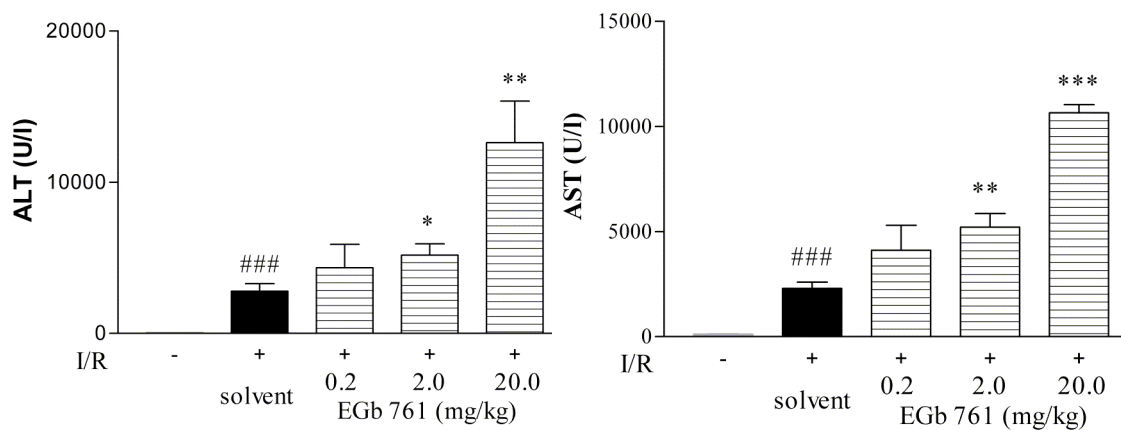


Figure 22 Transaminase levels (AST + ALT) of rats treated with EGb 761 (i.v.) in different concentrations or with solvent, respectively, prior to 1.5 hours of warm ischemia and 3 hours of warm reperfusion. Data are presented as mean  $\pm$  SEM (n=5, \*p<0.05 vs. solvent, #p<0.05 vs. control, Student's t-test).

##### 3.1.1.2 APOPTOSIS

Caspase-3 like activity of hepatic tissue was evaluated after IR, as caspase-3 is known to be the main effector molecule of apoptosis.<sup>133</sup> The hepatic caspase-3 activity was increased in rats subjected to warm ischemia followed by warm reperfusion (Figure 23). Preischemic EGb 761 treatment did not alter caspase-3 increase.

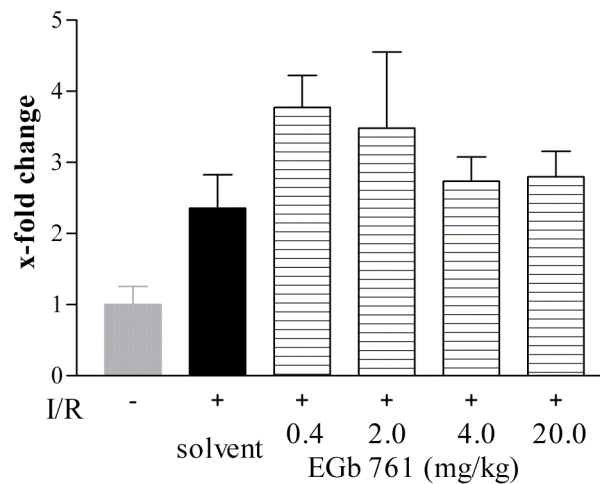


Figure 23 Caspase-3 like activity of animals pretreated with different concentrations of EGb 761 or solvent, respectively, prior to warm IR. Data are presented as mean  $\pm$  SEM (n=3).

### 3.1.1.3 BLOOD PRESSURE DEVELOPMENT DURING IR

Arterial blood pressure was monitored during the whole treatment period, starting right before solvent or EGb 761 application, respectively. Solvent treated animals showed blood pressure values around 100-110 mmHg preischemic, which tended to decrease during reperfusion and slightly recovered to the end (Figure 24).

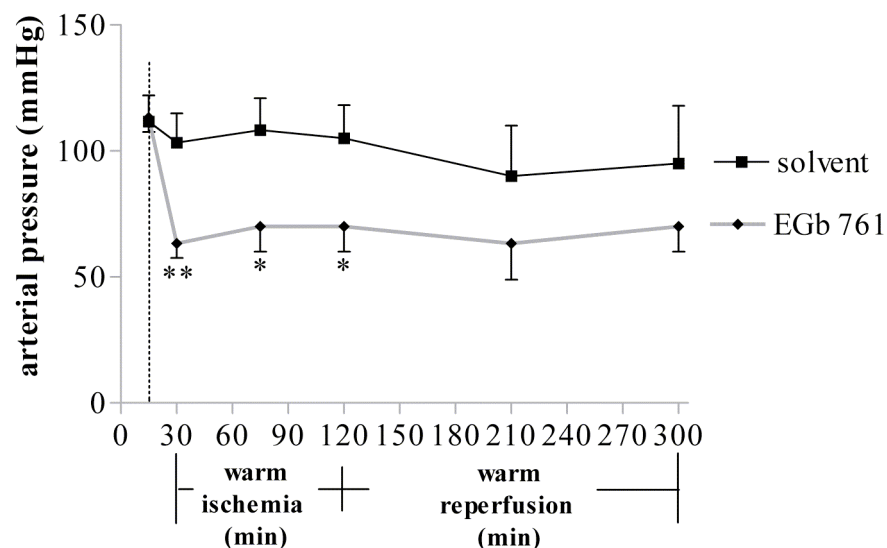


Figure 24 Blood pressure was monitored starting with the onset of solvent and EGb 761 (20 mg/kg) application, respectively, following 90 min of warm ischemia and 180 min of reperfusion. Data are presented as mean  $\pm$  SEM (n=3, \*p<0.05 vs. solvent, Student's t-test).

In contrast, blood pressure significantly collapsed straight after i.v. injection of EGb 761 to 63 mmHg  $\pm$  6 and kept constant with minimal variations during IR (Figure 24).

### 3.1.2 Investigation of arterial blood pressure drop

#### 3.1.2.1 eNOS INHIBITION – IN *VIVO*

In order to investigate the acute arterial blood pressure drop after EGb 761 administration *in vivo*, the impact of eNOS was elucidated. The generation of NO via eNOS is known to be involved in blood flow regulation as it functions as vasodilator.<sup>35</sup> Therefore, animals received 15 minutes before EGb 761 (20 mg/kg) administration either an intravenous injection of L-NAME (16 mg/kg), a selective eNOS inhibitor, or the respective solvent. Arterial blood pressure was monitored for 30 minutes. Blood pressure dropped significantly from 115 mmHg  $\pm$  10 to 63 mmHg  $\pm$  15 straight after EGb 761 application (Figure 25). Thereafter, blood pressure recovered continuously. L-NAME treatment impeded blood pressure collapse.

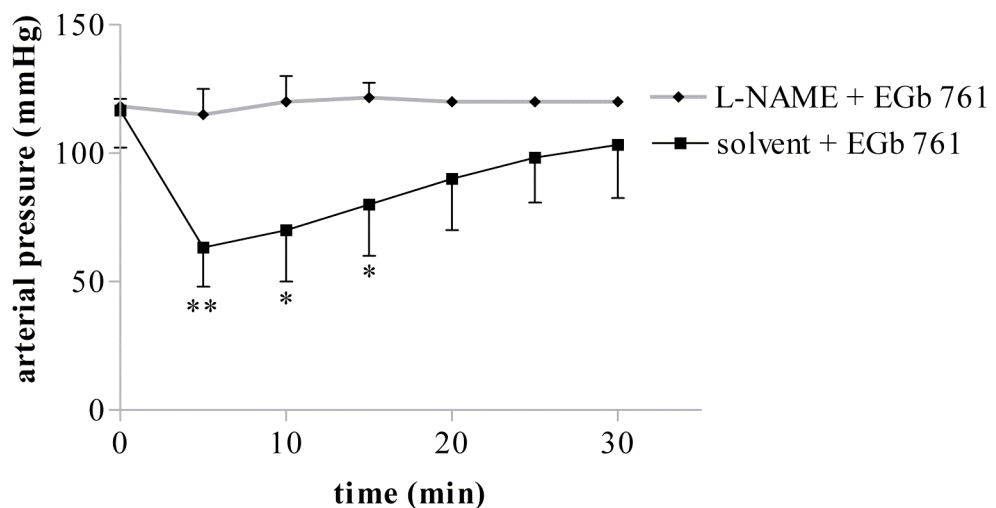


Figure 25 Blood pressure of rats was monitored for 30 min after i.v. EGb 761 application. Animals received L-NAME (grey line) or solvent (black line), respectively, 15 min prior to EGb 761 (20 mg/kg) application. Data are presented as mean  $\pm$  SEM (n=3, \*p<0.05 vs. L-NAME + EGb 761, Student's t-test).

#### 3.1.2.2 eNOS EXPRESSION IN ISOLATED THORACIC AORTA

Thoracic aortas were harvested from Sprague-Dawley rats pretreated with either solvent or EGb 761 (20 mg/kg), respectively. WB analysis shows that EGb 761 treatment increases eNOS phosphorylation (Ser-1177; upper panel), compared to solvent treated animals (Figure 15). Total eNOS protein confirmed equal protein loading (lower panel).

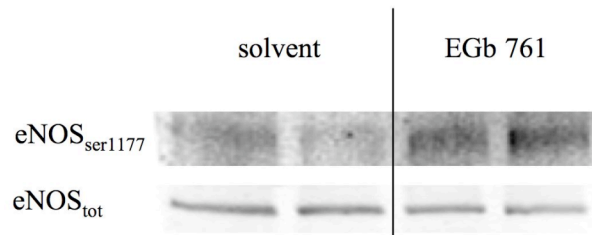


Figure 26 Western blot analysis of solvent or EGb 761 treated animals, respectively. Phosphorylated eNOS (Ser 1177; upper panel) and total eNOS (lower panel). All experiments were performed at least three times. One representative Western blot is shown.

## 3.2 XANTHOTHUMOL AND 3-HYDROXYXANTHOTHUMOL

### 3.2.1 Impact on ROS levels in a cell-free system

The ability of the compounds to scavenge superoxide radical was evaluated by chemiluminescence measurement using the xanthine/xanthine-oxidase assay.

The time course demonstrated that chemiluminescence is emitted right after luminol (0.66 mM) and xanthine-oxidase (0.33 U/ml) injection, peaking after approximately 8 seconds and declining continuously thereafter (Figure 27). Chemiluminescence was reduced by Xanthothumol in a concentration dependent manner.

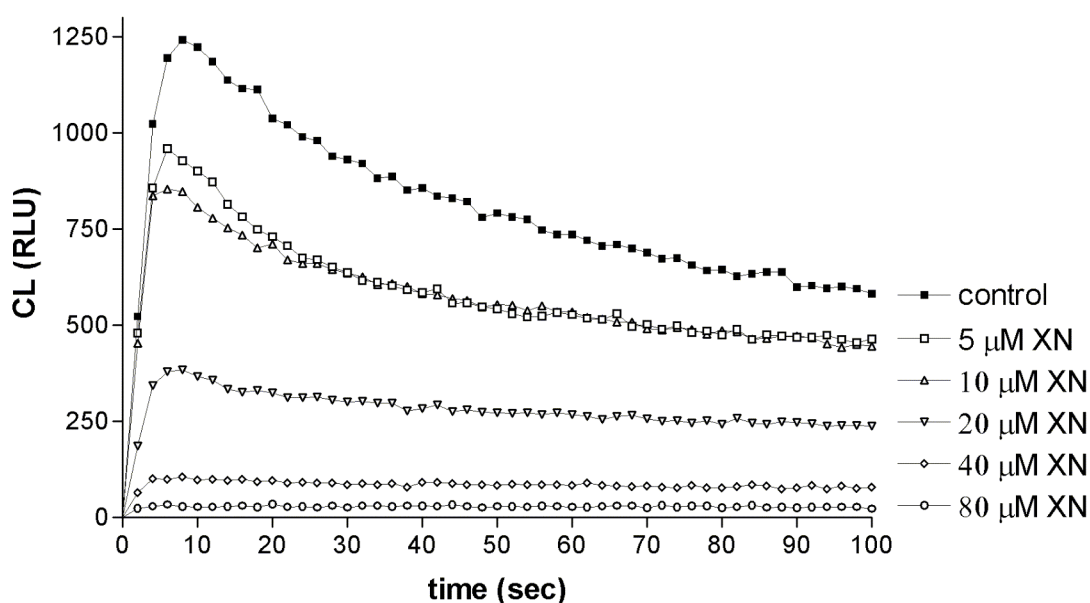


Figure 27 Chemiluminescence light emission for different XN concentrations in comparison to solvent treated samples (control). One representative time course for each concentration is shown.

When illustrated as area under the curve (AUC), XN (Figure 28) and OH-XN (Figure 29), respectively, showed both a dose-dependent reduction in chemiluminescence, indicating a reduction of ROS levels. The potency for each was assessed by the dilution that led to 50 % inhibition of ROS detection ( $IC_{50}$ ).  $IC_{50}$  was 15  $\mu$ M for XN and 25  $\mu$ M for OH-XN, respectively.

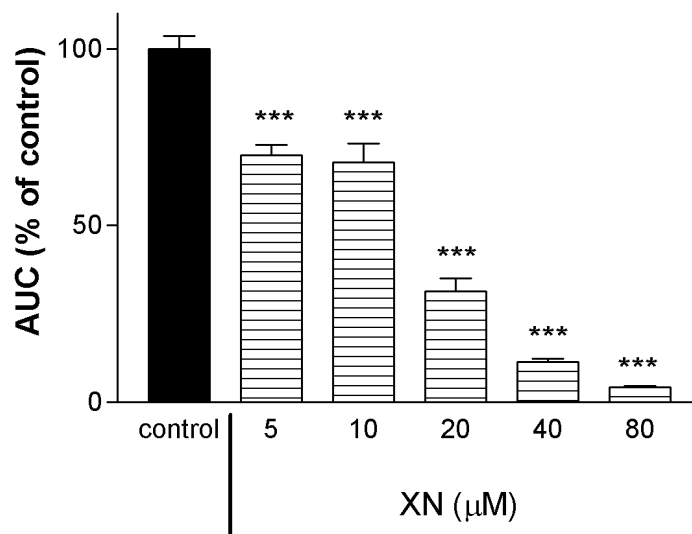


Figure 28 Area under the curve (AUC) of light emission from chemiluminescence reaction for different XN concentrations in comparison to solvent treated controls. Data are presented as mean  $\pm$  SEM (n=9, \*p<0.05 vs. control, Student's t-test).

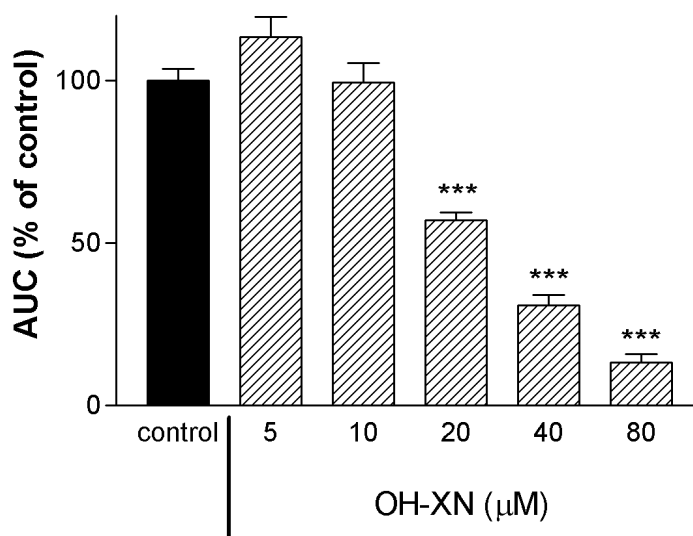


Figure 29 Area under the curve (AUC) of light emission from chemiluminescence reaction for different OH-XN concentrations in comparison to solvent treated controls. Data are presented as mean  $\pm$  SEM (n=9, \*p<0.05 vs. control, Student's t-test).

### 3.2.2 Influences on the redox status in a cellular system

Intracellular response to oxidative challenge with  $H_2O_2$  was measured by loading HEK 293 cells with 20  $\mu M$  dihydrofluorescein diacetat ( $H_2FDA$ ). After penetrating the cell membrane, ester groups are cleaved by esterases, which leads to the formation of dihydrofluorescein, a ROS-sensitive fluorescence dye. 40  $\mu M$  of XN and OH-XN, respectively, showed significant fluorescence reduction (XN = 71.91 %  $\pm$  9.2; OH-XN = 15.1 %  $\pm$  2.8) in comparison to the corresponding control (Figure 30). Moreover, OH-XN significantly exceeds the activity of the well-established antioxidant N-acetylcysteine (NAC; 1 mM).

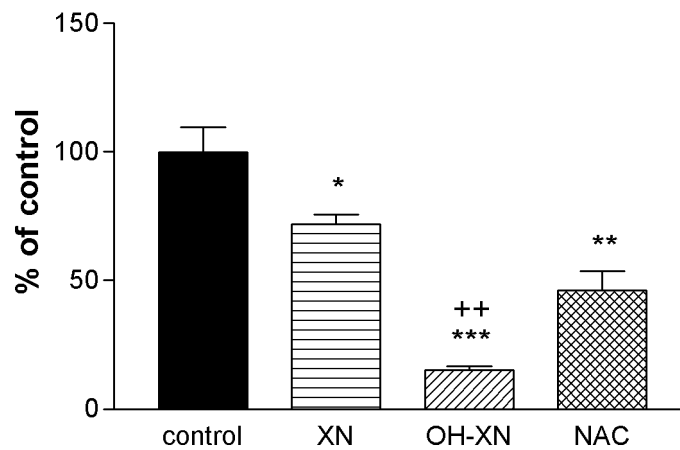


Figure 30 Fluorescence was measured of HEK 293 cells pretreated with 40 $\mu M$  XN or OH-XN prior to stimulation with  $H_2O_2$ . Significance was calculated at a 95 % concentration interval in comparison to the corresponding controls (\*) and NAC (+), respectively. Data are presented as mean  $\pm$  SEM (n=4; Student's t-test).

### 3.2.3 Influences on NF- $\kappa$ B activity in a reporter gene assay

As illustrated in Figure 31, TNF- $\alpha$  (1 ng/ml) induced an increase of NF- $\kappa$ B activity, which was dose-dependently reduced by pretreatment with XN and OH-XN (5 – 60  $\mu$ M), respectively. Pyrrolidine dithiocarbamate (PDTC; 50  $\mu$ M) pretreatment, which served as positive control, reduced the NF- $\kappa$ B activity to 53.9 %  $\pm$  7. Interestingly, OH-XN (IC<sub>50</sub> 13  $\mu$ M) showed greater inhibitory effects than XN (IC<sub>50</sub> 35  $\mu$ M). The capability was assessed by the dilution that produced 50 % inhibition of NF- $\kappa$ B activity (IC<sub>50</sub>).

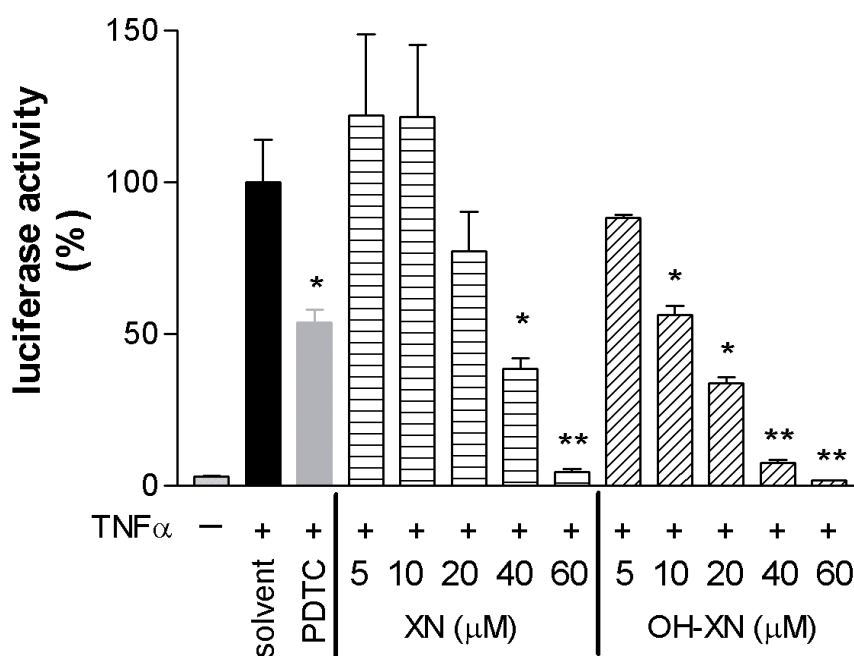


Figure 31 NF- $\kappa$ B promoter activity of HEK 293 cells treated with different concentrations of XN and OH-XN, respectively, prior to TNF- $\alpha$  stimulation. Cells treated with solvent served as control group and PDTC treated cells were used as a positive control. Data are presented as mean  $\pm$  SEM (n=3, \*p<0.05 vs. solvent, Student's t-test).

### 3.2.4 Impact on warm ischemia/warm reperfusion

#### 3.2.4.1 NF- $\kappa$ B BINDING ACTIVITY

The impact of XN on NF- $\kappa$ B binding activity was evaluated by EMSA of isolated nuclear extracts of the hepatic tissue samples. Figure 32 shows NF- $\kappa$ B inhibition of animals treated with both 8 mg/kg XN preischemic and 8 mg/kg XN postischemic, when subjected to 1 hour warm ischemia followed by 2 hours reperfusion.

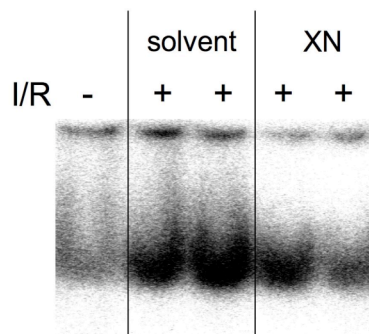


Figure 32 NF- $\kappa$ B binding activity was determined by EMSA of rat liver tissues harvested after 1 hour of warm ischemia followed by 2 hours of warm reperfusion. Animals were treated with both 8 mg/kg XN preischemic and 8 mg/kg XN postischemic or solvent, respectively. Control animals were left untreated. All experiments were performed at least three times. One representative gel shift experiment is shown.

NF- $\kappa$ B binding activity of animals subjected to long reperfusion periods (6 h; Figure 33) were treated with 8 mg/kg XN, administered pre- and postischemic. NF- $\kappa$ B activity induced by IR was markedly reduced by XN treatment.

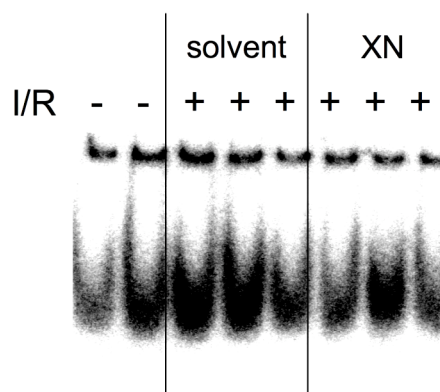


Figure 33 NF- $\kappa$ B binding activity was determined by EMSA of whole rat liver homogenates subjected to 1 hour of warm ischemia followed by 6 hours of reperfusion. Animals were treated with both 8 mg/kg XN preischemic and 8 mg/kg XN postischemic or solvent, respectively. Control animals were left untreated. All experiments were performed at least three times. One representative gel shift experiment is shown.

### 3.2.4.2 LIVER TISSUE INJURY

Blood samples were collected at the end of reperfusion time and were analyzed for liver enzymes (ALT + AST), which indicate the degree of liver injury. Animals subjected to 1 hour of warm ischemia followed by 2 hours of warm reperfusion showed significantly elevated liver enzyme levels, which kept unchanged after XN treatment (Figure 34).

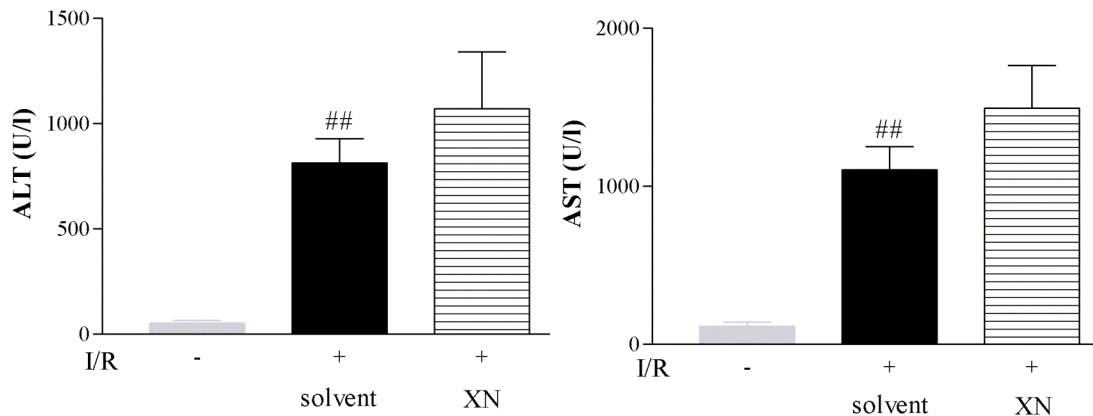


Figure 34 ALT + AST levels of rats subjected to 1 hour of warm ischemia followed by 2 hours of reperfusion, treated with both 8 mg/kg XN preischemic and 8 mg/kg XN postischemic or the respective solvent, respectively. Data represent means  $\pm$  SEM (n=3; #p<0.05 vs. untreated controls; Student's t-test).

Xanthohumol treatment did not alter the injury outcome after long reperfusion times either (6 hours; Figure 35).

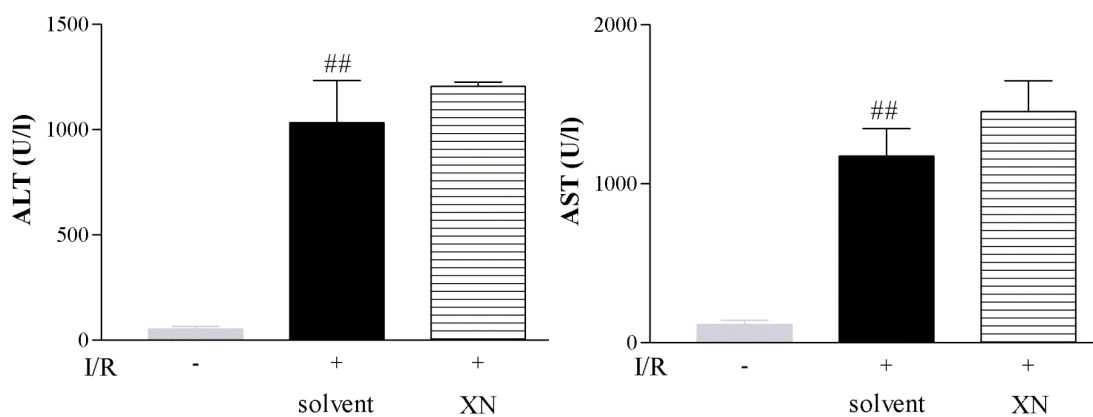


Figure 35 ALT + AST levels of rats subjected to 1 hour of warm ischemia followed by 6 hours of warm reperfusion, treated with both 8 mg/kg XN preischemic and 8 mg/kg XN postischemic or the respective solvent, respectively. Data represent means  $\pm$  SEM (n=3; #p<0.05 vs. untreated controls; Student's t-test).

### 3.2.5 Impact on cold ischemia/warm reperfusion

#### 3.2.5.1 ENDOGENOUS ANTIOXIDANT SYSTEM

The levels of the endogenous antioxidants GSH and SOD were significantly reduced in IR subjected animals compared to untreated controls. XN or OH-XN (2.26 mM) administration prior to the ischemic period, respectively, reversed that decrease (Figure 36; Figure 37).

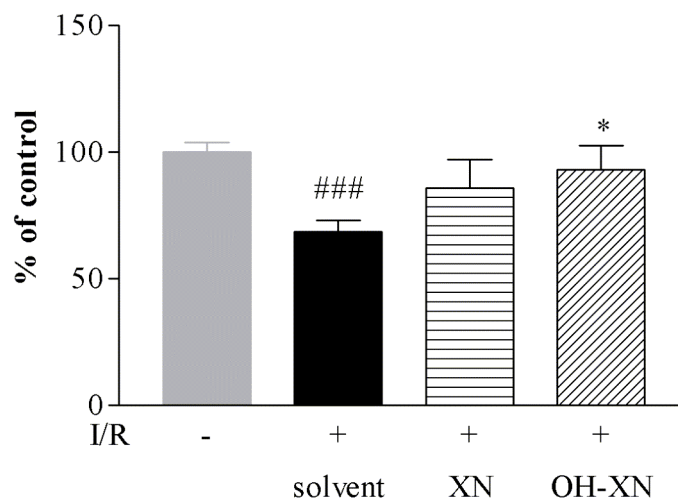


Figure 36 Tissue GSH levels of rats treated with 2.26 mM of XN, OH-XN or solvent, respectively, prior to cold hepatic IR. Control animals were left untreated. Data represent means  $\pm$  SEM of triplicates (3 animals each group). # $p < 0.05$  vs. untreated control or \* $p < 0.05$  vs. solvent (Student's t-test).

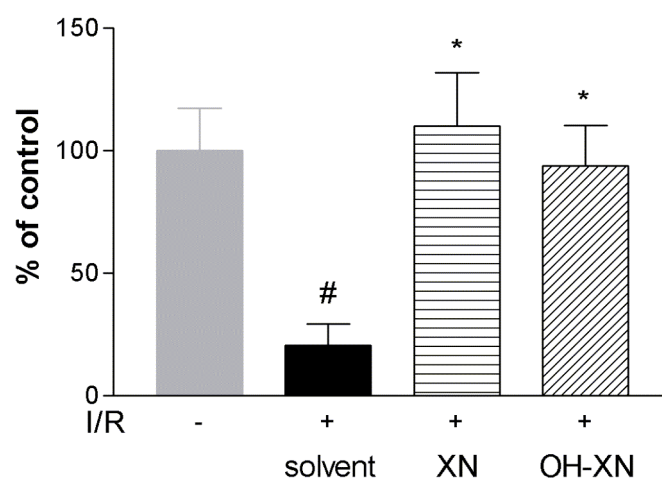


Figure 37 Tissue SOD levels of rats treated with 2.26 mM of XN, OH-XN or solvent, respectively, prior to cold hepatic IR. Control animals were left untreated. Data represent means  $\pm$  SEM (n=3). # $p < 0.05$  vs. untreated control or \* $p < 0.05$  vs. solvent (Student's t-test).

### 3.2.5.2 OXIDATIVE DAMAGE

Determination of lipid peroxidation was evaluated by quantifying the malondialdehyde (MDA) content with the thiobarbituric acid reactive substance (TBARS) assay. No differences could be observed between the untreated control animals, solvent treated IR group as well as the groups that received 2.26 mM XN or OH-XN, respectively, prior to the ischemic period (Figure 38).

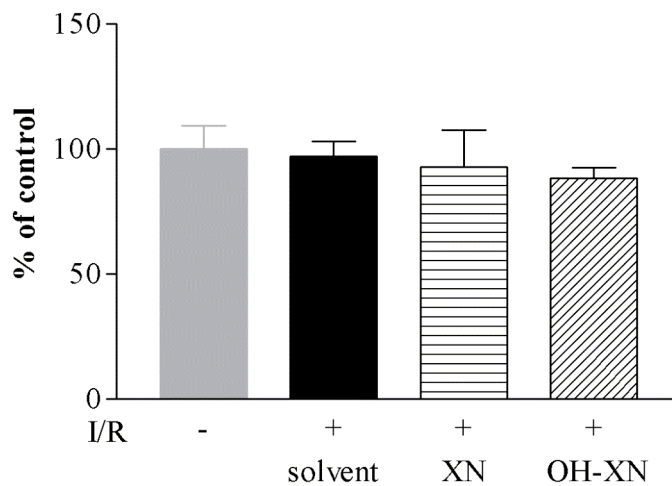


Figure 38 Tissue MDA levels of rats treated with 2.26 mM of XN, OH-XN or solvent, respectively, prior to 6 hours cold hepatic ischemia followed by 150 minutes of warm reperfusion. Control animals were left untreated. Data represent means  $\pm$  SEM (n=3).

### 3.2.5.3 NF- $\kappa$ B BINDING ACTIVITY

To investigate the impact of XN and OH-XN on NF- $\kappa$ B DNA binding activity, the electrophoretic mobility shift assay (EMSA) was performed with isolated nuclear extracts of the hepatic tissue samples. As shown in Figure 39, NF- $\kappa$ B activity of the solvent treated group is strongly increased after 6 hours of cold ischemia followed by reperfusion of 150 minutes with KH solution (pH 7.4, 37 °C, 95 % O<sub>2</sub> / 5 % CO<sub>2</sub> saturation) when compared to untreated controls. Animals treated with 2.26 mM XN prior to the ischemic period revealed attenuated DNA binding activity of NF- $\kappa$ B, whereas OH-XN (2.6 mM) administration had no impact.

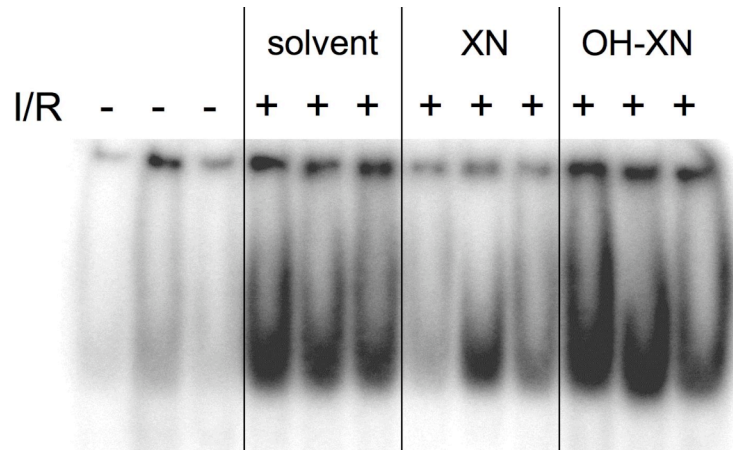


Figure 39 NF- $\kappa$ B binding activity was determined by EMSA of whole rat liver homogenates treated with 2.26 mM of XN, OH-XN or solvent, respectively, prior to IR. Control animals were left untreated. All experiments were performed at least three times. One representative gel shift experiment is shown.

#### 3.2.5.4 PROTEIN LEVELS

Akt is described as a typical antiapoptotic kinase involved in ischemia/reperfusion injury.<sup>134</sup> XN and OH-XN (2.26 mM) pretreatment, respectively, abrogated the phosphorylation on Ser-473 in comparison to solvent treated animals after cold IR (Figure 40).

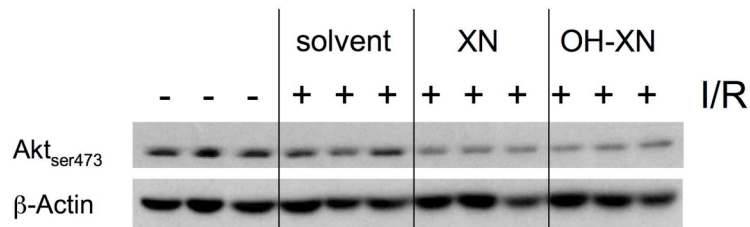


Figure 40 Hepatic protein levels of phosphorylated Akt (Ser-473; upper panel) and  $\beta$ -Actin (lower panel) by WB analysis of livers treated with 2.26 mM of XN, OH-XN or solvent, respectively, prior to IR. Control animals were left untreated. One representative blot is shown.

Interestingly, the phosphorylation on position Thr-308 was markedly abolished only after XN pretreatment after cold IR (Figure 41). It has been shown in literature, that Thr-308 is the main activating event of Akt, although phosphorylation of both domains might be necessary for full activation of Akt.<sup>134</sup>

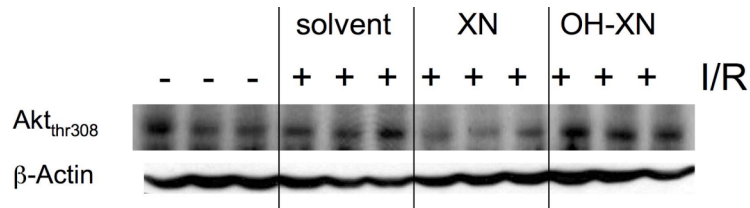


Figure 41 Hepatic protein level of phosphorylated Akt (threonin 308; upper panel) and  $\beta$ -Actin (lower panel) by WB analysis of livers treated with 2.26 mM of XN, OH-XN or solvent, respectively, prior to IR. Control animals were left untreated. One representative blot is shown.

The proteins of the Bcl-2 family exerts either pro- or antiapoptotic effects. Bcl-xl belongs to the group of antiapoptotic proteins.<sup>135</sup> XN (2.26 mM) reduced the protein level of Bcl-xl after cold IR, when administered before the ischemic period, whereas OH-XN (2.26 mM) had no effect (Figure 42).

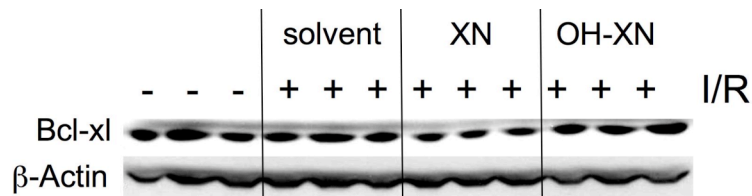


Figure 42 Hepatic protein level determination of Bcl-xl (upper panel) and  $\beta$ -actin (lower panel) by WB analysis of livers treated with 2.26 mM of XN, OH-XN or solvent, respectively, prior to IR. Control animals were left untreated. One representative blot is shown.

JNK activation occurs primarily in the reperfusion phase in response to ROS.<sup>22, 136</sup> Treatment with 2.26 mM of XN and OH-XN before the ischemic period reduced the protein level of phosphorylated JNK slightly after cold IR (Figure 43).

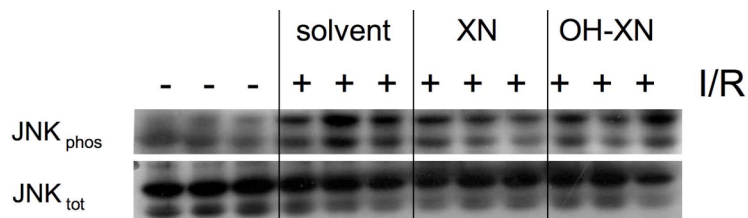


Figure 43 Hepatic protein level of phosphorylated JNK (upper panel) and total JNK (lower panel) by WB analysis of livers treated with 2.26 mM of XN, OH-XN or solvent, respectively, prior to IR. Control animals were left untreated. One representative blot is shown.

### 3.2.5.5 APOPTOSIS

Hepatic caspase-3 like activity was measured, as caspase-3 is known to be one of the main effector molecules of apoptosis.<sup>133</sup> Caspase-3 activity was induced by cold IR (Figure 44). XN (2.26 mM) treatment showed an additional increase in activity, which was not seen after OH-XN (2.26 mM) treatment.

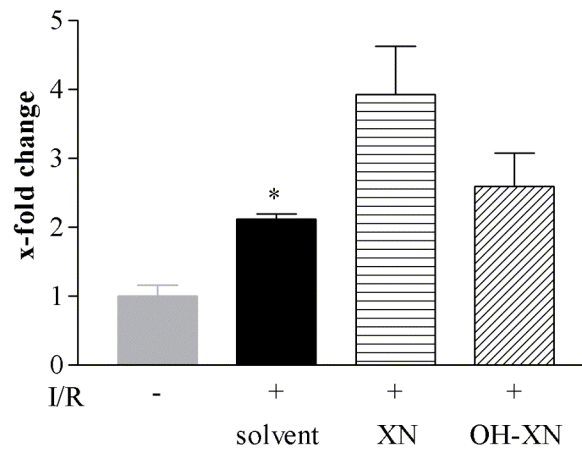


Figure 44 Caspase-3 like activity of animals treated with 2.26 mM of XN, OH-XN or solvent, respectively, prior to ischemia/reperfusion. Control animals were left untreated. Data are presented as mean  $\pm$  SEM (n=3, \*p<0.05 vs. untreated control, Student's t-test).

### 3.2.5.6 TNF- $\alpha$ LEVELS

Plasma levels of TNF- $\alpha$  were determined by ELISA (Figure 45). XN and OH-XN pretreatment, respectively, did not show significant changes compared to solvent treated animals.

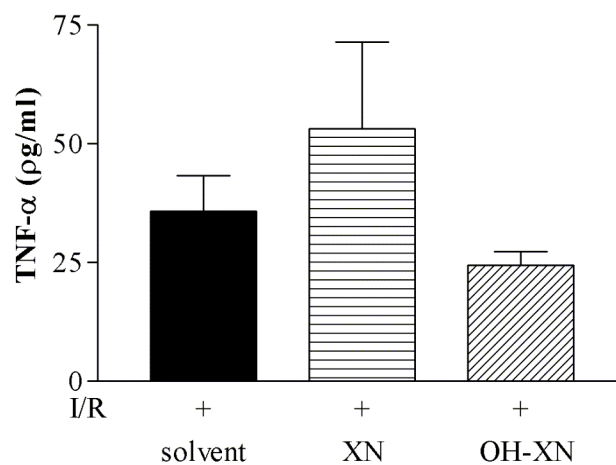


Figure 45 TNF- $\alpha$  levels of perfusates were determined by ELISA, of XN (2.26 mM), OH-XN (2.26 mM) or solvent treated animals, respectively. Data are presented as mean  $\pm$  SEM (n=3).

### 3.2.5.7 LIVER TISSUE INJURY

The perfusates were collected during the reperfusion period and LDH levels were determined, indicating hepatic tissue damage. Figure 46 demonstrates the time course of LDH development throughout the reperfusion period. LDH levels slightly decreased to the beginning and increased continuously to the end. XN and OH-XN pretreatment increased LDH levels to the end of reperfusion, although the results were not significant.

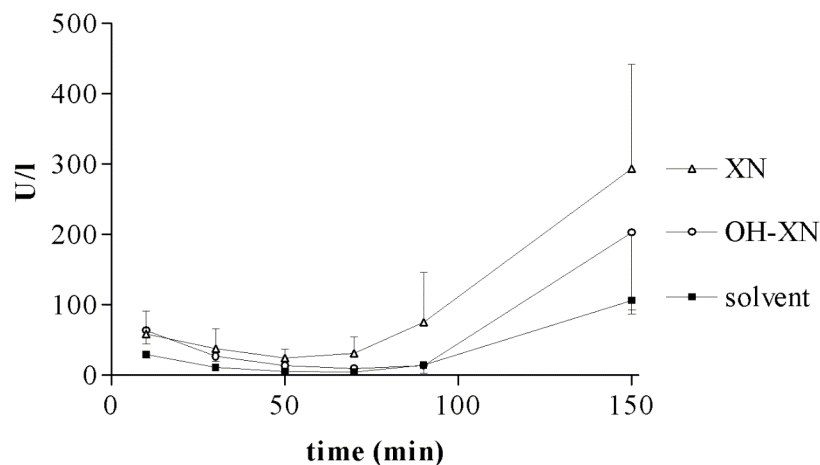


Figure 46 Time course of LDH levels throughout the reperfusion period from rats pretreated with 2.26 mM of XN, OH-XN or solvent, respectively. Data are presented as mean  $\pm$  SEM (n=3).

The transaminases (AST, ALT) were analyzed at the end of reperfusion (Figure 47). Interestingly, the XN treated group showed an obvious increase in the liver enzymes, whereas the levels of the OH-XN treated group remained unaltered.

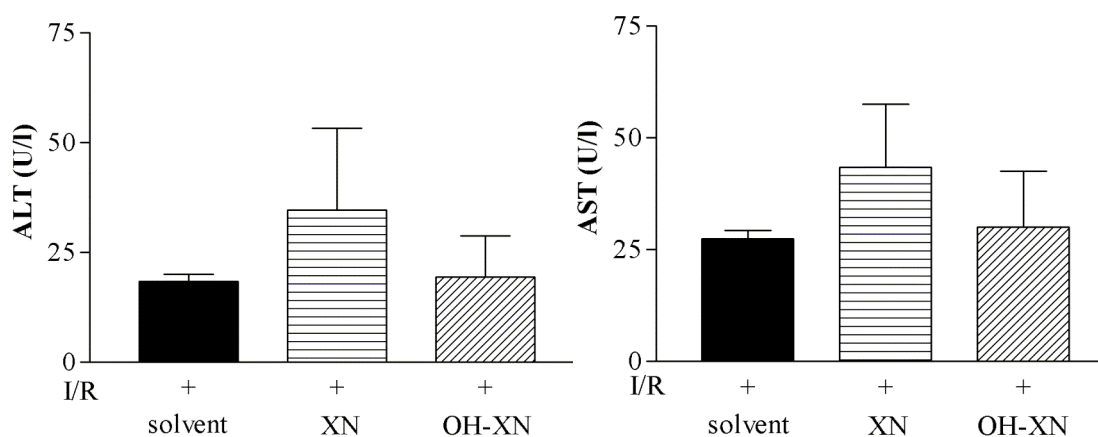


Figure 47 ALT + AST levels of rats treated with 2.26 mM of XN, OH-XN or solvent, respectively, prior to 6 hours of cold ischemia followed by 150 minutes of warm reperfusion. Data are presented as mean  $\pm$  SEM (n=3).

### 3.3 NF- $\kappa$ B DECOY NANOPARTICLES

#### 3.3.1 Biodistribution

Confocal laser scanning microscopy was performed to proof the suitability of decoy nanoparticles application in the *ex vivo* model of cold ischemia/warm reperfusion. Dr. Florian Hoffmann has already shown in his Ph.D. thesis, that decoy nanoparticles administered i.v. *in vivo* predominantly localize in hepatic tissue, moreover, selectively lead to colocalization in Kupffer cells. Therefore, the liver was treated with fluorescent labeled decoy ODNs loaded onto gelatin nanoparticles as described in chapter 2.4.5.3. Figure 48 displays that fluorescent labeled decoy ODNs (red) are selectively taken up by Kupffer cells (green), as indicated in the overlaid picture by the yellow color. No decoys were found in hepatocytes.

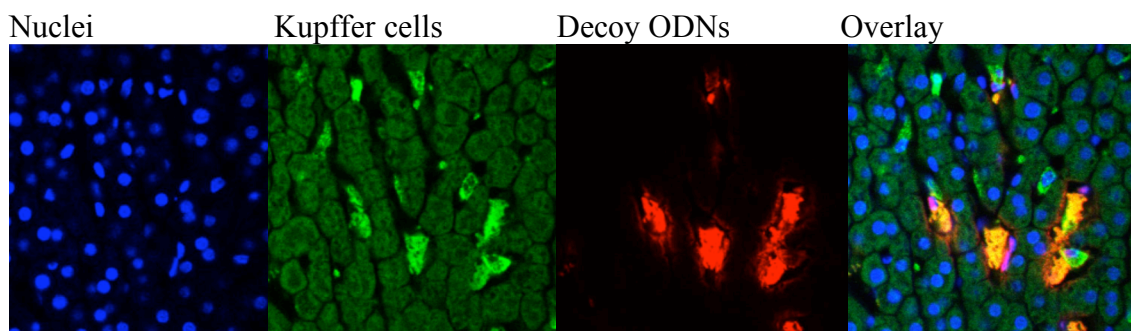


Figure 48 Confocal microscopy. Blue: Nuclei; Green: Kupffer cells; Red: Decoy ODNs. The yellow color indicates colocalization of Kupffer cells and decoy ODNs.

#### 3.3.2 Impact on cold ischemia/warm reperfusion

##### 3.3.2.1 NF- $\kappa$ B BINDING ACTIVITY

NF- $\kappa$ B DNA binding activity was elucidated with the electrophoretic mobility shift assay (EMSA), which was performed with isolated nuclear extracts of hepatic tissue samples, subjected to 6 hours cold ischemia followed by 150 minutes of warm reperfusion. As shown in Figure 49, ischemia/reperfusion induces NF- $\kappa$ B activation which was abolished by NF- $\kappa$ B decoy-NP (20 nM) treatment prior to the ischemic period. However, scrambled decoy-NP had no effect.

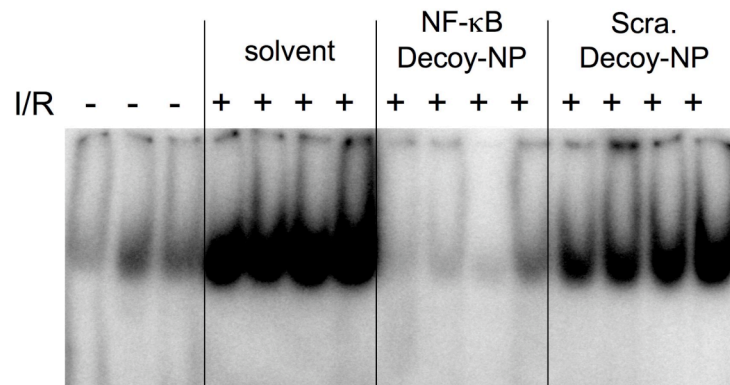


Figure 49 NF- $\kappa$ B binding activity was determined by EMSA of whole rat liver homogenates treated with 20 nM of NF- $\kappa$ B decoy-NP, scrambled decoy-NP or solvent, respectively, prior to 6 hours of cold ischemia followed by reperfusion. Control animals were left untreated. All experiments were performed at least three times. One representative gel shift experiment is shown.

### 3.3.2.2 LIVER TISSUE INJURY

Perfusate samples were collected throughout the reperfusion period and transaminases were determined. The liver enzymes (AST, ALT) were determined after 6 hours of cold ischemia followed by 150 minutes of warm reperfusion. No significant changes of NF- $\kappa$ B decoy-NP pretreatment could be observed, respectively (Figure 50).

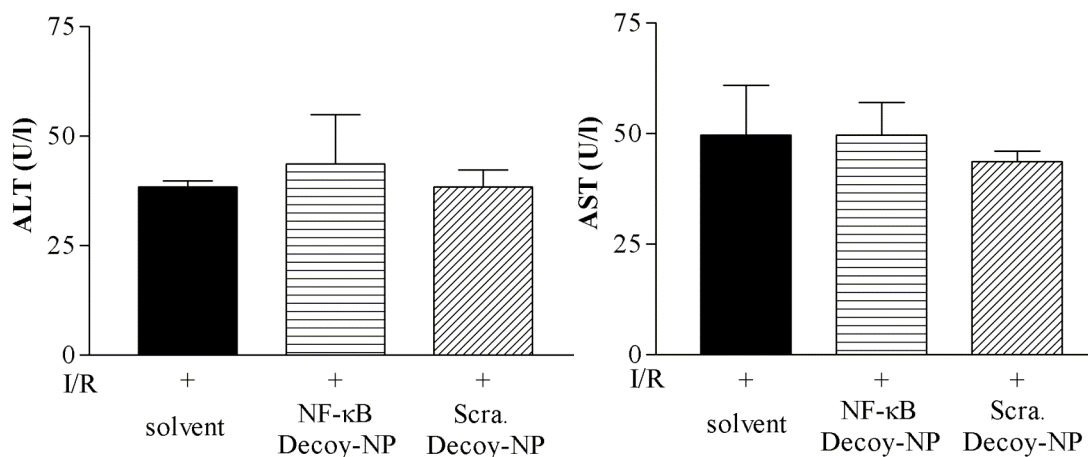


Figure 50 ALT + AST levels of livers subjected to 6 hours of cold ischemia followed by reperfusion. Rats were treated before the ischemic period with 20 nM of NF- $\kappa$ B decoy-NP solution, scrambled decoy-NP solution or solvent, respectively. Data are presented as mean  $\pm$  SEM (n=3).

# **DISCUSSION**

#### 4.1 GINKGO BILOBA EXTRACT – EGB 761

The standardized Ginkgo biloba leaf extract, EGb 761 from Dr. Willmar Schwabe Pharmaceuticals, has shown to have a multifaceted variety of molecular functions like antioxidant activities, vasoregulatory properties, beneficial actions on mitochondrial function and others, which are responsible for its therapeutic use.<sup>6</sup> The complementary actions of its different constituents possibly result in additive, synergistic as well as antagonistic properties. Therefore, studies elucidating single ingredients of this complex extract do not reflect doubtlessly the effect of the whole extract.

The pathomechanism of the hepatic IRI is very complex, resulting in severe hepatocellular injury. Several pathways participate in the injury cascade, such as mitochondrial function, redox system, sinusoidal microcirculation and the NF- $\kappa$ B signal transduction cascade. Therefore, it is difficult to achieve tissue protection by targeting single mediators. Hence, simultaneous interventions at several stages of this process could be advantageous. Thus, complex extracts offer a variety of opportunities as they address several molecular targets.

Grape seed<sup>137</sup>, green tea<sup>45</sup> and garlic extract<sup>138</sup> have previously demonstrated to be protective in different models of hepatic IRI. The beneficial effects were mainly referred to their antioxidant potential due to the high levels of polyphenols. Furthermore, the literature offers a large number of studies elucidating EGb 761 in IR of different organs like heart<sup>84</sup>, kidneys<sup>77</sup>, bladder<sup>139</sup>, brain<sup>140</sup>, intestine<sup>141</sup> and others, all demonstrating protective effects.

Interestingly, only two studies were previously performed to evaluate EGb 761 in hepatic IRI, both by Gundlach and colleagues.<sup>81, 142</sup> They revealed that intravenous EGb 761 (20 mg/kg) administration prior to warm IR, increases the hepatic microcirculation, due to attenuated leukocyte adherence and plugging in postsinusoidal vessels.<sup>81</sup> However, classic hepatic tissue injury markers (AST, ALT) were unaltered. In our studies, intravenous administration of different concentrations of EGb 761 revealed that 2 mg/kg significantly increased liver tissue damage after IR as measured by transaminases (Figure 22). Moreover, a further increase to 20 mg/kg EGb 761, the same dosage as Gundlach and colleagues used, showed an impressive augmentation of the

liver injury. These results indicate an enhanced toxicity of EGb 761, when given intravenously before warm IR. The differences to Gundlach and colleagues might be due to differences in the method applied, as we chose a longer ischemic period (1 hour vs. 1.5 hours) and a different race of rats (Lewis vs. Sprague-Dawley). The caspase-3 like activity levels did not correlate with the levels of transaminases, instead they remained unchanged (Figure 23). Hence, caspases do not seem to be involved in tissue injury followed by IR after EGb 761 treatment.

However, impressive acute blood pressure decrease came along with that, which could be a reason for impaired tissue damage. Within minutes after EGb 761 (20 mg/kg) administration (Figure 24), blood pressure dropped from approximately 110 mmHg to 60 mmHg. Obviously, the blood circulation was markedly hindered right after the onset of reperfusion, hence, macroscopic tissue vessel thrombosis was noticed more frequently. Interestingly, in literature no studies described an acute arterial blood pressure decrease by EGb 761 or Ginkgo biloba extract treatment so far, respectively. Although similar dosages of EGb 761 were administrated in the same mode (i.v.), indeed blood pressure was never monitored,<sup>141, 143</sup> except from three long-term feeding studies of Ginkgo biloba extract or EGb 761, respectively. These studies revealed blood pressure attenuation in hypertensive or physiologically healthy rats, respectively,<sup>144-146</sup> when pretreated orally. Sasaki et al. assumed that on the one hand, a decrease in oxidative stress reduces the withdrawal of NO for peroxynitrite formation, on the other hand, an increase of mRNA levels of eNOS were proposed to be responsible for elevated NO levels.<sup>145</sup> Additionally, Dr. Anja Koltermann revealed in her Ph.D. thesis that eNOS is activated by EGb 761 treatment *in vitro*, which is regulated by the phosphoinositide 3-kinase (PI3K)/Akt pathway.

Eventually, to investigate the underlying mechanism of acute hypotension and the involvement of eNOS in this process, a selective inhibitor of eNOS was given *in vivo* before EGb 761 administration. As seen in Figure 25, eNOS inhibition with L-NAME impeded the acute arterial blood pressure attenuation. Moreover, eNOS protein levels of isolated aortic rings, extracted from EGb 761 pretreated rats, were clearly elevated (Figure 26). Hence, the author concludes that the acute attenuation of the arterial blood pressure due to EGb 761 treatment is more likely eNOS regulated, than caused by a reduction of oxidative stress as claimed by Sasaki et al..<sup>145</sup>

In consideration of the increased tissue damage after treatment of EGb 761 prior to warm IR, at least two reasons can be assumed. On the one hand, the systemic blood pressure drop, mediated by the NO/GC pathway, leads to severe microcirculatory disturbances resulting in reduced liver blood flow and microvessel thrombosis. On the other hand, direct cytotoxicity, which is most likely caused by the generation of peroxynitrite. Since iNOS activation is known to be upregulated during IRI,<sup>44</sup> in this case both, iNOS and eNOS, might contribute to elevated NO levels thus favoring peroxynitrite generation.

In conclusion, EGb 761 administration prior to warm IR of the liver has no beneficial effect, on the contrary, it is rather toxic. Therefore, this project did not focus in more detail on the IR process, as the therapeutic use of EGb 761 in this model is not appropriate. Hence, acute hypotension after EGb 761 administration was the main interest, as it might be crucial for impaired tissue damage due to constricted microcirculation during reperfusion. Here, it could be demonstrated that EGb 761 upregulates eNOS activation, which is responsible for acute hypotension after intravenous administration (Figure 51). On the contrary, it can be hypothesized that the beneficial therapeutic effects of EGb 761 in vascular diseases might be also related to its molecular function on eNOS regulation.

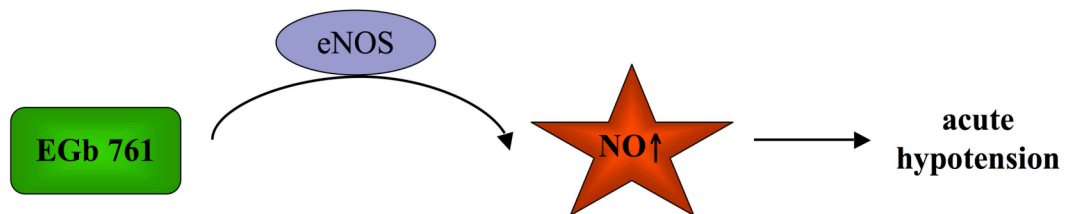


Figure 51 Concluding results of intravenous EGb 761 application *in vivo*.

However, the mode of EGb 761 application seems to be important, as oral or intraperitoneal administrations did not worsen hepatic tissue injury.<sup>146-148</sup> Studies on the pharmacokinetics of oral EGb 761 administration revealed that the bioavailability of the flavonol glycosides is either relatively low or the metabolic biotransformation is high. However, ginkgolide A and B as well as bilobalides were found to be bioavailable, despite high urinary excretion.<sup>149</sup> This recommends that the spectrum of active components of EGb 761 is strongly influenced by way of administration and thus is arbitrate for the toxicological impact of EGb 761 *in vivo*.

## 4.2 XANTHOTHUMOL AND 3-HYDROXYXANTHOTHUMOL

In the 1990<sup>th</sup>, epidemiological studies indicated that the French population suffers a relatively low incidence of coronary heart diseases despite high intake of saturated fat. It was assumed that the comparable high wine consumption of the French population is responsible for this phenomenon, today also referred to as “French paradox”.<sup>9, 150</sup> In the following years, research indicated that the polyphenol resveratrol is a main contributor, as it is in particular present in grapes, thus in red wine.<sup>151, 152</sup>

In recent years, several dietary polyphenols like epigallocatechine, quercetin, taxifolin, rutin and isoliquiritigenin to name a few, which are mainly found in fruits, vegetables, tea, grains and legumes, gained interest due to their health benefits and protective effects in different human disease models.<sup>2, 7</sup> Their antioxidant activities are assumed to be mainly responsible for these effects.<sup>8, 96</sup> In the oxidative stress driven hepatic IR model, several flavonoids and polyphenols showed beneficial effects in preventing hepatic tissue damage.<sup>99-103</sup>

The antioxidant activities of XN, the principal prenylated flavonoid of the hop plant, and of OH-XN, a metabolite occurring during XN biotransformation, were published *in vitro* by different groups.<sup>10, 107, 128</sup> In this work the antioxidant activity of both compounds were verified to provide a basis for following *in vivo* experiments. Both, XN and OH-XN, showed strong inhibitory activities on ROS production in the xanthine/xanthine-oxidase cell-free system (Figure 28; Figure 29). The IC<sub>50</sub> of XN (15µM) in comparison to the work of Gerhäuser was slightly different, what might be due to differences in the method applied.<sup>10</sup> Interestingly, in the cellular model (H<sub>2</sub>FDA assay) OH-XN showed a significant higher inhibitory capacity on oxidative stress induced by H<sub>2</sub>O<sub>2</sub> compared to XN (Figure 30). OH-XN even exceeded the activities of the well-known antioxidant N-acetylcysteine (NAC).<sup>153</sup> Structural differences of both compounds could explain these results, as structural activity relationship (SAR) studies for other polyphenolics showed that the amount of hydroxyl substituents and their specific arrangement affects their antioxidant activity. More precisely, an ortho-diphenoxyl functionality and an added hydroxyl group, as seen for OH-XN, did increase the antioxidant potential of these compounds.<sup>108-110</sup>

The activation of the redox sensitive transcription factor NF- $\kappa$ B was suggested to be relevant for hepatic IRI, as it upregulates the expression of different proinflammatory genes.<sup>66, 154</sup> Oral treatment of rats with green tea extract, which contains high levels of polyphenols, has demonstrated to inhibit NF- $\kappa$ B binding activity in hepatic warm IR.<sup>45</sup> Influences of XN on NF- $\kappa$ B were previously shown *in vitro* in different cancer cell models.<sup>117, 118</sup> In this study, XN and OH-XN reduced NF- $\kappa$ B activation dose-dependently in a NF- $\kappa$ B reportergene assay (Figure 31). Interestingly, the IC<sub>50</sub> of the compounds (XN = 35  $\mu$ M; OH-XN = 13  $\mu$ M) did correlate with their antioxidant activity in the cellular model (Figure 30), since OH-XN displayed a higher potential in both models. This could prove that NF- $\kappa$ B activation correlates with oxidative stress, as already shown in several models.<sup>15</sup> Moreover, the author illustrates for the first time that XN is able to inhibit NF- $\kappa$ B DNA binding activity *in vivo* in the complex process of warm IR, regardless of the duration of reperfusion (Figure 32; Figure 33). It is proposed in literature that hepatic NF- $\kappa$ B activation induced by IR correlates with the severity of tissue damage, thus, its inhibition is beneficial.<sup>33, 66, 154, 155</sup> Surprisingly, the tissue damage as indicated by the release of liver enzymes (AST, ALT) in the blood circulation, did not correlate with NF- $\kappa$ B inhibition after XN treatment in warm IR, instead levels were unaltered (Figure 34; Figure 35). Eventually, this could be an indication for the critical ambiguous role of NF- $\kappa$ B in the liver, since it is unlikely that XN inhibits NF- $\kappa$ B selectively in Kupffer cells, which are assumed to be mainly responsible for the transcription of proinflammatory mediators.<sup>24, 59, 60</sup> Therefore, the isolated cold IR model was chosen for further analysis of this complex mechanism, as extrahepatic factors such as interference with blood constituents as well as interactions with other organs can be excluded. Hence, the impact of the substances can be solely investigated on the liver.

Regarding their activity on the antioxidant system, XN and OH-XN treatment before cold IR displayed an impressive restoration of the superoxide dismutase (SOD) levels, which were strongly diminished by IR (Figure 37). SOD is an endogenous enzyme, which accounts for detoxification of a major proportion of the highly reactive superoxide anion radical in the liver tissue. The administration of SOD derivatives in the hepatic IR process has previously demonstrated to be protective.<sup>156</sup> Moreover, administration of the endogenous, non-enzymatic antioxidant GSH in different IR

models showed beneficial effects regarding the hepatic tissue injury.<sup>3, 157</sup> Both compounds were able to abrogate decreased GSH levels induced by cold IR (Figure 36). Furthermore, XN and OH-XN inhibited JNK activation slightly, which confirmed their impact on the antioxidant system, since JNK activation occurs primarily in the reperfusion phase in response to ROS (Figure 43).<sup>22, 136</sup> Lipid peroxidation is a parameter indicating oxidative damage to membrane lipids by ROS, which is assumed to be mainly involved in IRI. Here, no differences could be seen in the TBARS assay applied (Figure 38). This confirms the view of others, that lipid peroxidation is not necessarily an appropriate marker in the model of hepatic IRI.<sup>158</sup> Moreover, the TBARS assay determines malondialdehyde (MDA), which is a degradation product of polyunsaturated fatty acids. Its specificity toward other compounds than MDA is questionable,<sup>159</sup> although, it is the most widely performed assay to measure lipid peroxidation.

NF- $\kappa$ B activation was strongly reduced after XN treatment in cold IR, whereas, OH-XN did not have any impact (Figure 39), although its antioxidant activities were apparent as mentioned above. Interestingly, similar results were observed when the polyphenol curcumin is reduced to tetra-hydrocurcumin, which resulted in the loss of NF- $\kappa$ B inhibition although the antioxidant activity was still intact.<sup>160</sup> Moreover, it was demonstrated by Dell'Agli et al. that lipophilic catechin analogues inhibit NF- $\kappa$ B activity more potently than hydrophilic ones.<sup>161</sup> Furthermore, it can be assumed that the structural differences, which are associated with higher hydrophilicity of OH-XN, may impact the cellular uptake and the susceptibility for metabolic biotransformation, thus influencing the biological impact of OH-XN.

To investigate the way of NF- $\kappa$ B inhibition, the impact of XN and OH-XN on the Akt pathway was elucidated. Akt is an important upstream activator of NF- $\kappa$ B.<sup>134</sup> Activation leads to IKK phosphorylation in the cytoplasm, which in turn is able to phosphorylate I $\kappa$ B, thus, activating the translocation of NF- $\kappa$ B into the nucleus where it starts gene transcription. It has recently been reported *in vitro* that XN represses Akt phosphorylation.<sup>88</sup> Here, Akt inhibition of both phosphorylation domains (Thr-308; Ser-473) has been shown for XN (Figure 40; Figure 41), whereas OH-XN attenuated only phosphorylation on Ser-473. However, full activation of Akt requires phosphorylation of both domains, though it has been postulated that the first phosphorylation step on the

Thr-308 domain is the main activating event of Akt.<sup>134</sup> Thus, it can be assumed that the inhibition of Ser-473 phosphorylation by OH-XN results only in minimal Akt inhibition since Thr-308 is still phosphorylated. These results suggest that NF- $\kappa$ B inhibition by XN in cold IR is, at least in part, regulated by an Akt inhibition. However, the activation of NF- $\kappa$ B via ROS has to be challenged, since OH-XN showed no effect, although an impressive GSH and SOD upregulation was observed. Karin and colleagues confirmed these results as they found that endogenously produced ROS do not lead to NF- $\kappa$ B activation.<sup>153</sup>

Additionally, Akt is a central regulator of apoptosis as it inactivates proapoptotic molecules of the Bcl-2 family like Bad, thereby, antiapoptotic members such as Bcl-2 and Bcl-xl are activated.<sup>134</sup> Constitutively active Akt induced via adenoviral gene transfer, has shown to be protective as apoptosis is inhibited in the liver subjected to IR.<sup>162</sup> In contrast, inhibition of Akt with wortmannin is associated with reduced protection from hepatic IR.<sup>66</sup> In this work we could demonstrate that Akt inhibition by XN treatment correlates with diminished levels of the antiapoptotic protein Bcl-xl (Figure 42) as well as with an activation of caspase-3 (Figure 44). Caspases are intracellular cysteine proteases that mediate inflammation and cell-death. Caspase-3 in particular is the main effector molecule of apoptosis and a selective inhibition in the IR process effectively reduced hepatic IRI.<sup>133</sup> Eventually, liver tissue damage, as measured by the liver enzymes, was elevated by XN treatment and remained unchanged by OH-XN (Figure 47), furthermore the TNF- $\alpha$  levels correlated with the tissue damage (Figure 45).

In conclusion (Figure 52), these results indicate that the flavonoids Xanthohumol and 3-Hydroxyxanthohumol in the biological relevant model of hepatic IR, which is oxidative stress driven, do not improve tissue injury despite their extensive antioxidant activities. Moreover, based on these data, NF- $\kappa$ B activation in cold IR seems to be, at least in part, regulated over the Akt pathway, as its inhibition by Xanthohumol correlates with NF- $\kappa$ B attenuation. In contrast, the oxidative stress driven NF- $\kappa$ B activation is rather questionable, since 3-Hydroxyxanthohumol did not inhibit NF- $\kappa$ B activation at all, although its impact on the antioxidant system is impressive. Interestingly, tissue damage induced by IR does not correlate with NF- $\kappa$ B activation in this study. On the one hand

that might be due to cell-unspecific NF- $\kappa$ B inhibition in the entire liver, resulting in abolished proliferative i.e. protective properties of hepatocytes. On the other hand, NF- $\kappa$ B inhibition over the Akt pathway goes along with decreased levels of antiapoptotic protein levels, which could be responsible for elevated tissue damage followed by IR as well.

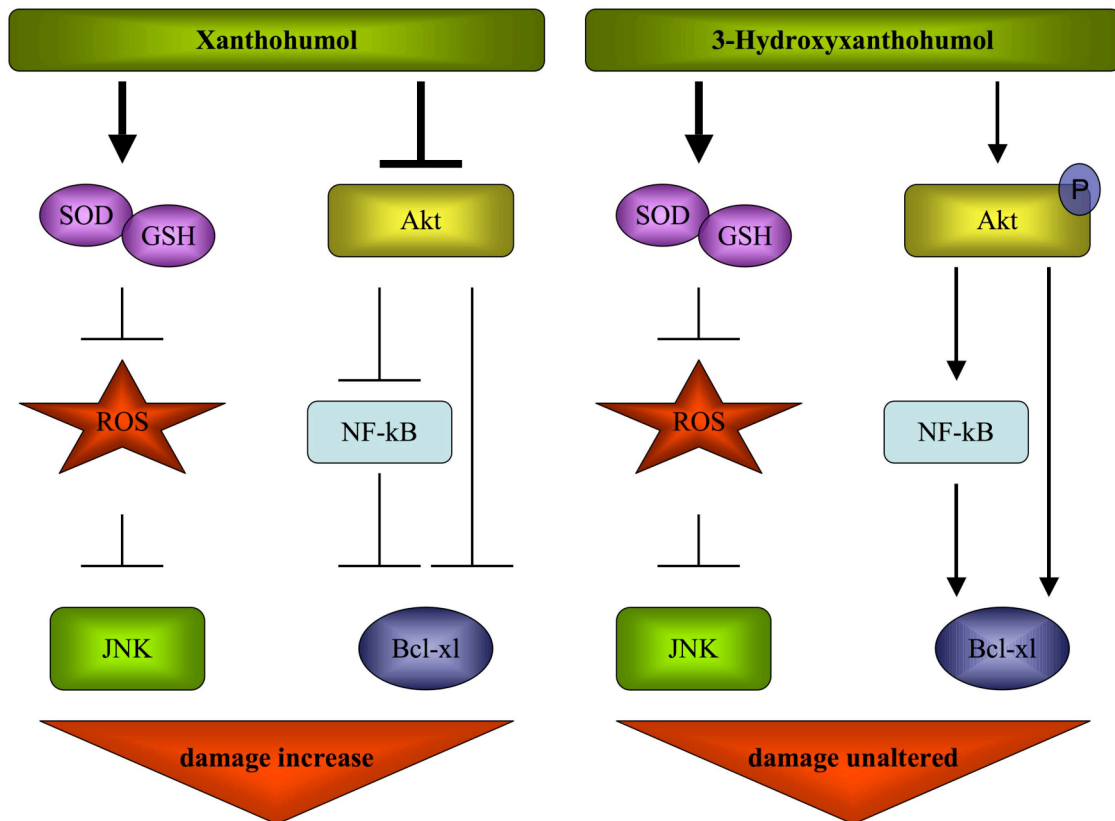


Figure 52 Concluding results of the impact of XN and OH-XN in hepatic IRI.

However, although the antioxidant activities of flavonoids are undisputable, the bioavailability of dietary flavonoids after oral consumption is limited due to the extensive metabolism.<sup>163</sup> Therefore, it is questionable whether the beneficial impact of flavonoid-rich nutrients can be solely referred to the flavonoids and their antioxidant activity. Concluding, flavonoids do not consequently warrant beneficial therapeutic use in oxidative stress driven injury models, as verified here for the hepatic IR injury.

### 4.3 NF- $\kappa$ B DECOY NANOPARTICLES

The NF- $\kappa$ B signal transduction pathway is assumed to be crucial during IR in the liver, as it has long been thought that its activation induces purely the expression of several proinflammatory cytokines such as TNF- $\alpha$  and IL-1 as well as adhesion molecules like ICAM-1, which contribute to hepatic tissue injury.<sup>15, 31</sup> The idea of targeting Kupffer cells exclusively derives from several studies, which revealed in recent years that NF- $\kappa$ B function is more likely different depending on the liver cell-type addressed and potentially opposing in nature. It is assumed that NF- $\kappa$ B in hepatocytes induces predominantly antiapoptotic proteins and participates in regeneration and proliferation, hence, in liver protection.<sup>22, 59</sup> However, NF- $\kappa$ B activation in Kupffer cells is assumed to be responsible for the inflammatory response after IR.<sup>24</sup> Alternatively, it was also proposed that TNF- $\alpha$  and IL-6 release of Kupffer cells driven by NF- $\kappa$ B activation, is responsible for hepatocyte proliferation and regeneration.<sup>15, 62</sup> Eventually, global modulations of NF- $\kappa$ B have previously shown that the desired therapeutic effect cannot be achieved with cell-unspecific targeting.<sup>54-58</sup>

Dr. Florian Hoffmann introduced gelatin NP as a new tool in his recent Ph.D. thesis, which selectively targets Kupffer cells. Administration of NF- $\kappa$ B oligonucleotides decoy loaded to gelatin NP *in vivo* prior to warm IR (1 h / 2 h) abolished NF- $\kappa$ B activation and reduced TNF- $\alpha$  release as well as expression. Astonishingly, liver tissue damage remained unaltered. Eventually, Dr. Hoffmann hypothesized that NF- $\kappa$ B activation in Kupffer cells is not crucial for liver damage.

Based on these interesting results, we wanted to elucidate the role of NF- $\kappa$ B in a model more closely related to the transplantation process, the cold IR process. This model is advantageous in our case for various reasons. On the one hand it solely focus on the liver. Interventions with blood constituents and influences of other organs can be avoided. Moreover, the tissue damage does entirely derive from the liver and hepatic factors. On the other hand, Kupffer cells, which are the main target of NF- $\kappa$ B decoy NP treatment, are vigorously activated during cold IR. That accounts to be a major difference compared to the warm IR model.<sup>15</sup>

The suitability of the application mode was proven by confocal laser scanning microscopy and revealed selective Kupffer cell targeting in the isolated cold IR model (6 h / 2.5 h). Parenchymal cells were not affected (Figure 48). NF- $\kappa$ B binding activity was analyzed by EMSA, which determines the NF- $\kappa$ B levels of whole liver tissue homogenates. As shown in Figure 49, NF- $\kappa$ B decoy-NP treatment completely abolished NF- $\kappa$ B activation. Interestingly, selective NF- $\kappa$ B inhibition in Kupffer cells in the cold IR model did not improve tissue damage, instead hepatic injury remained unaltered (Figure 50). However, Dr. Florian Hoffmann recently demonstrated that postischemic hepatic tissue injury followed by long reperfusion periods (24 h) increased markedly after decoy-NP treatment.

Based on these data two hypothesis are volunteered:

First, NF- $\kappa$ B activation in Kupffer cells is not responsible for acute hepatic tissue injury induced by either warm or cold IR. Although Lentsch et al. have recently shown that NF- $\kappa$ B activation in Kupffer cells correlates with hepatic tissue injury, selective NF- $\kappa$ B inhibition in Kupffer cells and direct correlation with hepatic injury, remains to be proven.<sup>60</sup> Indeed, it can be hypothesized that Kupffer cells seem to participate in other ways to early tissue damage, as their depletion has shown several times to be beneficial in IR.<sup>61</sup> Thus, other pathways than the NF- $\kappa$ B signal transduction cascade might be more likely implicated. Jaeschke et al. assumed that oxidative stress derived from the postischemic ROS release by Kupffer cells, which are the main sources of vascular ROS formation, is crucial for the subsequent injury cascade, thus for hepatocellular injury.<sup>1</sup> Since direct cytotoxicity of ROS is quantitatively insufficient to explain severe injury during reperfusion,<sup>32</sup> it was proposed by Bilzer and Gerbes that ROS mediate TNF- $\alpha$ , IL and PAF release of endothelial cells and monocytes, and modulate mitogen-activated protein kinases (e.g. JNK), which might also be implicated in tissue injury mediated by Kupffer cells.<sup>3</sup> However, it should be kept in mind that the essential role of Kupffer cells in the initial phase of reperfusion injury allows several pathways to be involved, which are not necessarily NF- $\kappa$ B regulated.

Second, NF- $\kappa$ B activation in Kupffer cells contributes to late tissue protection after hepatic IR. Whether Kupffer cells directly impact liver protection or indirectly by hepatocyte NF- $\kappa$ B activation, via TNF- $\alpha$  and IL-6 release, is not yet clear. However,

the latter is more likely, since NF- $\kappa$ B is downregulated in the entire liver, as mentioned above. Thus, downregulation of hepatocyte derived NF- $\kappa$ B would explain tissue injury after long periods of reperfusion, as its activation was reported to be responsible for regeneration and proliferation.<sup>120</sup>

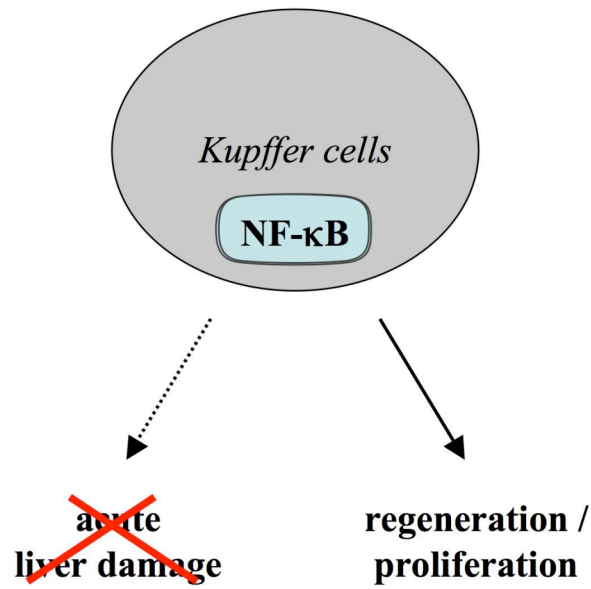


Figure 53 Role of NF- $\kappa$ B in Kupffer cells.

In conclusion, the role of NF- $\kappa$ B in Kupffer cells seems to be more complicated than generally proposed. Kupffer cells seem not to participate in acute IR damage triggered by NF- $\kappa$ B, other pathways are more likely to be involved (Figure 53). Moreover, hepatocellular protection after longer reperfusion periods seems to be an intrinsic function of NF- $\kappa$ B in Kupffer cells during IRI, whereas its detailed mechanism with special consideration of hepatocytes remains to be elucidated.

# SUMMARY

In the present study different approaches, from natural to synthetic origin, were investigated in the multifunctional IR model of the liver. First, EGb 761 (a) – a standardized extract of several ingredients, second, Xanthohumol (b) – a single compound of the hop plant and 3-Hydroxyxanthohumol a biotransformation product, third, NF- $\kappa$ B decoy-NP (c) – a tool targeting selectively the transcription factor NF- $\kappa$ B exclusively in Kupffer cells.

- a. Interestingly, EGb 761 did not show beneficial effects on hepatic IRI, this study rather revealed that intravenous administration implicates crucial toxic potential. Coincidentally, impressive acute hypotension was observed in that line, caused by eNOS activation triggered by the phosphoinositide 3-kinase (PI3K)/Akt pathway. The toxic effects might depend on the administration mode of EGb 761 and are assumed to result, at least in part, from systemic blood pressure drop which led to a decline in hepatic microcirculation.
- b. The flavonoids Xanthohumol and 3-Hydroxyxanthohumol have shown to be potent antioxidants *in vitro* and in the complex oxidative stress driven model of hepatic IR. Interestingly, Xanthohumol inhibited NF- $\kappa$ B activation by the Akt pathway, which correlates with downregulation of antiapoptotic and upregulation of proapoptotic markers. Since cell unspecific NF- $\kappa$ B inhibition with Xanthohumol is more likely to happen, it might explain that NF- $\kappa$ B inhibition results in increased tissue injury. In contrast, 3-Hydroxyxanthohumol had no impact on the NF- $\kappa$ B pathway, eventually tissue injury remained unaltered. In conclusion, flavonoids do not necessarily warrant beneficial usage due to their antioxidant capacity, more attention has to be paid on other pathways involved.
- c. Selective NF- $\kappa$ B inhibition in Kupffer cells with decoy-NP was achieved in an isolated model of hepatic IR. NF- $\kappa$ B activation was abolished without affecting tissue injury. Therefore, the NF- $\kappa$ B pathway derived from Kupffer cells does not contribute to acute IR injury. However, its impact on regeneration and proliferation of the liver is favored.

## **REFERENCES**

- 1 Jaeschke H. Molecular mechanisms of hepatic ischemia-reperfusion injury and preconditioning. *Am J Physiol Gastrointest Liver Physiol* 2003;284:G15-26.
- 2 Glantzounis GK, Salacinski HJ, Yang W, Davidson BR, Seifalian AM. The contemporary role of antioxidant therapy in attenuating liver ischemia-reperfusion injury: a review. *Liver Transpl* 2005;11:1031-47.
- 3 Bilzer M, Gerbes AL. Preservation injury of the liver: mechanisms and novel therapeutic strategies. *J Hepatol* 2000;32:508-15.
- 4 Carini R, Albano E. Recent insights on the mechanisms of liver preconditioning. *Gastroenterology* 2003;125:1480-91.
- 5 Kupiec-Weglinski JW, Busuttil RW. Ischemia and reperfusion injury in liver transplantation. *Transplant Proc* 2005;37:1653-6.
- 6 Smith JV, Luo Y. Studies on molecular mechanisms of Ginkgo biloba extract. *Appl Microbiol Biotechnol* 2004;64:465-72.
- 7 Hertog MG, Bueno-de-Mesquita HB, Fehily AM, Sweetnam PM, Elwood PC, Kromhout D. Fruit and vegetable consumption and cancer mortality in the Caerphilly Study. *Cancer Epidemiol Biomarkers Prev* 1996;5:673-7.
- 8 Rahman I, Biswas SK, Kirkham PA. Regulation of inflammation and redox signaling by dietary polyphenols. *Biochem Pharmacol* 2006;72:1439-52.
- 9 Das S, Das DK. Resveratrol: a therapeutic promise for cardiovascular diseases. *Recent Patents Cardiovasc Drug Discov* 2007;2:133-8.
- 10 Gerhauser C, Alt A, Heiss E, Gamal-Eldeen A, Klimo K, Knauff J, Neumann I, Scherf HR, Frank N, Bartsch H, Becker H. Cancer chemopreventive activity of Xanthohumol, a natural product derived from hop. *Mol Cancer Ther* 2002;1:959-69.
- 11 Nikolic D, Li Y, Chadwick LR, Pauli GF, van Breemen RB. Metabolism of xanthohumol and isoxanthohumol, prenylated flavonoids from hops (*Humulus lupulus* L.), by human liver microsomes. *J Mass Spectrom* 2005;40:289-99.
- 12 Kanoria S, Jalan R, Seifalian AM, Williams R, Davidson BR. Protocols and mechanisms for remote ischemic preconditioning: a novel method for reducing ischemia reperfusion injury. *Transplantation* 2007;84:445-58.
- 13 Montalvo-Jave EE, Escalante-Tattersfield T, Ortega-Salgado JA, Pina E, Geller DA. Factors in the pathophysiology of the liver ischemia-reperfusion injury. *J Surg Res* 2008;147:153-9.
- 14 Galaris D, Barbouti A, Korantzopoulos P. Oxidative stress in hepatic ischemia-reperfusion injury: the role of antioxidants and iron chelating compounds. *Curr Pharm Des* 2006;12:2875-90.

- 15 Fan C, Zwacka RM, Engelhardt JF. Therapeutic approaches for ischemia/reperfusion injury in the liver. *J Mol Med* 1999;77:577-92.
- 16 Arii S, Teramoto K, Kawamura T. Current progress in the understanding of and therapeutic strategies for ischemia and reperfusion injury of the liver. *J Hepatobiliary Pancreat Surg* 2003;10:189-94.
- 17 Serracino-Inglott F, Habib NA, Mathie RT. Hepatic ischemia-reperfusion injury. *Am J Surg* 2001;181:160-6.
- 18 Massip-Salcedo M, Rosello-Catafau J, Prieto J, Avila MA, Peralta C. The response of the hepatocyte to ischemia. *Liver Int* 2007;27:6-16.
- 19 Gujral JS, Bucci TJ, Farhood A, Jaeschke H. Mechanism of cell death during warm hepatic ischemia-reperfusion in rats: apoptosis or necrosis? *Hepatology* 2001;33:397-405.
- 20 Kohli V, Madden JF, Bentley RC, Clavien PA. Calpain mediates ischemic injury of the liver through modulation of apoptosis and necrosis. *Gastroenterology* 1999;116:168-78.
- 21 Kohli V, Gao W, Camargo CA, Jr., Clavien PA. Calpain is a mediator of preservation-reperfusion injury in rat liver transplantation. *Proc Natl Acad Sci U S A* 1997;94:9354-9.
- 22 Shin T, Kuboki S, Lentsch AB. Roles of nuclear factor-kappaB in postischemic liver. *Hepato Res* 2008;38:429-40.
- 23 Ke B, Lipshutz GS, Kupiec-Weglinski JW. Gene therapy in liver ischemia and reperfusion injury. *Curr Pharm Des* 2006;12:2969-75.
- 24 Bilzer M, Roggel F, Gerbes AL. Role of Kupffer cells in host defense and liver disease. *Liver Int* 2006;26:1175-86.
- 25 Kolios G, Valatas V, Kouroumalis E. Role of Kupffer cells in the pathogenesis of liver disease. *World J Gastroenterol* 2006;12:7413-20.
- 26 Karidis NP, Kouraklis G, Theocharis SE. Platelet-activating factor in liver injury: a relational scope. *World J Gastroenterol* 2006;12:3695-706.
- 27 Jaeschke H. Mechanisms of Liver Injury. II. Mechanisms of neutrophil-induced liver cell injury during hepatic ischemia-reperfusion and other acute inflammatory conditions. *Am J Physiol Gastrointest Liver Physiol* 2006;290:G1083-8.
- 28 Caldwell CC, Tschöep J, Lentsch AB. Lymphocyte function during hepatic ischemia/reperfusion injury. *J Leukoc Biol* 2007;82:457-64.
- 29 Arumugam TV, Shiels IA, Woodruff TM, Granger DN, Taylor SM. The role of the complement system in ischemia-reperfusion injury. *Shock* 2004;21:401-9.

- 30 Suzuki S, Toledo-Pereyra LH, Rodriguez FJ. Role of neutrophils during the first 24 hours after liver ischemia and reperfusion injury. *Transplant Proc* 1994;26:3695-700.
- 31 Hines IN, Harada H, Wolf R, Grisham MB. Superoxide and post-ischemic liver injury: potential therapeutic target for liver transplantation. *Curr Med Chem* 2003;10:2661-7.
- 32 Jaeschke H. Role of reactive oxygen species in hepatic ischemia-reperfusion injury and preconditioning. *J Invest Surg* 2003;16:127-40.
- 33 Matsui N, Kasajima K, Hada M, Nagata T, Senga N, Yasui Y, Fukuishi N, Akagi M. Inhibition of NF-kappaB activation during ischemia reduces hepatic ischemia/reperfusion injury in rats. *J Toxicol Sci* 2005;30:103-10.
- 34 Bergendi L, Benes L, Durackova Z, Ferencik M. Chemistry, physiology and pathology of free radicals. *Life Sci* 1999;65:1865-74.
- 35 Mungrue IN, Bredt DS, Stewart DJ, Husain M. From molecules to mammals: what's NOS got to do with it? *Acta Physiol Scand* 2003;179:123-35.
- 36 Isobe M, Katsuramaki T, Hirata K, Kimura H, Nagayama M, Matsuno T. Beneficial effects of inducible nitric oxide synthase inhibitor on reperfusion injury in the pig liver. *Transplantation* 1999;68:803-13.
- 37 Meguro M, Katsuramaki T, Nagayama M, Kimura H, Isobe M, Kimura Y, Matsuno T, Nui A, Hirata K. A novel inhibitor of inducible nitric oxide synthase (ONO-1714) prevents critical warm ischemia-reperfusion injury in the pig liver. *Transplantation* 2002;73:1439-46.
- 38 Takamatsu Y, Shimada K, Yamaguchi K, Kuroki S, Chijiwa K, Tanaka M. Inhibition of inducible nitric oxide synthase prevents hepatic, but not pulmonary, injury following ischemia-reperfusion of rat liver. *Dig Dis Sci* 2006;51:571-9.
- 39 Pannen BH, Al-Adili F, Bauer M, Clemens MG, Geiger KK. Role of endothelins and nitric oxide in hepatic reperfusion injury in the rat. *Hepatology* 1998;27:755-64.
- 40 Taniai H, Hines IN, Bharwani S, Maloney RE, Nimura Y, Gao B, Flores SC, McCord JM, Grisham MB, Aw TY. Susceptibility of murine periportal hepatocytes to hypoxia-reoxygenation: role for NO and Kupffer cell-derived oxidants. *Hepatology* 2004;39:1544-52.
- 41 Zhang C, Zu J, Shi H, Liu J, Qin C. The effect of Ginkgo biloba extract (EGb 761) on hepatic sinusoidal endothelial cells and hepatic microcirculation in CCl4 rats. *Am J Chin Med* 2004;32:21-31.
- 42 He SQ, Zhang YH, Venugopal SK, Dicus CW, Perez RV, Ramsamooj R, Nantz MH, Zern MA, Wu J. Delivery of antioxidative enzyme genes protects against

- ischemia/reperfusion-induced liver injury in mice. *Liver Transpl* 2006;12:1869-79.
- 43 Vertuani S, Angusti A, Manfredini S. The antioxidants and pro-antioxidants network: an overview. *Curr Pharm Des* 2004;10:1677-94.
- 44 Hur GM, Ryu YS, Yun HY, Jeon BH, Kim YM, Seok JH, Lee JH. Hepatic ischemia/reperfusion in rats induces iNOS gene transcription by activation of NF-kappaB. *Biochem Biophys Res Commun* 1999;261:917-22.
- 45 Zhong Z, Froh M, Connor HD, Li X, Conzelmann LO, Mason RP, Lemasters JJ, Thurman RG. Prevention of hepatic ischemia-reperfusion injury by green tea extract. *Am J Physiol Gastrointest Liver Physiol* 2002;283:G957-64.
- 46 Kumar A, Takada Y, Boriek AM, Aggarwal BB. Nuclear factor-kappaB: its role in health and disease. *J Mol Med* 2004;82:434-48.
- 47 Collins T, Cybulsky MI. NF-kappaB: pivotal mediator or innocent bystander in atherogenesis? *J Clin Invest* 2001;107:255-64.
- 48 Hart LA, Krishnan VL, Adcock IM, Barnes PJ, Chung KF. Activation and localization of transcription factor, nuclear factor-kappaB, in asthma. *Am J Respir Crit Care Med* 1998;158:1585-92.
- 49 Bharti AC, Aggarwal BB. Nuclear factor-kappa B and cancer: its role in prevention and therapy. *Biochem Pharmacol* 2002;64:883-8.
- 50 Valen G, Yan ZQ, Hansson GK. Nuclear factor kappa-B and the heart. *J Am Coll Cardiol* 2001;38:307-14.
- 51 Liu SF, Malik AB. NF-kappa B activation as a pathological mechanism of septic shock and inflammation. *Am J Physiol Lung Cell Mol Physiol* 2006;290:L622-L645.
- 52 Gloire G, Legrand-Poels S, Piette J. NF-kappaB activation by reactive oxygen species: fifteen years later. *Biochem Pharmacol* 2006;72:1493-505.
- 53 Karin M, Ben-Neriah Y. Phosphorylation meets ubiquitination: the control of NF-[kappa]B activity. *Annu Rev Immunol* 2000;18:621-63.
- 54 Beg AA, Sha WC, Bronson RT, Ghosh S, Baltimore D. Embryonic lethality and liver degeneration in mice lacking the RelA component of NF-kappa B. *Nature* 1995;376:167-70.
- 55 Imose M, Nagaki M, Naiki T, Osawa Y, Brenner DA, Asano T, Hayashi H, Kato T, Moriwaki H. Inhibition of nuclear factor kappaB and phosphatidylinositol 3-kinase/Akt is essential for massive hepatocyte apoptosis induced by tumor necrosis factor alpha in mice. *Liver Int* 2003;23:386-96.

- 56 Guicciardi ME, Deussing J, Miyoshi H, Bronk SF, Svingen PA, Peters C, Kaufmann SH, Gores GJ. Cathepsin B contributes to TNF-alpha-mediated hepatocyte apoptosis by promoting mitochondrial release of cytochrome c. *J Clin Invest* 2000;106:1127-37.
- 57 Lavon I, Goldberg I, Amit S, Landsman L, Jung S, Tsuberi BZ, Barshack I, Kopolovic J, Galun E, Bujard H, Ben-Neriah Y. High susceptibility to bacterial infection, but no liver dysfunction, in mice compromised for hepatocyte NF-kappaB activation. *Nat Med* 2000;6:573-7.
- 58 Luedde T, Beraza N, Trautwein C. Evaluation of the role of nuclear factor-kappaB signaling in liver injury using genetic animal models. *J Gastroenterol Hepatol* 2006;21 Suppl 3:S43-6.
- 59 Iimuro Y, Nishiura T, Hellerbrand C, Behrns KE, Schoonhoven R, Grisham JW, Brenner DA. NFkappaB prevents apoptosis and liver dysfunction during liver regeneration. *J Clin Invest* 1998;101:802-11.
- 60 Kuboki S, Okaya T, Schuster R, Blanchard J, Denenberg A, Wong HR, Lentsch AB. Hepatocyte NF-kappaB activation is hepatoprotective during ischemia-reperfusion injury and is augmented by ischemic hypothermia. *Am J Physiol Gastrointest Liver Physiol* 2007;292:G201-7.
- 61 Shiratori Y, Kiriyaama H, Fukushi Y, Nagura T, Takada H, Hai K, Kamii K. Modulation of ischemia-reperfusion-induced hepatic injury by Kupffer cells. *Dig Dis Sci* 1994;39:1265-72.
- 62 Olthoff KM. Molecular pathways of regeneration and repair after liver transplantation. *World J Surg* 2002;26:831-7.
- 63 Abshagen K, Eipel C, Kalff JC, Menger MD, Vollmar B. Loss of NF-kappaB activation in Kupffer cell-depleted mice impairs liver regeneration after partial hepatectomy. *Am J Physiol Gastrointest Liver Physiol* 2007;292:G1570-7.
- 64 Meijer C, Wiezer MJ, Diehl AM, Schouten HJ, Meijer S, van Rooijen N, van Lambalgen AA, Dijkstra CD, van Leeuwen PA. Kupffer cell depletion by CI2MDP-liposomes alters hepatic cytokine expression and delays liver regeneration after partial hepatectomy. *Liver* 2000;20:66-77.
- 65 Watanabe M, Chijiwa K, Kameoka N, Yamaguchi K, Kuroki S, Tanaka M. Gadolinium pretreatment decreases survival and impairs liver regeneration after partial hepatectomy under ischemia/reperfusion in rats. *Surgery* 2000;127:456-63.
- 66 Muller C, Dunschede F, Koch E, Vollmar AM, Kiemer AK. Alpha-lipoic acid preconditioning reduces ischemia-reperfusion injury of the rat liver via the PI3-kinase/Akt pathway. *Am J Physiol Gastrointest Liver Physiol* 2003;285:G769-78.
- 67 Kiemer AK, Gerbes AL, Bilzer M, Vollmar AM. The atrial natriuretic peptide and cGMP: novel activators of the heat shock response in rat livers. *Hepatology* 2002;35:88-94.

- 68 Murry CE, Jennings RB, Reimer KA. Preconditioning with ischemia: a delay of lethal cell injury in ischemic myocardium. *Circulation* 1986;74:1124-36.
- 69 Matsumoto K, Honda K, Kobayashi N. Protective effect of heat preconditioning of rat liver graft resulting in improved transplant survival. *Transplantation* 2001;71:862-8.
- 70 Jacobs BP, Browner WS. Ginkgo biloba: a living fossil. *Am J Med* 2000;108:341-2.
- 71 Bastianetto S, Zheng WH, Quirion R. The Ginkgo biloba extract (EGb 761) protects and rescues hippocampal cells against nitric oxide-induced toxicity: involvement of its flavonoid constituents and protein kinase C. *J Neurochem* 2000;74:2268-77.
- 72 Bors W, Michel C, Stettmaier K. Antioxidant effects of flavonoids. *Biofactors* 1997;6:399-402.
- 73 Gohil K, Packer L. Bioflavonoid-rich botanical extracts show antioxidant and gene regulatory activity. *Ann N Y Acad Sci* 2002;957:70-7.
- 74 DeFeudis FV, Drieu K. Ginkgo biloba extract (EGb 761) and CNS functions: basic studies and clinical applications. *Curr Drug Targets* 2000;1:25-58.
- 75 Mahadevan S, Park Y. Multifaceted therapeutic benefits of Ginkgo biloba L.: chemistry, efficacy, safety, and uses. *J Food Sci* 2008;73:R14-9.
- 76 Liu KX, Wu WK, He W, Liu CL. Ginkgo biloba extract (EGb 761) attenuates lung injury induced by intestinal ischemia/reperfusion in rats: roles of oxidative stress and nitric oxide. *World J Gastroenterol* 2007;13:299-305.
- 77 Sener G, Sener E, Sehirli O, Ogunc AV, Cetinel S, Gedik N, Sakarcan A. Ginkgo biloba extract ameliorates ischemia reperfusion-induced renal injury in rats. *Pharmacol Res* 2005;52:216-22.
- 78 Koch E. Inhibition of platelet activating factor (PAF)-induced aggregation of human thrombocytes by ginkgolides: considerations on possible bleeding complications after oral intake of Ginkgo biloba extracts. *Phytomedicine* 2005;12:10-6.
- 79 Akiba S, Kawauchi T, Oka T, Hashizume T, Sato T. Inhibitory effect of the leaf extract of Ginkgo biloba L. on oxidative stress-induced platelet aggregation. *Biochem Mol Biol Int* 1998;46:1243-8.
- 80 Zablocka B, Lukasiuk K, Lazarewicz JW, Domanska-Janik K. Modulation of ischemic signal by antagonists of N-methyl-D-aspartate, nitric oxide synthase, and platelet-activating factor in gerbil hippocampus. *J Neurosci Res* 1995;40:233-40.

- 81 Topp S, Knoefel WT, Schutte A, Brilloff S, Rogiers X, Gundlach M. Ginkgo biloba (EGB 761) improves microcirculation after warm ischemia of the rat liver. *Transplant Proc* 2001;33:979-81.
- 82 Janssens D, Remacle J, Drieu K, Michiels C. Protection of mitochondrial respiration activity by bilobalide. *Biochem Pharmacol* 1999;58:109-19.
- 83 Janssens D, Michiels C, Delaive E, Eliaers F, Drieu K, Remacle J. Protection of hypoxia-induced ATP decrease in endothelial cells by ginkgo biloba extract and bilobalide. *Biochem Pharmacol* 1995;50:991-9.
- 84 Kusmic C, Basta G, Lazzerini G, Vesentini N, Barsacchi R. The effect of Ginkgo biloba in isolated ischemic/reperfused rat heart: a link between vitamin E preservation and prostaglandin biosynthesis. *J Cardiovasc Pharmacol* 2004;44:356-62.
- 85 Varga E, Bodi A, Ferdinandy P, Droy-Lefaix MT, Blasig IE, Tosaki A. The protective effect of EGb 761 in isolated ischemic/reperfused rat hearts: a link between cardiac function and nitric oxide production. *J Cardiovasc Pharmacol* 1999;34:711-7.
- 86 Park YM, Won JH, Yun KJ, Ryu JH, Han YN, Choi SK, Lee KT. Preventive effect of Ginkgo biloba extract (GBB) on the lipopolysaccharide-induced expressions of inducible nitric oxide synthase and cyclooxygenase-2 via suppression of nuclear factor-kappaB in RAW 264.7 cells. *Biol Pharm Bull* 2006;29:985-90.
- 87 Kobuchi H, Droy-Lefaix MT, Christen Y, Packer L. Ginkgo biloba extract (EGb 761): inhibitory effect on nitric oxide production in the macrophage cell line RAW 264.7. *Biochem Pharmacol* 1997;53:897-903.
- 88 Albin A, Dell'Eva R, Vene R, Ferrari N, Buhler DR, Noonan DM, Fassina G. Mechanisms of the antiangiogenic activity by the hop flavonoid xanthohumol: NF-kappaB and Akt as targets. *Faseb J* 2006;20:527-9.
- 89 Winkel-Shirley B. Flavonoid biosynthesis. A colorful model for genetics, biochemistry, cell biology, and biotechnology. *Plant Physiol* 2001;126:485-93.
- 90 Zanolini P, Zavatti M. Pharmacognostic and pharmacological profile of *Humulus lupulus* L. *J Ethnopharmacol* 2008;116:383-96.
- 91 Gerhauser C. Beer constituents as potential cancer chemopreventive agents. *Eur J Cancer* 2005;41:1941-54.
- 92 Gerhauser C, Frank N. Xanthohumol, a new all-rounder? *Mol Nutr Food Res* 2005;49:821-3.
- 93 Avula B, Ganzera M, Warnick JE, Feltenstein MW, Sufka KJ, Khan IA. High-performance liquid chromatographic determination of xanthohumol in rat plasma, urine, and fecal samples. *J Chromatogr Sci* 2004;42:378-82.

- 94 Yilmazer M, Stevens JF, Deinzer ML, Buhler DR. In vitro biotransformation of xanthohumol, a flavonoid from hops (*Humulus lupulus*), by rat liver microsomes. *Drug Metab Dispos* 2001;29:223-31.
- 95 Nookandeh A, Frank N, Steiner F, Ellinger R, Schneider B, Gerhauser C, Becker H. Xanthohumol metabolites in faeces of rats. *Phytochemistry* 2004;65:561-70.
- 96 Teixeira S, Siquet C, Alves C, Boal I, Marques MP, Borges F, Lima JL, Reis S. Structure-property studies on the antioxidant activity of flavonoids present in diet. *Free Radic Biol Med* 2005;39:1099-108.
- 97 Stevenson DE, Hurst RD. Polyphenolic phytochemicals--just antioxidants or much more? *Cell Mol Life Sci* 2007;64:2900-16.
- 98 Zhan C, Yang J. Protective effects of isoliquiritigenin in transient middle cerebral artery occlusion-induced focal cerebral ischemia in rats. *Pharmacol Res* 2006;53:303-9.
- 99 Lanteri R, Acquaviva R, Di Giacomo C, Sorrenti V, Li Destri G, Santangelo M, Vanella L, Di Cataldo A. Rutin in rat liver ischemia/reperfusion injury: effect on DDAH/NOS pathway. *Microsurgery* 2007;27:245-51.
- 100 Su JF, Guo CJ, Wei JY, Yang JJ, Jiang YG, Li YF. Protection against hepatic ischemia-reperfusion injury in rats by oral pretreatment with quercetin. *Biomed Environ Sci* 2003;16:1-8.
- 101 Plin C, Tillement JP, Berdeaux A, Morin D. Resveratrol protects against cold ischemia-warm reoxygenation-induced damages to mitochondria and cells in rat liver. *Eur J Pharmacol* 2005;528:162-8.
- 102 Fiorini RN, Donovan JL, Rodwell D, Evans Z, Cheng G, May HD, Milliken CE, Markowitz JS, Campbell C, Haines JK, Schmidt MG, Chavin KD. Short-term administration of (-)-epigallocatechin gallate reduces hepatic steatosis and protects against warm hepatic ischemia/reperfusion injury in steatotic mice. *Liver Transpl* 2005;11:298-308.
- 103 Tsuda T, Horio F, Osawa T. The role of anthocyanins as an antioxidant under oxidative stress in rats. *Biofactors* 2000;13:133-9.
- 104 Miranda CL, Stevens JF, Ivanov V, McCall M, Frei B, Deinzer ML, Buhler DR. Antioxidant and prooxidant actions of prenylated and nonprenylated chalcones and flavanones in vitro. *J Agric Food Chem* 2000;48:3876-84.
- 105 Stevens JF, Miranda CL, Frei B, Buhler DR. Inhibition of peroxynitrite-mediated LDL oxidation by prenylated flavonoids: the alpha,beta-unsaturated keto functionality of 2'-hydroxychalcones as a novel antioxidant pharmacophore. *Chem Res Toxicol* 2003;16:1277-86.

- 106 Rodriguez RJ, Miranda CL, Stevens JF, Deinzer ML, Buhler DR. Influence of prenylated and non-prenylated flavonoids on liver microsomal lipid peroxidation and oxidative injury in rat hepatocytes. *Food Chem Toxicol* 2001;39:437-45.
- 107 Plazar J, Zegura B, Lah TT, Filipic M. Protective effects of xanthohumol against the genotoxicity of benzo(a)pyrene (BaP), 2-amino-3-methylimidazo[4,5-f]quinoline (IQ) and tert-butyl hydroperoxide (t-BOOH) in HepG2 human hepatoma cells. *Mutat Res* 2007;632:1-8.
- 108 Rice-Evans C. Implications of the mechanisms of action of tea polyphenols as antioxidants in vitro for chemoprevention in humans. *Proc Soc Exp Biol Med* 1999;220:262-6.
- 109 Feng Y, Lu YW, Xu PH, Long Y, Wu WM, Li W, Wang R. Caffeic acid phenethyl ester and its related compounds limit the functional alterations of the isolated mouse brain and liver mitochondria submitted to in vitro anoxia-reoxygenation: Relationship to their antioxidant activities. *Biochim Biophys Acta* 2008;1780:659-672.
- 110 Cai YJ, Fang JG, Ma LP, Yang L, Liu ZL. Inhibition of free radical-induced peroxidation of rat liver microsomes by resveratrol and its analogues. *Biochim Biophys Acta* 2003;1637:31-8.
- 111 Zhao F, Nozawa H, Daikonnya A, Kondo K, Kitanaka S. Inhibitors of nitric oxide production from hops (*Humulus lupulus* L.). *Biol Pharm Bull* 2003;26:61-5.
- 112 Tanigawa S, Fujii M, Hou DX. Action of Nrf2 and Keap1 in ARE-mediated NQO1 expression by quercetin. *Free Radic Biol Med* 2007;42:1690-703.
- 113 Dietz BM, Kang YH, Liu G, Eggler AL, Yao P, Chadwick LR, Pauli GF, Farnsworth NR, Mesecar AD, van Breemen RB, Bolton JL. Xanthohumol isolated from *Humulus lupulus* Inhibits menadione-induced DNA damage through induction of quinone reductase. *Chem Res Toxicol* 2005;18:1296-305.
- 114 Cai Q, Rahn RO, Zhang R. Dietary flavonoids, quercetin, luteolin and genistein, reduce oxidative DNA damage and lipid peroxidation and quench free radicals. *Cancer Lett* 1997;119:99-107.
- 115 Ricciardi R, Shah SA, Wheeler SM, Quarfordt SH, Callery MP, Meyers WC, Chari RS. Regulation of NFkappaB in hepatic ischemic preconditioning. *J Am Coll Surg* 2002;195:319-26.
- 116 Ricciardi R, Schaffer BK, Kim RD, Shah SA, Donohue SE, Wheeler SM, Quarfordt SH, Callery MP, Meyers WC, Chari RS. Protective effects of ischemic preconditioning on the cold-preserved liver are tyrosine kinase dependent. *Transplantation* 2001;72:406-12.
- 117 Dell'Eva R, Ambrosini C, Vannini N, Piaggio G, Albini A, Ferrari N. AKT/NF-kappaB inhibitor xanthohumol targets cell growth and angiogenesis in hematologic malignancies. *Cancer* 2007;110:2007-11.

- 118 Colgate EC, Miranda CL, Stevens JF, Bray TM, Ho E. Xanthohumol, a prenylflavonoid derived from hops induces apoptosis and inhibits NF-kappaB activation in prostate epithelial cells. *Cancer Lett* 2007;246:201-9.
- 119 Beraza N, Ludde T, Assmus U, Roskams T, Vander Borgh S, Trautwein C. Hepatocyte-specific IKK gamma/NEMO expression determines the degree of liver injury. *Gastroenterology* 2007;132:2504-17.
- 120 Maeda S, Kamata H, Luo JL, Leffert H, Karin M. IKKbeta couples hepatocyte death to cytokine-driven compensatory proliferation that promotes chemical hepatocarcinogenesis. *Cell* 2005;121:977-90.
- 121 Kawakami S, Wong J, Sato A, Hattori Y, Yamashita F, Hashida M. Biodistribution characteristics of mannosylated, fucosylated, and galactosylated liposomes in mice. *Biochim Biophys Acta* 2000;1524:258-65.
- 122 Yoshida M, Yamamoto N, Uehara T, Terao R, Nitta T, Harada N, Hatano E, Iimuro Y, Yamaoka Y. Kupffer cell targeting by intraportal injection of the HVJ cationic liposome. *Eur Surg Res* 2002;34:251-9.
- 123 Romero EL, Morilla MJ, Regts J, Koning GA, Scherphof GL. On the mechanism of hepatic transendothelial passage of large liposomes. *FEBS Lett* 1999;448:193-6.
- 124 Melgert BN, Weert B, Schellekens H, Meijer DK, Poelstra K. The pharmacokinetic and biological activity profile of dexamethasone targeted to sinusoidal endothelial and Kupffer cells. *J Drug Target* 2003;11:1-10.
- 125 Bijsterbosch MK, Manoharan M, Dorland R, Waarlo IH, Biessen EA, van Berkel TJ. Delivery of cholesteryl-conjugated phosphorothioate oligodeoxynucleotides to Kupffer cells by lactosylated low-density lipoprotein. *Biochem Pharmacol* 2001;62:627-33.
- 126 Crettaz J, Berraondo P, Mauleon I, Ochoa L, Shankar V, Barajas M, van Rooijen N, Kochanek S, Qian C, Prieto J, Hernandez-Alcoceba R, Gonzalez-Aseguinolaza G. Intrahepatic injection of adenovirus reduces inflammation and increases gene transfer and therapeutic effect in mice. *Hepatology* 2006;44:623-32.
- 127 Lambert G, Fattal E, Couvreur P. Nanoparticulate systems for the delivery of antisense oligonucleotides. *Adv Drug Deliv Rev* 2001;47:99-112.
- 128 Vogel S, Ohmayer S, Brunner G, Heilmann J. Natural and non-natural prenylated chalcones: synthesis, cytotoxicity and anti-oxidative activity. *Bioorg Med Chem* 2008;16:4286-93.
- 129 Marklund S, Marklund G. Involvement of the superoxide anion radical in the autoxidation of pyrogallol and a convenient assay for superoxide dismutase. *Eur J Biochem* 1974;47:469-74.

- 130 Kiemer AK, Weber NC, Vollmar AM. Induction of IkappaB: atrial natriuretic peptide as a regulator of the NF-kappaB pathway. *Biochem Biophys Res Commun* 2002;295:1068-76.
- 131 Smith PK, Krohn RI, Hermanson GT, Mallia AK, Gartner FH, Provenzano MD, Fujimoto EK, Goeke NM, Olson BJ, Klenk DC. Measurement of protein using bicinchoninic acid. *Anal Biochem* 1985;150:76-85.
- 132 Bradford MM. A rapid and sensitive method for the quantitation of microgram quantities of protein utilizing the principle of protein-dye binding. *Anal Biochem* 1976;72:248-54.
- 133 Mueller TH, Kienle K, Beham A, Geissler EK, Jauch KW, Rentsch M. Caspase 3 inhibition improves survival and reduces early graft injury after ischemia and reperfusion in rat liver transplantation. *Transplantation* 2004;78:1267-73.
- 134 Mullonkal CJ, Toledo-Pereyra LH. Akt in ischemia and reperfusion. *J Invest Surg* 2007;20:195-203.
- 135 Jaeschke H, Lemasters JJ. Apoptosis versus oncotic necrosis in hepatic ischemia/reperfusion injury. *Gastroenterology* 2003;125:1246-57.
- 136 Johnson GL, Nakamura K. The c-jun kinase/stress-activated pathway: regulation, function and role in human disease. *Biochim Biophys Acta* 2007;1773:1341-8.
- 137 Sehirli O, Ozel Y, Dulundu E, Topaloglu U, Ercan F, Sener G. Grape seed extract treatment reduces hepatic ischemia-reperfusion injury in rats. *Phytother Res* 2008;22:43-8.
- 138 Sener G, Sehirli O, Ipci Y, Ercan F, Sirvanci S, Gedik N, Yegen BC. Aqueous garlic extract alleviates ischaemia-reperfusion-induced oxidative hepatic injury in rats. *J Pharm Pharmacol* 2005;57:145-50.
- 139 Yenilmez A, Kilic FS, Sirmagul B, Isikli B, Aral E, Oner S. Preventive effects of Ginkgo biloba extract on ischemia-reperfusion injury in rat bladder. *Urol Int* 2007;78:167-72.
- 140 Urikova A, Babusikova E, Dobrota D, Drgova A, Kaplan P, Tatarkova Z, Lehotsky J. Impact of Ginkgo Biloba Extract EGb 761 on ischemia/reperfusion - induced oxidative stress products formation in rat forebrain. *Cell Mol Neurobiol* 2006;26:1343-53.
- 141 Pehlivan M, Dalbeler Y, Hazinedaroglu S, Arikan Y, Erkek AB, Gunal O, Turkcapar N, Turkcapar AG. An assessment of the effect of Ginkgo Biloba EGb 761 on ischemia reperfusion injury of intestine. *Hepatogastroenterology* 2002;49:201-4.
- 142 Schutte A, Topp SA, Knoefel WT, Brilloff S, Mueller L, Rogiers X, Gundlach M. Influence of Ginkgo Biloba extract (EGB 761) on expression of EGR-1 mRNA

- and HSP-70 mRNA after warm ischemia in the rat liver. *Transplant Proc* 2001;33:3724-5.
- 143 Chen SH, Liang YC, Chao JC, Tsai LH, Chang CC, Wang CC, Pan S. Protective effects of Ginkgo biloba extract on the ethanol-induced gastric ulcer in rats. *World J Gastroenterol* 2005;11:3746-50.
- 144 Umegaki K, Shinozuka K, Watarai K, Takenaka H, Yoshimura M, Daohua P, Esashi T. Ginkgo biloba extract attenuates the development of hypertension in deoxycorticosterone acetate-salt hypertensive rats. *Clin Exp Pharmacol Physiol* 2000;27:277-82.
- 145 Sasaki Y, Noguchi T, Yamamoto E, Giddings JC, Ikeda K, Yamori Y, Yamamoto J. Effects of Ginkgo biloba extract (EGb 761) on cerebral thrombosis and blood pressure in stroke-prone spontaneously hypertensive rats. *Clin Exp Pharmacol Physiol* 2002;29:963-7.
- 146 Shinozuka K, Umegaki K, Kubota Y, Tanaka N, Mizuno H, Yamauchi J, Nakamura K, Kunitomo M. Feeding of Ginkgo biloba extract (GBE) enhances gene expression of hepatic cytochrome P-450 and attenuates the hypotensive effect of nicardipine in rats. *Life Sci* 2002;70:2783-92.
- 147 Sener G, Kabasakal L, Yuksel M, Gedik N, Alican Y. Hepatic fibrosis in biliary-obstructed rats is prevented by Ginkgo biloba treatment. *World J Gastroenterol* 2005;11:5444-9.
- 148 Ding J, Yu J, Wang C, Hu W, Li D, Luo Y, Luo H, Yu H. Ginkgo biloba extract alleviates liver fibrosis induced by CCl in rats. *Liver Int* 2005;25:1224-32.
- 149 Biber A. Pharmacokinetics of Ginkgo biloba extracts. *Pharmacopsychiatry* 2003;36 Suppl 1:S32-7.
- 150 Renaud S, de Lorgeril M. Wine, alcohol, platelets, and the French paradox for coronary heart disease. *Lancet* 1992;339:1523-6.
- 151 Ray PS, Maulik G, Cordis GA, Bertelli AA, Bertelli A, Das DK. The red wine antioxidant resveratrol protects isolated rat hearts from ischemia reperfusion injury. *Free Radic Biol Med* 1999;27:160-9.
- 152 Shigematsu S, Ishida S, Hara M, Takahashi N, Yoshimatsu H, Sakata T, Korthuis RJ. Resveratrol, a red wine constituent polyphenol, prevents superoxide-dependent inflammatory responses induced by ischemia/reperfusion, platelet-activating factor, or oxidants. *Free Radic Biol Med* 2003;34:810-7.
- 153 Hayakawa M, Miyashita H, Sakamoto I, Kitagawa M, Tanaka H, Yasuda H, Karin M, Kikugawa K. Evidence that reactive oxygen species do not mediate NF-kappaB activation. *Embo J* 2003;22:3356-66.

- 154 Liu ZJ, Yan LN, Li SW, You HB, Gong JP. Glycine blunts transplantative liver ischemia-reperfusion injury by downregulating interleukin 1 receptor associated kinase-4. *Acta Pharmacol Sin* 2006;27:1479-86.
- 155 Suetsugu H, Iimuro Y, Uehara T, Nishio T, Harada N, Yoshida M, Hatano E, Son G, Fujimoto J, Yamaoka Y. Nuclear factor  $\kappa$ B inactivation in the rat liver ameliorates short term total warm ischaemia/reperfusion injury. *Gut* 2005;54:835-42.
- 156 Yuzawa H, Fujioka H, Mizoe A, Azuma T, Furui J, Nishikawa M, Hashida M, Kanematsu T. Inhibitory effects of safe and novel SOD derivatives, galactosylated-SOD, on hepatic warm ischemia/reperfusion injury in pigs. *Hepatology* 2005;52:839-43.
- 157 Bilzer M, Baron A, Schauer R, Steib C, Ebensberger S, Gerbes AL. Glutathione treatment protects the rat liver against injury after warm ischemia and Kupffer cell activation. *Digestion* 2002;66:49-57.
- 158 Silver EH, Szabo S. Possible role of lipid peroxidation in the actions of acrylonitrile on the adrenals, liver and gastrointestinal tract. *Res Commun Chem Pathol Pharmacol* 1982;36:33-43.
- 159 Lykkesfeldt J. Malondialdehyde as biomarker of oxidative damage to lipids caused by smoking. *Clin Chim Acta* 2007;380:50-8.
- 160 Sandur SK, Pandey MK, Sung B, Ahn KS, Murakami A, Sethi G, Limtrakul P, Badmaev V, Aggarwal BB. Curcumin, demethoxycurcumin, bisdemethoxycurcumin, tetrahydrocurcumin and turmerones differentially regulate anti-inflammatory and anti-proliferative responses through a ROS-independent mechanism. *Carcinogenesis* 2007;28:1765-73.
- 161 Dell'agli M, Bellosta S, Rizzi L, Galli GV, Canavesi M, Rota F, Parente R, Bosisio E, Romeo S. A structure-activity study for the inhibition of metalloproteinase-9 activity and gene expression by analogues of gallic acid. *Cell Mol Life Sci* 2005;62:2896-903.
- 162 Harada N, Hatano E, Koizumi N, Nitta T, Yoshida M, Yamamoto N, Brenner DA, Yamaoka Y. Akt activation protects rat liver from ischemia/reperfusion injury. *J Surg Res* 2004;121:159-70.
- 163 Lotito SB, Frei B. Consumption of flavonoid-rich foods and increased plasma antioxidant capacity in humans: cause, consequence, or epiphenomenon? *Free Radic Biol Med* 2006;41:1727-46.

**ALPHABETIC LIST OF  
COMPANIES**

---

Abbott	Wiesbaden, Germany
AbD Serotec GmbH	Duesseldorf, Germany
Agfa-Gevaert AG	Cologne, Germany
Air Liquide	Duesseldorf, Germany
Amersham Bioscience	Freiburg, Germany
Amersham Pharmacia	Uppsala, Sweden
Appli Chem	Darmstadt, Germany
Applied Biosystems	Hamburg, Germany
ATCC	Rockville, USA
Beckman Coulter	Krefeld, Germany
Berthold detection systems	Pforzheim, Germany
Berthold Technologies	Bad Wildbad, Germany
Biomers.net	Ulm, Germany
BioRad	Munich, Germany
Biosource	Camarillo, USA
Braun Melsungen AG	Melsungen, Germany
Cambrex Profarmaco	Landen, Belgium
Canberra-Packard	Schwadorf, Austria
Cayman Chemical	Michigan, USA
Charles-River Laboratories	Sulzfeld, Germany
Dr. Willmar Schwabe GmbH	Karlsruhe, Germany
Fermentas	St. Leon-Rot, Germany
Fuji	Duesseldorf, Germany
Gerhardt GmbH & Co. KG	Koenigswinter, Germany
GraphPad Software	San Diego, USA
Henke Sass Wolf	Tuttlingen, Germany
Heraeus	Hanau, Germany
Interdim	Montulocon, France
Invitrogen	Karlsruhe, Germany
Janssen-Cilag	Neuss, Germany
Labvision	Fremont, USA
Masterflex	Gelsenkirchen, Germany

---

Millipore	Billerica, USA
Minerva Biolabs	Berlin, Germany
Olympus	Hamburg, Germany
Oxford Biomedical Research	Oxford, USA
PAA Laboratories	Linz, Austria
Peske	Aindling-Pichl, Germany
Portex	Kent, UK
Promega	Heidelberg, Germany
Qiagen	Hilden, Germany
Ratiopharm	Ulm, Germany
Roche Diagnostics	Mannheim, Germany
Serotec	Duesseldorf, Germany
Sigma-Aldrich	Taufkirchen, Germany
Ssniff	Soest, Germany
Stratagene	LaJolla, USA
Tecan	Crailsheim, Germany
Thermo Shandon	Frankfurt, Germany
USB	Cleveland, USA
VWR	Ismaning, Germany
Watson-Marlow GmbH	Rommerskirchen, Germany
Zeiss	Jena, Germany

# **CURRICULUM VITAE**

**ANDREAS HARTKORN**PERSONAL DETAILS

---

- Born 23. January 1980 in Koblenz
- Marital status single
- Nationality German

Ph.D.

---

11/05 – 07/08 **Ludwig-Maximilians-University**, Munich  
Department of Pharmacy  
Center of Drug Research / Pharmaceutical Biology  
Prof. Dr. Angelika M. Vollmar

EDUCATION

---

10/05 **Degree as pharmacist**, Munich

04/00 – 04/04 **Ludwig-Maximilians-University**, Munich

- 3. State examination at 19.09.2005
- 2. State examination at 19.04.2004
- 1. State examination at 15.03.2002

06/90 - 06/99 **Privates Johannesgymnasium**, grammar school, Lahnstein

86-90 **Willi-Graf-Schule**, primary school, Koblenz

WORK EXPERIENCE

---

Since 01/06 **Apotheke am Hauptzollamt**, Munich

Since 11/05 **Löwen Apotheke**, Munich

11/04 – 05/05 **Curtin University of Technology**, Perth, Australia

05/04 – 10/04 **Asam Apotheke**, Munich

# **PUBLICATIONS**

ORIGINAL PUBLICATIONS

---

**07/08** Hoffmann, F. PhD; Sass, G. PhD; Zillies, J. PhD; Zahler, S. PhD; Tiegs, G. PhD; Hartkorn, A.; Winter, G. PhD; Coester, C. PhD; Gerbes, A.L. MD and Vollmar, A.M. PhD

*Selective NF- $\kappa$ B inhibition in Kupffer cells shows controversial effects in fulminant hepatitis and ischemia/reperfusion*

**Submitted Gut**

**06/08** Hartkorn, A.; Hoffmann, F. PhD; Ajamieh H. PhD; Vogel S. PhD; Heilmann J. PhD; Gerbes A.L. MD; Zahler S. PhD and Vollmar A.M. PhD

*Xanthohumol is not protective in hepatic ischemia-reperfusion injury despite its antioxidant effects*

**Submitted Biochemical Pharmacology**

**04/07** Koltermann, A.; Hartkorn, A.; Koch, E. PhD; Fürst, R. PhD; Vollmar, A.M. PhD and Zahler, S. PhD

*Ginkgo Biloba Extract EGb 761 Increases Endothelial Nitric Oxide Production In Vitro and In Vivo.*

Cellular and Molecular Life Science; 2007; 64:1715-22

POSTER

---

**05/06** Wimmer, W.; Hartkorn, A. and Locher, C.

*Benzotriazole-mediated synthesis of 1-substituted 1,2,3,4-tetrahydro-isoquinolines.*

International Symposium on Chemistry, Biology and Medicine  
Paphos, Greece

**04/05**

Hartkorn, A. and Locher, C.

*Successful synthesis of 1-substituted 1,2,3,4-tetrahydroisoquinoline derivatives from N-benzotriazol-1-ylalkyl-N-tosyl- $\beta$ -phenylethylamines.*

Western Australian Biomedical Research Institute

Research Symposium

Perth, Australia

# **ACKNOWLEDGEMENTS**

First and foremost, I would like to thank Prof. Dr. Angelika M. Vollmar for giving me the opportunity to perform this project in her laboratories. Her trust, advices and never-ending optimism – her great style of leadership, intrigued me. After all, I have learned a lot during my time and I am proud of being a member of her research group.

I am further very grateful to PD Dr. Stefan Zahler. For his support and patience throughout this project combined with his special sense of humor giving a pleasant atmosphere. And for acting as second examiner, thank you.

Sincere thanks is given to all members of my thesis committee for their time and effort.

For experimental support I thank Andrea Rothmeier for her great help in the plasmid preparations, Dr. Hussam Ajamieh for carrying out the GSH and SOD assays, Babett Rannefeld for her kind support in measuring the liver enzymes and Dr. Anja Koltermann for great cooperation in the Ginkgo biloba project.

Special thanks goes to Dr. Willmar Schwabe Pharmaceuticals for providing EGb 761 extract, Prof. Dr. J. Heilmann and Susanne Vogel from the University of Regensburg for the synthesis of Xanthohumol and 3-Hydroxyxanthohumol and last but not least to the Department of Technology (Prof. Dr. G. Winter, Dr. C. Coester and Sebastian Fuchs) for preparation and supply of decoy nanoparticles.

I want to thank each and every one of our working group most sincerely for providing a cooperative and enjoyable ambience, in which boundless helpfulness was always guaranteed. Several friendships have formed and turned out to be of great value for me, which I don't want to miss any longer.

Very special thanks go to my research fellow and friend Dr. Florian Hoffmann. For numerous discussions, helpful advices and continuous motivation, no matter of which concern. Thank you.

Special thanks go to all my friends!

Personal financial support and thematic distraction was given by my future employer "Hartkorn Gewürzmühle GmbH" - Thank you!

Most important, I am happy to thank my parents. With their endless understanding, support and encouragement they gave me the best basis to fulfill the "*Ph.D. project*" successfully. Thank you so much.

